Characterization of an Arsenite-Oxidizing *Caballeronia* sp. Soil Bacterium and its Mutualistic Relationship with *Trifolium pratense* for Arsenic Remediation

A thesis presented to

The Faculty of Graduate Studies

of

Lakehead University

by

Jessie McFadden

In partial fulfillment of the requirements
for the degree of
Master of Science in Biology

January, 2021

Abstract

The proposed application of the mutualistic interaction between a native arsenic-oxidizing soil bacteria and *Trifolium pratense* in Northwestern Ontario mine sites is a novel approach to remediation. This thesis studies the characteristics of an arsenic-oxidizing bacterium isolated from a gold mine in Hemlo, Ontario; observes the variance in arsenic (As) toxicity to three different plant species commonly used as phytoremediators; and analyzes the interaction of one of these three plant species with the isolated soil bacterium. The conversion of trivalent inorganic As(III) to its pentavalent form (As(V)) is a widely accepted detoxification pathway. By enriching soil samples collected from the mine's tailing areas with 1 mM sodium arsenite (As(III)) mineral salt solution, 125 As-tolerant soil bacteria were isolated. Silver nitrate ($AgNO_3$) screening and subsequent ICP-AES analysis determined that isolate LU-71 was the only As-oxidizer. An As(III)-induced LU-71 culture had a 74±19% conversion efficiency of As(III) to As(V) in 18 h. The isolate was identified as a novel As-oxidizer in the *Caballeronia* genus by 16S rDNA sequencing and the bacterium also had the ability to produce siderophores. The As-oxidizing bacteria experienced optimal growth at 25°C and pH 7, and was determined to be a heterotroph with a minimum inhibitory concentrations of As(III) and As(V) of 8 and 200 mM, respectively. The LD_{50} of As(III) was 11 times less than As(V) to the germination of *T. pratense*, *F. rubra*, and *M. sativa* seeds. The LD_{50} of As(III) to seeds inoculated with the As-oxidizing bacteria was about 6 times greater than the LD_{50} of As(III) to uninoculated seeds. To *T. pratense* plant growth and biomass production, the As-oxidizing bacteria increased yield by 43%. Given its success promoting plant germination and growth in As-stressed environments, the As-oxidizing *Caballeronia* bacteria is a potentially cost-effective remediation approach to mines in Ontario.

Objectives

Current strategies to restore As-contaminated sites often neglect to consider the entire scope of ecosystem health. Arsenic contamination is multifaceted and each case reserves its own approach. Phytoextraction is a widely used remediation strategy, for nonpoint source contamination though this is not an appropriate solution; before plant matter can be removed and incinerated, wildlife and runoff will further contribute to the contaminant's ubiquity. Bioremediation in the form of non-native bacterial species also neglects to consider the implications of its presence in soil communities. Although numerous studies on the effects of plant growth promoting rhizobacteria (PGPR) to enhance As phytoremediation have been carried out (Srivastava *et al*, 2013b; Wang *et al*, 2011; Funes Pinter *et al*, 2018), to the best of our knowledge, using plant growth promoting As-oxidizing bacteria to promote phytoremediation has not yet been determined. Therefore, this thesis aims to (1) isolate and characterize As(III) oxidizers native to the Northwestern Ontario region, (2) characterize and determine their PGP abilities, and (3) study their effect on germination and growth of phytoremediating plants. The combined approach of phyto- and bio-remediation will be analyzed in the following chapters for its potential as a holistic alternative to current nonpoint source As remediation strategies.

Acknowledgements

Sincerest thanks are extended to my supervisor, Dr. Kam Leung, for his support, constant guidance, and unfaltering patience throughout the past two years. Dr. Kam Leung along with committee member, Dr. Peter Lee, welcomed me into this program with trusting open minds, for which I am forever grateful. Both members of my committee, Dr. Peter Lee and Dr. Heidi Schraft, have continuously supported and encouraged my research, and I am especially grateful for their valuable recommendations that shaped my studies. Dr. Baoqiang Liao has kindly offered his time and energy as my external examiner and I wish to extend my thanks for his knowledgeable feedback on my project. Dr. Wensheng Qin and Grzegorz Kepka at the Lakehead University Instrument Laboratory, and Johane Joncas at the Lakehead University Environmental Laboratory shared their knowledge and time and were integral to the analytical components of my research. I wish to thank Nicholas Ek for orienting me to the lab and offering guidance and a friendly face during the first few months of this project, along with Devon Prontack for laying the foundation for this study. A big thank you as well to Catherine Kibiuk, Paige Perrons, Karissa Kilby, Ashley Faulkner, and Adam Taylor who offered their summer to this research. They contributed countless hours to the characterization of the As-oxidizing bacteria and were instrumental in the efficiency with which my lab work was undertaken. Catherine Kibiuk demonstrated her dedication to the project through her continued involvement and was a constant source of encouragement and a joy to work with. I wish to thank Paridhi Singh for her support in and outside of the lab, and her valuable contributions to this research; I wish her all the best with hers. To all those who have helped shape my path and inspired me thus far, thank you. Without the endless support of my parents and sister, I would not be where I am today, my warmest thanks to my family, forever. Thanks as well to my partner, Cody, for his ceaseless encouragement and for his ability to listen to my heart, even when I did not.

Table of Contents

List of Tables

List of Figures

1. Plant-Bacteria Interactions to Increase Effectiveness of Arsenic Remediation: A Review

1.1. Introduction

Mining is quickly becoming the primary anthropogenic cause of arsenic (As) contamination worldwide (Simmler *et al*, 2016). As a national leader in mining, Ontario is responsible for one-third of Canada's total mined metal production (Burkhardt *et al*, 2017). With 253,000 active mining claims in the region, a vast distribution of land and underground resources are required to meet these demands; this same land requires timely and effective remediation (Ontario OFB, 2020).

Remediation today can take the shape of many different activities: from clean up to revegetation. When soil conditions are poor and contamination is present, revegetation becomes a complex task. Soil following mining generally displays low nutrients, minimal organic matter, decreased water potential, acidic or alkaline pH, and elevated metal contamination such as As toxicity (Renault, 2004). In some cases, plants tolerant to the poor soil conditions just described have successfully returned barren landscapes to their original states; however, the process takes decades and in certain sites contamination is so acute that revegetation is unsuccessful.

The process of integrating plants to rehabilitate soils, sludges, sediments, and water to contain, degrade, or remove contaminants is known as phytoremediation (UNEP, 2002). Phytoremediation is a low-cost approach, effective in addressing low levels of contamination. For this reason, it often represents a significant component of mine closure agreements. Most commonly in industrial applications, phytoremediation moves contaminants from the soil into plant tissues; the plants are then harvested and incinerated (Weis and Weis, 2004).

Remediation can also take the form of a more active approach. Mechanical and chemical techniques such as dredging and filtering soil, soil washing, and soil relocation are

conventional methods of remediation. Unlike phytoremediation, these approaches are costly and disruptive. Contaminated soil is excavated, processed with chemical agents such as sulphuric or nitric acid, and relocated to a waste site (Mulligan *et al*, 2001). Such techniques are generally applied in situations where contamination is high, toxicity becomes an issue downstream, or in the event of land sales (Lim *et al*, 2014). The waste generated from washing the soil, and soil that is simply relocated to reduce acute toxicity at mine sites, does not address the root of the contamination.

Another remediation strategy employs soil microbial activity to neutralize contaminants. Bioremediation, the use of microorganisms to uptake or detoxify environmental pollutants, is an effective method of remediation but its application in open mine sites is limited. Microorganisms often exist in codependent relationships with higher plants, requiring root exudates in the rhizosphere to survive (Ahmad *et al*, 2008). Contaminated soils are in some cases too toxic for plant germination (Lim *et al*, 2014). With an aim of holistic ecosystem recovery in mind, the interaction between bioremediation and phytoremediation is where novel potential lies.

1.2. Arsenic in the Environment

Arsenic is the twentieth most abundant element in the earth's crust, existing in soil and aquatic environments in four different oxidation states: As(-ve III), As(0), As(III), or As(V). Arsenate (As(V)) and arsenite (As(III)) prevail in the natural environment, and are more toxic and mobile than their organic As counterparts (Abbas *et al*, 2017; Sarkar and Paul, 2016). Abbas *et al* (2018) found that arsenite is 60 times more toxic than arsenate. This is due primarily to arsenite's affinity to attack sulfide moieties of proteins, leading to degraded cellular function and cell death. In defining As toxicity, many factors require assessment; the organism or system being affected, the source of contamination, and the chemical state of As are just a few

examples. In examining the toxicity of As to an organism, successful detoxification would include (but is not limited to) As(III) being extruded back to the environment. Hence, As detoxification for a eukaryote or prokaryote is not necessarily synonymous with detoxifying the environment.

Recently, there has been some debate in the literature regarding the toxicity of organic versus inorganic As. Past studies reported organic forms of arsenic (monomethylarsonate (MMA^{V}), dimethylarsinate (DMA^{V}), monomethylarsonite (MMA^{III}), and dimethylarsenite (DMA^{III})) to be less toxic than their inorganic counterparts (As(III) and As(V)) (US NRC, 1999); however, recent evidence suggests that the conversion of inorganic arsenic into organic arsenic may not represent a detoxification pathway. Work on human hepatocytes and chromosomes performed by Petrick *et al* (2000) and Mass *et al* (2001), respectively, concluded the following relative order of toxicity: MMA^{III} > As(III) > As(V) > MMA^{V} = DMA^{V}. The Canada Health Services Drinking Water Quality Guideline (2008) advises that the "oxidation of As(III) to As(V) is the preferred method of removing inorganic arsenic [in combination with other treatment technologies], as it ensures that total arsenic is reduced in an efficient manner".

Provincial soil quality regulations in Ontario, Canada, limit total As concentrations to less than 11 $mg \cdot kg^{-1}$ in all agricultural soils, less than 13 $\mu g \cdot L^{-1}$ in ground water, and less than 6 $mg \cdot kg^{-1}$ in all sediment (Ministry of the Environment, 2011). Federal soil quality guidelines for the protection of environmental and human health restrict As levels in agricultural, residential, commercial, and industrial soils to less than 12 $mg \cdot kg^{-1}$ (Canadian Council of Ministers of the Environment, 2001). The ubiquitous nature of As in soil demands that water quality be closely monitored as well; the Canadian guidelines for total arsenic in drinking water is 10 $\mu g \cdot L^{-1}$, about 1000 times less arsenic than is permitted in soils (Canadian Water Network, 2015). The mineral sector uses about 1.7 billion cubic metres of fresh water per year and is the fourth largest water

user in Canada. Of the 1.7 billion cubic metres, about 78% are discharged directly into lakes and rivers without treatment (Burkhardt *et al*, 2017).

Soil contamination contributes significantly to the bioaccumulation of waste toxins within watersheds, and the bioavailability of As in soils is dictated by three main factors: soil redox potential, pH, and organic matter. Ascar *et al* (2008) found that under redox conditions (-200, 0, and 200 mV redox potential) with organic biosolid incorporation, an increase in all soluble arsenic species occurred. At high (500-200 mV) soil redox levels, however, arsenic solubility is generally low and is primarily present as As(V) (Masscheleyn *et al*, 1991). Low levels of soil pH (< 5.2) have been found to enhance plant uptake of As (Tu and Ma, 2003). The extensive factors at play during As absorption and transformation are under continued study but provide important insights into the role the rhizosphere plays in reducing As contamination.

1.3. Bioremediation

Given the exposure of soil communities to elevated As since the dawn of the industrial revolution, many As-tolerant and -oxidizing species have been identified and well studied, for example: *Rhizobium* NT-26, *Agrobacterium tumefaciens* 5A, and many strains of *Alcaligenes faecalis* and *Pseudomonas aeruginosa,* among others (Kashyap *et al*, 2006; Kaushik *et al*, 2012; Santini *et al*, 2000; Wang *et al*, 2009; Yamamura and Amachi, 2014). These examples form the basis of current bioremediation techniques. Bioremediation is the microbial detoxification of harmful compounds through transformation, containment, or elimination (Mulligan *et al*, 2001). Changes to the chemical properties of metals and metalloids is accomplished by microorganisms by altering oxidation states, e.g. the conversion of As(III) to As(V) (Sher and Rehman, 2019). Some microorganisms immobilize metal ions through processes like biosorption and bioaccumulation, sequestering metals in the cell cytoplasm or periplasm (Okoduwa *et al*, 2018; Sher and Rehman, 2019). Others eliminate contaminants by increasing their solubility, making

the metal ions more mobile and available for extraction processes such as phytoremediation or soil washing (Kapahi and Sachdeva, 2019; Sher and Rehman, 2019).

1.3.1. Reducing As Toxicity in Soil

Bacteria take up As via transport systems such as phosphate transporters (As(V)) and aquaglyceroporins (As(III)). Structural similarities between As(III) and glycerol allow bacteria to employ their glycerol facilitator channel to take up As (Garbinski *et al*, 2019; Meng *et al*, 2004). Bacterial species lacking a glycerol facilitator channel are in most cases still able to uptake As; more research is required to determine these additional mechanisms of As uptake (Kruger *et al*, 2013). Given the resemblance between As(V) and phosphate, bacteria employ phosphate transport systems to take up As(V) (Garbinski *et al*, 2019). Once within the bacteria, As may be oxidized, reduced, methylated, vaporized, or tolerated (Tripathi *et al*, 2007; Yan *et al*, 2019).

Since As(III) is about 60 times more toxic than As(V), the oxidation from As(III) to (V) is an applicable form of bioremediation used in As-contaminated areas (Belval *et al,* 2009). In addition to being less toxic than As(III), arsenate is less bioavailable and mobile due to its affinity for iron oxides, which bind it to the soil (Chen *et al*, 2005). Bacteria with the ability to oxidize As are classified as As-oxidizing bacteria, and may be either aerobic heterotrophs or anaerobic chemolithoautotrophs (Kumari and Jagadevan, 2016; Stolz *et al,* 2010). Heterotrophic species obtain their energy from organic carbon sources while chemolithoautotrophic species are able to obtain energy directly from oxidizing As(III) to As(V) (Kumari and Jagadevan, 2016). The majority of As-oxidizing bacteria are heterotrophs; their oxidation of As is carried out to reduce the toxicity of the metalloid, rather than to produce energy (Santini *et al,* 2000). The following exergonic reaction represents this As-oxidation mechanism: $2H_3AsO_3 + O_2 \rightarrow HAsO_4^{-2} + H_2AsO_4^{-1} + 3H^+$ (Santini *et al*, 2000). Two main mechanisms of As oxidation exist in bacteria, each catalyzed by a different arsenite oxidase enzyme: the AioAB and ArxA systems (Yan *et al*, 2019).

First discovered in the well-studied As-oxidizer *Alcaligenes faecalis*, the *aioAB* operon encodes AioAB, or the aerobic arsenite oxidase enzyme (Lett *et al*, 2012). Anaerobic oxidation of As when nitrate is present is catalyzed by the ArxA system, encoded by the *arxA* gene. The ArxA system is able to both oxidize and reduce As (Kruger *et al*, 2013; Yan *et al*, 2019;). Once converted within bacterial cells via the AioAB or ArxA system, As(V) can be excreted by a membrane protein (Sizova *et al*, 2006). Given the decreased toxicity of As(V), as compared to As(III), this is an advantageous manipulation of the metalloid (Rahman *et al*, 2014).

Immobilization of heavy metals is another methodology employed to reduce As toxicity in soil. Conventionally, immobilization of As using cement, quick lime, fly ash, phosphate, and organic matter has been applied (Basta and McGowen, 2004; Brown *et al*, 2004; Ko *et al*, 2017). More and more, economical and eco-conscious alternatives such as microbial sorption are gaining popularity (Ko *et al*, 2017). It has been found that sulfate reduction interacts with As in soil, decreasing its mobility through the generation of sulfide minerals; bacteria that reduce sulfate thus become valuable tools in As immobilization and remediation. Contrastingly, microbial iron reduction encourages the mobilization of As. Arsenic is often bound to iron minerals, making it insoluble (Tu *et al*, 2004). Iron solubilization by bacteria thus releases As from the minerals, making it bioavailable to plants and other soil microorganisms (Ghosh *et al*, 2011).

1.4. Phytoremediation

1.4.1. Arsenic Uptake and Detoxification in Plants

As a non-essential metal for plants and other organisms, As uptake by plants is dependent on concentration and speciation of As in soil. Arsenic enters plant tissue primarily in its inorganic form of As(III) or As(V). Given that As(III) is primarily associated with anaerobic soil environments, while As(V) is associated with aerobic soil, the transport system involved in As-

uptake is dependent on the soil redox potential (Fayiga and Saha, 2016; Sarkar and Paul, 2016). Similar to bacterial cells, As(V) in plants is primarily taken up by a family of PHT1 phosphate transporters, discovered in *Arabidopsis thaliana*. The analogous nature of As(V) and phosphate encourages competition between the metalloid and phosphate, causing both toxic effects to the plant and nutrient deficiencies (Catarecha *et al,* 2007; Coelho *et al,* 2020; Fayiga and Saha, 2016; Nussaume *et al,* 2011).

Arsenite is taken up by nodulin-26-like intrinsic proteins (NIPs) which are also able to transport As(III) back out of the cell (Abbas *et al,* 2018; Punshon *et al,* 2017; Zhao *et al,* 2009). Once within the plant, As affects growth and productivity through many avenues. Arsenite reacts with sulfhydryl groups and inhibits catalytic functions, leading to membrane degradation and eventual cell death (Farooq *et al*, 2016). Perhaps the most dangerous biochemical impact of As on plant function is the production of reactive oxygen species (ROS), including superoxide radicals (O_2^-), hydroxyl radicals (·OH), and hydrogen peroxide (H_2O_2). Arsenic induces the formation of singlet oxygen molecules, superoxide radical ions, hydrogen peroxide, hydroxyl radicles, and peroxyl radicles ($ROO^\bullet$) through toxicity inhibition of mitochondrial function, as a by-product in the formation of intermediate arsine species, and interference with cellular antioxidants (Hu *et al*, 2020). These ROS disrupt metabolism by damaging lipids, proteins, carbohydrates and DNA (Gunes *et al*, 2008; Meharg and Hartley-Whitaker, 2002). As defense against ROS, many plant species increase the production of antioxidant enzymes, bind and compartmentalize As with ligands in plant vacuoles, and benefit from increased salicylic acid, nitric oxide, and phosphorous (Begum *et al*, 2016; Chandrakar *et al*, 2016; Ozturk *et al*, 2010).

Once As is taken up into the plant, there are five main strategies employed to control the impact of As on the plant: vacuolar sequestration (Mateo *et al,* 2019; Verbruggen *et al,* 2009), extrusion (Mateo *et al,* 2019), translocation (Fayiga and Saha, 2016; Verbruggen *et al,*

2009), volatilization (Fayiga and Saha, 2016), and degradation of organic As in the roots to less toxic forms (Pilon-Smits, 2005). The most studied mechanism, vacuolar sequestration, involves reducing As(V) to As(III). Arsenate is reduced to As(III) which forms a complex with phytochelatins, allowing it to be sequestered into the root vacuoles (Abbas *et al,* 2018; Catarecha *et al,* 2007; Kamiya *et al,* 2009). To cope with heavy metal stress phytochelatins are produced, and are often synthesized more readily in the presence of heavy metals due to the binding of the metals to glutathione causing phytochelatin synthase to work faster (Mirza *et al,* 2014). Reduced glutathione (GSH) is a precursor to phytochelatins and is also needed for the reduction of As(V) to As(III) to occur, since As(V) needs to be reduced in order for the As(III)-phytochelatin complex to form (Meharg and Hartley-Whitaker, 2002; Souri *et al,* 2017). Not only is this complexation of As(III) to phytochelatins thought to be a key As detoxification mechanism, but also a way to achieve As tolerance in plants (Zhao *et al*, 2009).

Another As-detoxification mechanism is the extrusion of As(III), controlled by the same NIPs used for As intake (Mateo *et al,* 2019). Volatilization to control As involves the conversion of inorganic As from soil to gaseous organic forms, then released into the atmosphere (Fayiga and Saha, 2016). In some cases, a plant may degrade organic As to species of lesser toxicity through the use of enzymes, or by the assistance of bacteria (Pilon-Smits, 2005). Restricting As uptake to limit entry of toxic As into cells is another mechanism that certain plants may use to avoid As toxicity, achieved by suppressing the phosphate transport system so that As(V) cannot use it to enter the cell (Tripathi *et al,* 2007). Translocation is a method mainly employed by hyperaccumulator species where inorganic As from the plant's roots is moved to their shoots via xylem (Fayiga and Saha, 2016; Suriyagoda *et al,* 2018; Verbruggen *et al,* 2009).

1.4.2. Types of As Phytoremediation

The three main methods of applied phytoremediation are phytoextraction,

phytovolatilization, and phytostabilization. The most commonly used remediation method is phytoextraction, a process by which plants accumulate metals in their above-ground biomass, which are later harvested and incinerated. Hyperaccumulators, plants with metal-accumulating capabilities 10-500 times greater than average species, are frequently used in phytoextraction (Chibuike and Obiora, 2014). A second approach in phytoextraction applies plants with high biomass in combination with soil amendments (chelates) that foster metal mobilization for ease of uptake by the plant (Chibuike and Obiora, 2014). Concerns surrounding contamination of the food chain exist in applications of phytoextraction. However, recent studies suggest that hyperaccumulators within the Brassicaceae family could provide a solution to these concerns, given their high quantities of thiocyanates making them unpalatable to animals (El Mehdawi *et al*, 2018; Navari-Izzo and Quartacci, 2001).

Phytovolatilization is the transformation of pollutants into chemical compositions that allow the plant to transpire the pollutants into the atmosphere. Hyperaccumulators are often selected for this approach as well (Chibuike and Obiora, 2014). Phytostabilization uses plants to immobilize contaminants, decreasing bioavailability within the ecosystem (Segura and Ramos, 2013). This method is recommended for areas where widespread, non-point source contamination has occurred, and where phytoextraction is not a feasible option (Marques *et al*, 2009). In vast Northwestern Ontario mine sites, benefits of phytostabilization include the eliminated need to remove or dispose of soil, reduced costs and extent of disruption at the regenerating site, and the hastened ecosystem restoration provided by the vegetation (Pivetz, 2001).

1.5. A Mutualistic Approach: Combining Phytoremediation and Bioremediation for Enhanced As Remediation

1.5.1. Plant-Bacteria Interactions

The rhizosphere, the largest ecosystem on Earth, is a system in continual flux, changing depending on the plant species present, the age of the plants, the root area, light availability, humidity, temperature and plant nutrition (Ahmad *et al*, 2008). Direct pressures on plant growth impact root exudation patterns, and in turn microbial communities in coexistence. This same effect is observed in reverse; poor soil quality and an unhealthy microflora will negatively impact the growth of the above-soil vegetation (Salles *et al*, 2004). In remediating contaminated soil, both systems must be addressed.

Rhizobacteria may live in the soil influenced by plant roots or they may directly colonize the root surface, known as the rhizoplane. They may also colonize the endoplant habitat; intercellular spaces of plant vasculature (Elsas *et al*, 2007). Plant root exudates supply an important energy source for soil microorganisms (Salles *et al*, 2004). Some plants provide additional support to rhizospheric bacteria by secreting compounds that stimulate the degradation activities of the bacteria involved in the elimination of the targeted contaminant (Toussaint et al, 2012). Further emphasizing the complexity of soil microbe and plant interactions, Siciliano *et al* (2001) tested the hypothesis that plants situated in contaminated environments show preference to contaminant-degrading bacteria in their rhizosphere.

All these processes occurring in the rhizosphere significantly impact As concentrations and bioavailability due to their associated alterations to soil redox potential, pH and organic matter content. All plant species contribute to rhizosphere acidification through the uptake of iron which releases protons into the surrounding soil (Punchon *et al*, 2016). In addition, approximately 10-40% of a plant's total photosynthetically-fixed carbon is excreted into the soil surrounding the roots, contributing to elevated organic carbon in the rhizosphere compared to bulk soil (Acosta *et al*, 2015; Punchon *et al*, 2016).

The use of rhizosphere microorganisms to enhance phytoremediation of arsenic-contaminated environments is gaining interest (Ma *et al*, 2016). In recent years, several arsenic-resistant microorganisms that decrease arsenic's toxic effects and enhance plant growth have been discovered in various genera, e.g. *Bacillus, Achromobacter, Brevundimonas, Microbacterium, Ochrobactrum, Pseudomonas, Comamonas, Stenotrophomonas,* and *Ensifer* (Cavalca *et al*, 2010; Ghosh *et al*, 2011; Mallick *et al*, 2014; Mesa *et al*, 2017; Pandey *et al*, 2013; Plewniak e*t al*, 2018; Wang *et al*, 2011; Yang *et al*, 2012). In some cases, contaminant-degrading microorganisms have been combined with other plant growth-promoting rhizobacteria for the interacting effect of the detoxification and benefits to plant health (Segura and Ramos, 2013); As-oxidation and plant growth-promoting (PGP) traits in one bacterial strain would offer an ideal candidate for remediation. From a comprehensive literature review, only one study has been found that combines these two traits; Das *et al* (2016) studied the effect of an As-oxidizing PGP bacterium on rice for application in agricultural settings.

1.5.2. Plant Growth-Promoting Rhizobacteria

The rhizosphere is the region of soil closely associated with plant roots. A healthy rhizosphere is nutrient-rich and biologically diverse due to the interactions between plants and soil bacteria; bacteria capable of colonizing this environment are denominated rhizobacteria (Funes Pinter *et al*, 2018). Plant growth-promoting rhizobacteria (PGPR) are bacteria that associate with plant roots, characterized by their ability to increase nutrient uptake by plants through the production of plant growth hormones or macronutrients (Wang *et al*, 2011). Stimulating growth of phytoremediators through the use of PGPR is a valuable approach to soil rehabilitation.

Phytohormones are responsible for the regulation of plant growth and development. Microbes that synthesize phytohormones generally live in association with plants; the synthesis

of phytohormones that encourage plant growth, in turn, generate more food for the associated rhizobacteria (Egamberdieva *et al*, 2017; Ronzan *et al*, 2018). In conditions of As stress, phytohormone production by microbes can improve both plant growth and stress tolerance (Egamberdieva *et al*, 2017). One class of phytohormones, auxins, affect plant growth by responding to environmental stimuli. Indoleacetic acid (IAA) is the main auxin in plants and is responsible for regulating plant growth under stress, such as exposure to acute As toxicity, and controlling root and shoot development (Upadhyay *et al*, 2018; Zhao, 2010). Bacteria already adapted to As-contaminated environments produce excess IAA for use by associated plants (Soto *et al*, 2019).

The production of siderophores is another method employed by PGPR to promote plant growth. Siderophores are molecules with high affinity for ferric iron (Fe(III)) and membrane receptors with the ability to bind the Fe-siderophore complex, thereby facilitating iron uptake (Glick, 2012). Once siderophores have bound iron, microbial iron-siderophore complexes become accessible to plants, despite exposure to heavy metals that inhibit iron uptake (Cavalca *et al*, 2010; Genrich *et al*, 2000). Siderophore production by bacteria mobilizes Fe(III), releasing the As(V) bound to Fe(III) in soil (Chen *et al*, 2005; Sarkar *et al*, 2013). The freed As(V) can then be taken up by plants. A study by Jeong *et al* (2014) on the hyperaccumulator species *P. cretica* found that the presence of siderophore increased As uptake and translocation within the plant.

One of three main nutrients required for plant growth, phosphorous also plays an important role in healthy plant function; however, in its insoluble form, phosphorous is inaccessible to plants. Bacteria able to solubilize inorganic phosphorous in the soil surrounding plant roots provide important nourishment to plant associates (Ullah *et al*, 2015). In As-contaminated soils, the uptake of available phosphate is significantly lower than in healthy soils due to the analogous nature of phosphorous and As (Singh and Ma, 2006). Moreover,

phosphorous amendments to As-spiked soil has been recorded to significantly improve plant growth at high concentrations of As (400 mg kg^{-1}) (Singh and Ma, 2006; Tu and Ma, 2003). The production of phosphate-solubilizing enzymes by bacteria not only provides plants phosphate required for their growth, but has also been shown to mobilize As for uptake (Sarkar *et al*, 2013; Srivastava *et al*, 2013b).

ACC (1-aminocyclopropane-1-carboxylate) deaminase and ethylene production, nitrogen fixation, and xenobiotic activity are all additional characteristics of PGP bacteria. Similar to phosphorous, nitrogen is a nutrient integral to plant health; however, it must be converted from N_2 to NH_3 through a process commonly known as nitrogen fixation (Olanrewaju *et al*, 2017). It has been found that the presence of As in soil decreases nitrogen fixation by limiting the root nodule area on plants, as a direct result of limiting their growth. As-resistant, nitrogen-fixing bacteria are beneficial to plants in these elevated As environments (Mandal *et al*, 2011; Pajuelo *et al*, 2008). Ethylene is a plant hormone that is increased under conditions of stress and leads to decreased overall plant growth (Ullah *et al*, 2015). Given that ACC is the precursor of ethylene, bacteria that produce ACC deaminase are able to reduce ethylene production in plants, balancing ethylene levels and supporting continued growth (Olanrewaju *et al*, 2007; Saleem *et al*, 2007). Antibiotic production by soil bacteria is another indirect method of support through the suppression of disease (Ullah *et al*, 2015). Antibiotics produced by bacteria have been shown to prevent disease, especially valuable to plants under As stress, which otherwise weakens plant health (Glick, 2012; Ullah et al, 2015).

1.5.2.1. As Oxidation

Promotion of plant growth by soil and rhizosphere bacteria can also be achieved by a reduction in soil contamination. The toxicity discrepancy between the two forms of inorganic As, As(V) and As(III), support oxidation as a detoxification method; bacterial species with the ability to

convert As(III) to As(V) can reduce the toxicity of As contamination by 60 times (Abbas *et al*, 2018). Over 30 bacterial strains from genera *Bacillus, Deinococcus, Achromobacter, Thiobacillus, Ancylobacter, Hydrogenophaga, Microbacterium, Herminiimonas,* and *Pseudomonas* have been characterized as As-oxidizing (Yang *et al*, 2016). One of the main problems encountered in the application of these bacteria in bioremediation is their establishment in appropriate numbers within the contaminated environment (Segura and Ramos, 2013). Apart from the study by Das *et al* (2016), the use of plants to aid in the establishment of soil bacteria in As-contaminated soil has not been well studied. By examining As-oxidizing remediation through the lens of combined microbial and plant activities, significant contributions can be made to the industry. Bacteria are able to withstand harsher conditions than plants, with greater flexibility in their molecular processes; we hypothesize that the use of bacteria to oxidize As to a less toxic form in soil will increase plant germination and growth for phytoremediation in contaminated mine sites.

1.6. Scope and Organization of the Thesis

The research presented in the following chapters was undertaken to advance our knowledge of native As-oxidizing soil microbes and their interactions with phytoremediating plants. Once an As-oxidizing bacteria had been isolated and characterized, its plant-growth promoting characteristics and effect on germination and growth rates of T. pratense were assessed. The impact of T. pratense on bacterial cell density was also considered. The thesis is presented in three parts to address the multifaceted approach to remediation proposed. Chapter one provides a general introduction to rehabilitation practices specific to As. Chapter two focuses on identifying and characterizing a potential As-oxidizing soil bacteria. Chapter three presents the plant germination and growth study and their interaction with the As-oxidizing bacteria identified and characterized in Chapter two. Additional data, procedures and maps are included in an appendix section.

2. Arsenic Contamination in Northwestern Ontario and the Isolation and Characterization of an Arsenic-Oxidizing Soil Bacterium

2.1. Abstract

Arsenic (As) contamination in the mining industry is a common concern, and one not addressed by phytoremediation alone. The mutualistic interactions between soil bacteria and plants present considerable potential in remediation strategies. The current study aims to isolate and characterize a soil bacterium indigenous to Northwestern Ontario, with the ability to reduce the toxicity of As. The pentavalent form of As(V) is significantly less toxic than its trivalent counterpart, As(III); hence, As-oxidizing bacteria can be employed to reduce As-toxicity in contaminated soils. Soil samples were collected from a Barrick Gold mine site in Hemlo, Ontario and enriched with As(III) to isolate potential As-oxidizing bacteria. From 125 isolated As-resistant soil bacteria, only two isolates showed positive results in a qualitative $AgNO_3$ screening test for As oxidation. Subsequent characterization of As oxidation using quantitative As speciation and ICP-AES analysis revealed that only one of the two isolates was an As-oxidizing bacterium. 16S ribosomal RNA gene (16S rDNA) sequencing tentatively identified the As-oxidizing bacterium as a *Caballeronia* sp. LU-71 strain. Optimal growth conditions for LU-71 were 25°C and pH 7. The bacteria relied on a carbon source for growth and was determined to be 25 times more tolerant to As(V) than to As(III). An As(III)-induced LU-71 culture had 74±19% conversion efficiency of As(III) to As(V) in 18 h. The As-oxidation efficiency of this *Caballeronia* strain may provide opportunities to lower the toxicity of As and improve phytoremendation of As-contaminated sites.

Keywords: Arsenite Oxidation, Contaminated, *Caballeronia*, Bioremediation, ICP-AES

2.2. Introduction

One of the primary anthropogenic causes of arsenic (As) contamination worldwide is the mining of gold and copper (Simmler *et al*, 2016). Ore extraction and processing expose the surrounding environment to the ubiquitous metalloid, impacting groundwater, watersheds, ecosystem and human health. As a class I carcinogen, the threat of As to human and ecosystem health is imminent and thus its management is integral (Zhao *et al*, 2010). Current strategies to remediate As contamination involve decades of waiting, or inefficient filtration processes; in the case of open mine sites, these are not viable solutions. Given the exposure of soil and plant communities to elevated As since the dawn of the industrial revolution, many As-tolerant and As-oxidizing bacterial species have been identified and well-studied: *Pseudomonas arsenicoxydans* VC-1T, *Rhizobium* sp. NT-26, and *Paraburkholderia insulsa* strain 194 to name a few (Andres *et al*, 2013; Rusch *et al*, 2014; Valenzuela *et al*, 2015).

Modern remediation strategies often involve phytoremediation, with revegetation requirements representing a significant component of mine closure agreements. In this industrial application phytoextraction moves contaminants from the soil into plant tissues; the plants are then harvested and incinerated (Weis and Weis, 2004). Mine sites, however, often encompass hundreds of acres; these phytoextractors provide forage for neighbouring biodiversity, augmenting As contamination within the ecosystem. Another remediation strategy employs soil microbial activity to reduce the toxicity of contaminants. Bioremediation, the use of microorganisms to uptake or detoxify environmental pollutants, is an effective method of remediation but its application in open mine sites is limited. Often existing in codependent relationships with higher plants, microorganisms depend on root exudates for their survival (Ahmad *et al*, 2008). Given the acute toxicity of contaminants in mine soils, seed germination is often inhibited (Chibuike and Obiora, 2014). The combination of bioremediation and phytoremediation holds promise to surpass some of these obstacles.

Arsenic has an affinity for numerous different oxidation states, yet naturally it exists most frequently in its two inorganic forms: arsenate (As(V)) and arsenite (As(III)) (Sarkar and Paul, 2016). Amongst its inorganic forms, As(III) is more soluble and about 60 times more toxic than As(V), reacting with sulfhydryl (-SH) groups of proteins and enzymes to inhibit cellular function and cause cell death (Abbas *et al*, 2017). The oxidation state of As is highly dependent on the environment in which it is found; As(III) is associated with anaerobic soil environments, while As(V) is associated with aerobic soil environments (Sarkar and Paul, 2016). Once As is absorbed into the bacterial cell, detoxification mechanisms include oxidation, reduction, resistance, methylation, and volatilization (Li *et al* 2014; Mukhopadyay *et al*, 2002; Tripathi *et al*, 2007; Yan *et al*, 2019). Arsenic resistance systems in bacteria are the most extensively studied As detoxification pathway (Yan *et al*, 2018). However, many bacteria are able to do more than just resist As. Given the significant difference in toxicity between the trivalent and pentavalent forms of As, bacteria with the mechanisms in place to oxidize As(III) to As(V) would detoxify soils.

Oxidation of As from the trivalent to pentavalent form is catalyzed by As(III) oxidase enzymes (Kruger *et al*, 2013). Arsenic oxidation by two main mechanisms, the AioAB and ArxA systems, leads to the formation of the less toxic and less bioavailable As(V) (Yan *et al*, 2019). As(V) has a much higher affinity for iron oxides making it significantly less mobile than its As(III) counterpart. Given arsenate's similarities to phosphate in structure, the same transporters are employed to move As(V) and phosphate across the plasma membrane of the root cell. It is hypothesized that activity of arsenic-oxidizing bacteria may be elevated by root exudates and oxygen released by higher plants (Das *et al*, 2016). It is in the coupling of As-oxidizing bacteria and plants that effective remediation can be found.

As a national leader in mining, Ontario is responsible for one-third of Canada's total mined metal production (Burkhardt *et al*, 2017). Northwestern Ontario boasts natural resources, producing 720,000 ounces of gold and 232,000 ounces of palladium in 2019 (Thunder Bay CEDC, 2020). Barrick Gold Hemlo Mine is located in the Hemlo mining camp on the north shore of Lake Superior, just 16 kilometres east of the town of Marathon, Ontario (Appendix A). As one of three gold mines established on the Hemlo deposit, 6 million ounces of gold were extracted between 1985 and 2006 (Dawson, 2004). The area of study is a naturally revegetating region between an Unnamed Lake and tailings pond of the Barrick Gold Hemlo Mine. A mining area adjacent to the tailings pond has been previously studied and elevated amounts of As, Mo and Sb were determined to be present (Mol, 2018). Therefore, these contaminants may also exist in the naturalizing area near Unnamed Lake.

The objectives of this chapter are: (1) to provide a full profile of the current soil chemistry at the Barrick Hemlo study area to inform regional soil quality characteristics; (2) to isolate As-oxidizing bacteria from the tailings area of the Barrick Hemlo Gold Mine; and (3) to identify and characterize the As-oxidizing bacteria for potential application to enhance phytoremediation for the rehabilitation of As-contaminated soil.

2.3. Materials and Methods

2.3.1 Soil Characterization

Soil was sampled from Barrick Gold Mine in Hemlo, Ontario. Samples were retrieved from the area surrounding Unnamed Lake and associated tailings ponds. Samples were collected using a sterile scoop and stomacher bags; the bags were sealed and stored at 4°C until use. Ten samples were collected from different locations. At sampling site 1, two field replicates were collected. At sites 2 through 10, three field replicates were collected for each site. A map of the sampling area is included in Appendix A. Samples were collected randomly in

the vegetating area near Unnamed Lake. Total and extractable soil chemistry was assessed for Barrick Hemlo soil samples. For analysis of total metals soil samples were dried in a drying oven at 105°C prior to digestion, for up to 72 hours. Samples were homogenized to pass through a 2 mm mesh and a 0.2 gram aliquot was allowed to predigest in microwave digestion tubes overnight in a 3:1 ratio of concentrated HNO_3:HCl acids. Samples were then digested in a MARS 5 microwave digestion oven for 45 minutes at 175°C.

After digestion the samples were diluted with Type I DDW to 40 mL and concentrations of Al, As, Ba, Be, Ca, Cd, Co, Cr, Cu, Fe, K, Mg, Mo, Na, Ni, P, Pb, Sb, Sr, Ti, Va, and Zn were analyzed by ICP-AES Varian in the Lakehead University Instrument Laboratory (see Appendix C). Extractable soil data was assessed using a 1 M ammonium acetate (pH=7) solution in a 1:10 ratio of soil to solution for Ca, Mg, K and Na. To extract metals, 0.1 N HCl was used (LUEL, 2019). The concentrations of the cations were determined by ICP-AES in the Lakehead University Instrument Lab. Replicate, QC, and lab blank samples were included in each batch of samples.

The percent moisture of the samples was determined by gravimetry on a separate aliquot of sample. A 2.0-gram aliquot of soil was weighed and dried at 105°C overnight. Given the dry weight, moisture content was calculated by dividing the weight of the water in the wet soil by the dry weight of the soil. pH and conductivity were measured using a Mettler Model SevenMulti benchtop pH meter, in a 1:1 ratio of dry sample to DDW. The meter was equipped with a conductivity cell and pH probe. As an estimate of organic matter, loss on ignition was determined by placing 2.0 g of soil sample into a crucible and ashing it overnight at 550°C. Ash weight subtracted from dry weight calculated the total organic matter in the soil sample.

2.3.2 Media Preparation

2.3.2.1 Modified Minimal Salts Media (MSM)

In a final volume of 1 L of distilled deionized water (DDW) the following was dissolved: 2 g of $MgSO_4 \cdot 7H_2O$, 1 g of NH_4Cl, 0.505 g of K_2HPO_4, 0.05 g of $CaCl_2 \cdot H_2O$, and 0.0015 g of $FeCl_2$. To this mixture was added a 1 mL trace element solution, prepared by combining 10 mL of 7.7M HCl, 0.19 g of $CoCl_2 \cdot 6H_2O$, 0.1 g of $MnCl_2 \cdot 4H_2O$, 0.07 g of $ZnCl_2$, 0.006 g of H_3BO_3, 0.036 g of $Na_2MoO_4 \cdot 2H_2O$, 0.024 g of $NiCl_2$, 0.002 g of $CuCl_2$ in 1 L of DDW. An additional 1 mL of vitamin solution was added to the 1 L of MSM, prepared by combining 50 mg of thiamine-HCl, 100 mg of pyridoxine-HCl, 50 mg of niacinamide, 50 mg of D-Ca-pantothenate, 1 mg of cyanocobalamin (B12), 20 mg of biotin, 50 mg of p-aminobenzoic acid, 50 mg of riboflavin, and 20 mg of folic acid in 1 L of distilled water. All solutions can be autoclaved, with the exception of the vitamin solution, which should be filter sterilized using a 0.22 μm filter. For MSM agar, 1.5% agar was added before autoclaving (BD Difco Nutrient Agar 1.5%, Franklin Lakes, NJ, USA).

2.3.2.2 Phosphate Buffer Solution (PBS)

Into a final volume of 1 L DDW, the following was combined: 8.475 g NaCl, 1.093 g Na_2HPO_4, 0.276 g NaH_2PO_4. After all of the components were dissolved, the stir bar was removed and the pH adjusted to 7.4. PBS was autoclaved before use.

2.3.2.3 Tryptic Soy Broth (TSB)

Tryptic soy broth (TSB) was prepared by adding 3% broth (BD Bacto Soybean-Casein Digest Medium, Franklin Lakes, NJ, USA) to DDW, and autoclaving before use. For TSB agar, 1.5% agar (BD Difco Nutrient Agar 1.5%, Franklin Lakes, NJ, USA) was added before autoclaving.

2.3.3 Culture Preservation

Frozen bacterial cultures were prepared from the samples analyzed by ICP-AES and determined to have As(III) oxidation. These cultures were mixed 1:1 with sterile 50% glycerol and stored at -80°C. Samples were preserved in replicates of ten and labelled with date and strain.

2.3.4 Enrichment and Isolation of the As(III)-Oxidizing Bacteria

Soil samples were collected from ten sampling sites between a run-off pond and Unnamed Lake in Hemlo, Ontario and screened for As(III)-oxidizing bacteria (as described in *Section 2.3.1*). Samples were collected using a sterile scoop and stomacher bags; the bags were sealed and stored at 4°C until use. To enrich for the As(III)-oxidizing bacteria, ten grams of each soil sample was added to 100 mL of sterile mineral salt medium (MSM) (see *Section 2.3.2.1*) enriched with 1 mM $NaAsO_2$ (sodium arsenite, As(III)). Antimony potassium tartrate ($C_8H_4K_2O_{12}Sb_2 \cdot 3H_2O$, 0.1 mM) and Sodium molybdate (Na_2MoO_4, 10 mM) were also added to the enrichment due to the high concentrations of these heavy metals detected at the Hemlo Mine in a previous study (Mol, 2018). The enrichment was incubated at 25°C with shaking (150 rpm) for 1 week. A second enrichment followed: 1 mL of the first enrichment samples was combined with 100 mL of the same enriched MSM (with 1 mM $NaAsO_2$, 0.1 mM $C_8H_4K_2O_{12}Sb_2 \cdot 3H_2O$ and 10 mM Na_2MoO_4) used in the first enrichment. The 2nd enrichment samples were grown for one week at 150 rpm and 25°C before plating on arsenite selective agar.

The enriched soil samples were plated on sterile mineral salt glucose medium agar (MSMGA, MSM with 0.5% glucose and 1.5% agar) with 1, 5 and 10 mM $NaAsO_2$. To the MSM described in *Section 2.3.2.1*, 1.5% agar was added. The plates were incubated at 25°C for 72-96 hours before 125 bacteria were randomly isolated and screened for As(III) oxidizing activity. Silver nitrate ($AgNO_3$) was used to detect the presence of As(V); a brown precipitate formed in the presence of As(V), but a colourless to pale yellow reaction was observed with As(III). After growth in MSMG growth medium with 1 mM $NaAsO_2$, 1.5 mL of the culture was pipetted into 1.5 mL Eppendorf tubes and centrifuged at 10,000 rpm for 8 minutes. The supernatant was discarded, and the pellet was resuspended in 200 µL DDW. The $AgNO_3$ test was performed by mixing 80 µL of 1.25 mM As(III), 20 µL of the washed bacteria and 100 µL of 0.1 M silver nitrate, and the colour change was observed after incubation in darkness at 25°C for 24 hours.

2.3.5 Fractionation of As(III) and As(V)

Isolates positive to the $AgNO_3$ screening were further tested for As oxidation. As oxidation of the isolates was determined quantitatively by measuring the amount of As(III) being converted to As(V). The ammonium pyrrolidinedithiocarbamate (APDC) protocol was used to fractionate As(III) and As(V) of the samples. A 1% solution of APDC was prepared by dissolving 0.102 g APDC (Millipore Sigma, Oakville, ON, Canada) in 10 mL of double distilled water (DDW) (extra 0.02 g accounts for impurities). The 10 mL solution was pushed through a syringe filter (0.22 µm) into a test tube. This solution was made fresh for each experiment. The following was mixed into a 15 mL centrifuge tube: 1 mL of 0.1 M Sodium acetate (adjusted to pH 5), 1.25 mL Millipore DDW, 0.5 mL of sample, and 0.25 mL of 1% APDC solution. The solution was mixed and allowed to react for 5 minutes. Samples that contained As(III) showed a white precipitate, indicative of complexation. After 5 minutes, 2 mL of Carbon tetrachloride (CCl_4) was added and shaken for 3 minutes. The tubes were then centrifuged for 5 minutes at 4000 rpm. Half a mL of the upper aqueous layer was then added to 11.5 mL of DDW in a new tube for a final volume of 12mL. These samples were then analyzed using ICP-AES carried out by the Lakehead University Instrument Lab (LUEL). A complete protocol is included in Appendix B.

2.3.6 Inductively Coupled Plasma Atomic Electron Spectroscopy (ICP-AES) Analysis

Inductively coupled plasma atomic electron spectroscopy analysis was carried out by the LUIL. Sample introduction settings remained constant with a 40 second sample uptake delay, a pump rate of 20 rpm, and a rinse time of 35 seconds. Conditions for use were maintained as follows: 1.10 kW power, 15.0 L/min plasma flow, 1.50 L/min auxiliary flow, 0.70 L/min nebulizer flow, 7 mm viewing height, 20 s replicate read time, and a 20 s instrument stabilization delay. A standard operating procedure from the LUIL is included in Appendix B.

2.3.7 PCR and 16S rDNA Sequencing

To identify the As(III) oxidizing bacterial isolate, a 1260-base pair fragment of its 16S ribosomal DNA gene (rDNA) was sequenced and matched with the Genbank Sequence Database of the US National Centre for Biotechnology Information. DNA extraction was achieved following a xanthogenate-SDS (XS) DNA extraction method described by Tillet and Nielan (Tillet and Neilan, 2000). Isolates were grown in MSMG for 72 h before 1.5 mL was pipetted into a centrifuge tube and centrifuged for 10 minutes at 15,000 g, washed once with DDW and centrifuged again. The supernatant was discarded and 800 µL of XS Buffer (1% potassium ethyl xanthogenate, 100 mM Tris-HCl, 20 mM EDTA, 1% sodium dodecyl sulfate, and 800 mM ammonium acetate) was added. The pellet was resuspended by vortexing and incubated at 70°C for 2 h in a water bath. The lysed bacteria were vortexed for 10 s before being placed on ice for 30 minutes. Precipitated debris was removed by centrifugation at 15,000 g for 10 min. A 750 µL portion of the supernatant was then transferred to sterile Eppendorf tubes and an equal volume of 100% isopropanol was added. Tubes were inverted several times and placed in the -80°C freezer for 10 min. DNA was pelleted by centrifugation for 20 min at 15,000 g and washed with 100% ethanol, air dried, and resuspended in 100 µL of UV-treated DDW. Purified DNA was stored at -30°C prior to use.

Polymerase chain reaction was used to amplify a 1356 bp fragment of the 16S rRNA gene. The primers were synthesized by Eurofins Genomics (Toronto, ON, Canada). The final PCR reaction solution was 50 µL with a final concentration of 0.2 mM of dNTP, 2.5 mM of $MgCl_2$, Taq DNA polymerase buffer (1 X), 0.2 µM 63f (5'-CAGGCCTAACATGCAAGTC-3') primer and 0.2 µM 1401-r (5'-CGGTGTGTACAAGACCC-3') primer. Finally, 1 U of TAQ DNA polymerase and 1 µL of template DNA were added to the PCR reaction mixture prior to the assay. Conditions for the PCR reaction were as follows: 95°C for 5 minutes, then 34 cycles of 95°C for 1 min, 55°C for 1 min, 72°C for 1 min, and a final extension at 72°C for 10 min.

The PCR products were visualized using 1% agarose gel electrophoresis with 1 mg/ml ethidium bromide (Bio Rad Gel Doc XR System and Gel Doc software, Bio-Rad, Mississauga, ON, Canada). The PCR product was then purified using Thermoscientific GeneJET column (Thermo Fisher Scientific, Toronto, ON, Canada). The purified PCR products were sent to Eurofin Genomics for DNA sequencing. The isolate was identified by matching its rDNA sequence to the GenBank DNA database using BLAST. 16S rDNA sequences of well-studied As-oxidizing bacteria were compiled and aligned to produce a phylogenetic tree using a neighbour joining method in MEGA 7 (Kumar *et al*, 2019; Naruya and Nei, 1987). The evolutionary distances were computed using the Maximum Likelihood method (Tamura *et al*, 2004).

2.3.7.1 SEM and Gram Stain

The As(III)-oxidizing strain (LU-71) was examined under a Scanning Electron Microscope (SEM/EDS: Hitachi Su-70 Schottky Field Emission) and stained to observe phenotypic characteristics. The bacterium was grown in sterile TSB; three replicate cultures were centrifuged and suspended in 5 mL of 4% paraformaldehyde in PBS (Chao and Zhang, 2011). Cultures then underwent chemical dehydration in a series of 10 mL ethanol washes: 25%, 50%, 60%, 70%, 80%, 90%, 95%, 100%, and again with 100%. After the final wash, cultures were resuspended to a 2mL DDW solution of OD 1.0, and filtered through sterile 0.22 µm filters. The filters were allowed to dry at 4°C in sterile petri dishes, parafilmed shut, prior to SEM analysis. LU-71 gram stain analysis used classical gram staining techniques; crystal violet primary stain was used followed by iodine, both were rinsed with ethanol to decolorize and counterstained with safarin.

2.3.8 Characterization of LU-71

2.3.8.1 Optimal Temperature

The bacterium was grown at 25°C with 150 rpm shaking in sterile tryptic soy broth (TSB) for 18 hours before being washed and resuspended in sterile PBS and DDW ($OD_{600ηm}$ 0.1) respectively. Three replicates were grown in MSMG (0.5% glucose) at five different temperatures: 15, 20, 25, 30, and 35°C. The $OD_{600ηm}$ was measured every 2.5 hours, 5 times a day from 8 am to 6 pm.

2.3.8.2 Optimal pH

LU-71 culture was grown in TSB at 25°C with 150 rpm shaking. Five pH treatments were prepared in MSMG (0.5%): pH 5-9. pH was adjusted using a pH probe and either NaOH to raise the pH, or HCl to lower the pH. LU-71 was washed and resuspended in sterile PBS and DDW, respectively. Ten µL of the cell suspension was added to the 96 well plate containing 240 µL of sterile MSMG at various pH, and the experiment was begun at $OD_{500ηm}$ 0.08. The bacteria were grown in the five different treatments at 25°C in microtiter plates with 40 rpm shaking. The plate was sealed with parafilm and placed in a sealed container. There were ten replicates of each pH. A Microplate Absorbance Reader (MRX TC II, Dynex Technologies, Chantilly, VA, USA) was used to determine the OD measurements every three hours, from 9am to 6pm, for 51 hours.

2.3.8.3 Energy Source for the Growth of LU-71

The bacterium was grown in MSM+$NaAsO_2$ with and without glucose to determine its preferred energy source. A sterile MSM base growth medium (MSM + trace element solution + vitamin solution) was divided into two separate aliquots of 500 mL. To the first, filter-sterilized $NaHCO_3$ and $NaAsO_2$ stock solutions were added to reach final concentrations of 0.1 g/L (5 mM) and 1 mM, respectively. To the second, $NaHCO_3$, $NaAsO_2$ and glucose were added to achieve final concentrations of 5 mM, 1 mM and 0.5%, respectively (Santini *et al*, 2000). Each growth medium was further aliquoted into four sterile 250 mL flasks containing 50 mL of each medium type. The LU-71 inoculum was grown in sterile TSB at 25°C with 150 rpm shaking for 18 hours. The cells were washed three times with sterile PBS and suspended in sterile DDW at $OD_{600ηm}$ 1.0.

The cell suspension was added to 3 flasks of each type of media at a starting $OD_{600\eta m}$ of 0.2. Media was grown at 25°C with 150 rpm shaking. $OD_{600\eta m}$ measured from 0.75 mL aliquots were taken over the course of 50 hours.

2.3.8.4 Minimum Inhibitory Concentrations (MIC) of As(III) and As(V)

LU-71 was grown in MSMG and exposed to varying concentrations of sodium arsenite ($NaAsO_2$) and sodium arsenate (Na_3AsO_4). Arsenic stock solutions were filter sterilized before being added to autoclaved MSMG (0.5% glucose) at concentrations of 0 to 8 mM $NaAsO_2$ and 10 to 200 mM Na_3AsO_4. Each treatment included three replicates of each As concentration and LU-71, three replicates without As, and three replicates without LU-71. Optical density was recorded every 12 hours until growth reached the stationary phase. The experiment was conducted at As concentrations of 0.5, 1, 2, 4, 5, 6, 7 and 8 mM arsenite. Experiments were also conducted with 10, 20, 30, 40, 100, 120, 140, 160, 180 and 200 mM arsenate.

2.3.8.5 Growth and Oxidation of LU-71 Under Optimal Conditions

A sterile MSMG medium with 1 mM of $NaAsO_2$ was prepared and 50 mL of this growth medium was aliquoted into four sterile 250 mL Erlenmeyer flasks. LU-71 culture, grown in TSB, was rinsed three times with sterile PBS, centrifuged for 8 min at 15,000 g, the supernatant discarded and pellet resuspended through vortexing each time. The washed culture was then added to each media to obtain a starting OD of 0.08 and grown at 25°C at 150 rpm. Three flasks were left sterile as a control for the experiment. Over the course of 54 hours, two aliquots were taken from each sample every 3 hours from 8 am to 5 pm. The first of the two aliquots (750 μL) taken at each sampling time was used to measure $OD_{600\eta m}$. The second aliquot (1.25 mL) was centrifuged at 13,000 rpm for 5 minutes. From the supernatant, a 1 mL sample was placed in a 1.5 mL Eppendorf tube. Samples were then processed for As speciation and ICP analysis, as described in *Section 2.3.5* and *Section 2.3.6,* respectively.

2.3.8.6 Induction of As-Oxidation

LU-71 was cultured in sterile TSB in two separate treatments. One treatment had $NaAsO_2$ (at a final concentration of 0.5 mM) added to the growth medium to induce As-oxidation in the bacteria, while the other Erlenmeyer flask contained only TSB and LU-71, no arsenic. After 36 hours at 25°C and 150 rpm shaking, the two cultures were harvested and rinsed three times with sterile PBS before being resuspended in sterile MSMG containing 1 mM $NaAsO_2$ at OD_{600nm} 1. For each treatment (As(III)-induced or non-induced LU-71), three 50 mL sample replicates were prepared in sterile 250 mL Erlenmeyer flasks. Three additional flasks containing 50 mL of the sterile MSMG medium (with 1 mM $NaAsO_2$) were used as the control to monitor contamination throughout the experiment. Aliquots were taken every three hours for the first 18 hours. Samples were also taken at 33 and 57 h to complete the experiment. Samples were preserved in the -80 freezer until they could be prepped for As speciation and ICP-AES analysis. OD measurements were also recorded every 6 hours to track the growth of LU-71.

2.3.9 Statistical Analysis

Statistical analysis was performed using SigmaPlot 12 Software integrated with SigmaStat (Systat Software Inc, 2020) unless otherwise stated. A one-way repeated measures ANOVA was carried out to compare optimal temperatures and pH for the growth of LU-71. Following one-way ANOVAs, Tukey Tests and a Bonferroni T-Test (for the temperature experiment) were used to analyze pairwise combinations of the data. In order to distinguish between sampling sites at Barrick Hemlo Gold Mine, mean and standard deviation of metals were determined for each site. Statistical significance was defined as $p \leq 0.05$.

2.4 Results

2.4.1 Soil Analysis

A summary of the soil analyses from Barrick Hemlo mine sampling sites is given in Table 2.1. Both total and extractable chemical parameters were assessed. Data for all the sampling sites is provided in Appendix B. The Barrick Hemlo mine displayed As concentrations hovering around provincial limits, with an average level of 9.85 mg As kg^{-1}. In Ontario, provincial regulations require As concentrations less than 11 mg·kg^{-1} in all agricultural soils, less than 13 µg·L^{-1} in ground water, and less than 6 mg·kg^{-1} in all types of sediment (Ministry of the Environment, 2011). Federal guidelines on inorganic As in soil recommend less than 12 mg kg^{-1} in all agricultural, residential, commercial and industrial soils (Canadian Council of Ministers of the Environment, 2001). While some sample sites at Barrick Hemlo mine showed inconsequential concentrations of As, other sites had As concentrations of 28.76 and 38.41 mg As kg^{-1} (± 3.68 and 0.12 mg As kg^{-1}, respectively).

Regional soil studies have highlighted As as a metal of concern, along with molybdenum (Mo), antimony (Sb), and zinc (Zn) (Mol, 2018). Elevated concentrations of these metals were observed at Steep Rock Mine, Atikokan ON, Premier Mine in Beardmore, ON, and Winston Lake Mine near Schreiber, ON. At Steep Rock Mine, 320.65 mg As kg^{-1}, 4.46 mg Mo kg^{-1} and 674.91 mg Sb kg^{-1} were observed, and at Premier Mine sites levels of 2245.36 mg As kg^{-1}, 7.74 mg Mo kg^{-1} and 1472.3 mg Sb kg^{-1} (Mol, 2018). Winston Lake had elevated amounts of zinc at 787.61 mg Zn kg^{-1} due to ore mined at the site. Comparatively, Hemlo Mine soil health is stable (see Table 2.1). Canadian Soil Quality Guidelines for Sb, Mo and Zn are 40, 40 and 360 mg kg^{-1}, respectfully. The levels of As contamination found at the Barrick Hemlo Gold Mine suggest that bacteria at the site may have evolved an ability to tolerate and detoxify As. As oxidation is one

of the most common mechanisms for bacteria to detoxify As, hence, the As-oxidizing bacterium under study was isolated from these soil samples.

Table 2.1 Soil chemistry characteristics of Barrick Gold, Hemlo sampling sites (mg kg^{-1}), includes total metal concentrations in mg kg^{-1}, % moisture, conductivity, bulk density, % organic matter and pH.

	Total	± STD	Extractable	± STD
% Moisture	48.07	23.12	48.07	23.12
Conductivity (us/cm)	474.99	254.89	474.99	254.89
Bulk Density (g/cm^3)	0.45	0.30	0.45	0.30
Organic Matter	29.1	27.52	--	--
pH	6.72	1.2	6.72	1.2
Aluminium	9414.5	3605.9	77.06	56.53
Arsenic	9.85	14.06	0.088	0.087
Barium	199.59	235.68	3.84	4.11
Beryllium	0.00	0.00	0.004	0.004
Calcium	14502.6	12481.6	719.4	1007.6
Cadmium	0.17	0.71	0.027	0.054
Cobalt	11.06	5.96	0.199	0.152
Chromium	27.74	21.76	0.028	0.024
Copper	25.10	15.52	0.377	0.345
Iron	10898.0	4749.8	28.98	25.73
Potassium	1606.4	2047.13	10.63	5.23
Magnesium	4051.8	2236.1	37.59	66.46
Manganese	822.27	865.83	23.34	18.74
Molybdenum	33.91	47.31	0.003	0.009
Sodium	17.69	20.45	16.78	20.54
Nickel	22.05	13.12	0.250	0.156
Phosphorous	523.28	268.40	4.322	3.292
Lead	31.03	51.83	0.20	0.159
Antimony	0.00	0.00	0.00	0.00
Strontium	144.11	146.83	4.384	2.19
Titanium	680.78	345.12	0.174	0.228
Vanadium	25.29	13.46	0.094	0.091
Zinc	166.46	313.37	4.765	12.99

Average of 10 different sample locations; site 1 had 2 replicates, sites 2 through 10 had 3 experimental replicates. Total metals were assessed using a nitric and hydrochloric acid digest. Extractable metals were determined using 1 M ammonium acetate (pH=7) solution in a 1:10 ratio of soil to solution.

2.4.2 Isolation and Screening

A total of 125 isolates from Barrick Hemlo soil samples were tested for their ability to oxidize As(III). Two isolates showed positive reactions to the $AgNO_3$ screening test indicating potential of As(III) oxidation (see *Figure 2.1*). In the presence of silver nitrate, sodium arsenite reacts to form a clear or bright yellow colour (Simeonova *et al*, 2004). Sodium arsenate reacts with silver nitrate to create a brown precipitate. This qualitative test was used to screen the isolates for As oxidation; one isolate, referred to as LU-49, demonstrated an orange colour in the presence of silver nitrate. It suggested the presence of both silver arsenite and silver arsenate, implying an incomplete oxidation of As(III) by the bacteria. The second isolate, LU-71, when grown in sodium arsenite and exposed to silver nitrate, changed to a brown colour; suggesting a greater rate of conversion of As(III) to As(V) by LU-71 than LU-49.

In later experiments, all LU-49 frozen cultures were found to be contaminated and no longer exhibited As oxidation. This lack of As oxidation was confirmed with ICP-AES analysis. Thus, one As-oxidizing bacterium was the focus of this study, LU-71. ICP analysis of LU-71 grown in sodium arsenite concluded 88% oxidation of As(III) to As(V) after 3 days of growth (see *Figure 2.2*).

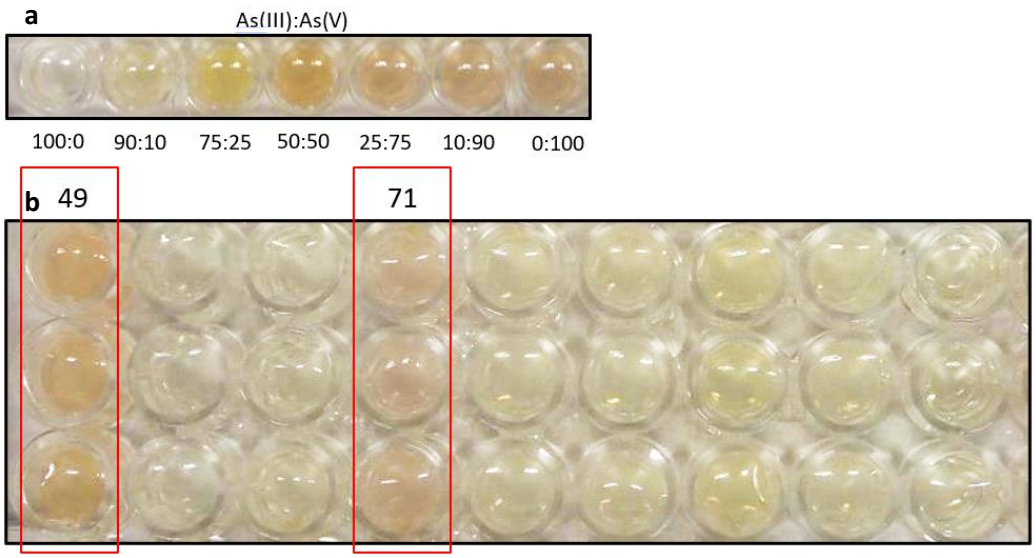

Figure 2.1. Silver nitrate arsenic oxidation test calibration **(a)** and screening tests **(b)**. The lighter orange colouring of the LU-49 samples indicates the presence of approximately 50% As(III) and 50% As(V). The light brown colouring of LU-71 samples suggests approximately 10% As(III) and 90% As(V). Other columns represent non-As-oxidizing isolates.

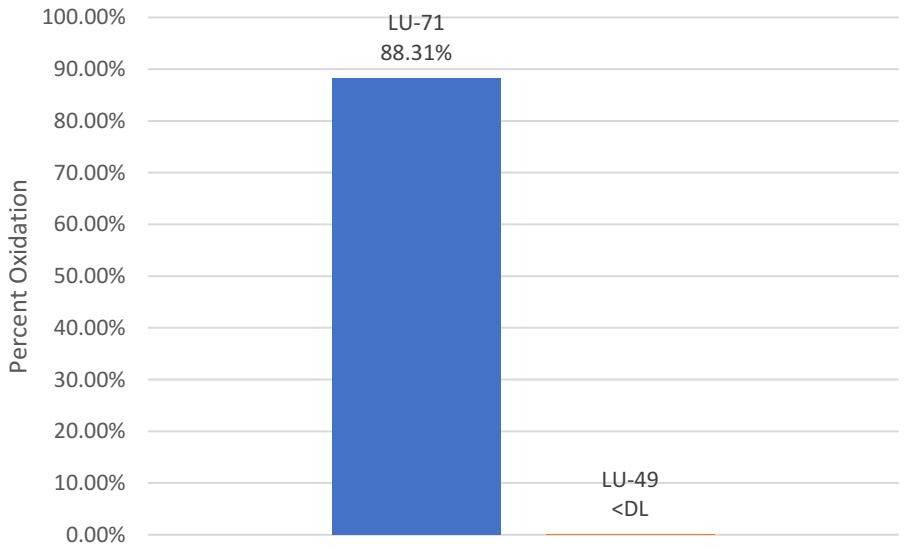

Figure 2.2. Oxidation of As(III) to As(V) by two bacterial isolates: LU-71 and LU-49. LU-71 converted 88.31% of As(III) to As(V), whereas LU-49 did not oxidize any As(III).

2.4.3 Identification of LU-71

The 1356 bp fragment of the 16S rRNA gene (rDNA) of LU-71 was amplified. A 1260 bp region of the amplified fragment was sequenced (see *Figure 2.3*). The 16S rDNA sequence of LU-71 was matched with the Genbank Sequence Database of the US National Centre for Biotechnology Information. Using a Blast search, the bacterium belonged to the β-Proteobacteria phylogenetic class and was tentatively classified as a *Caballeronia* sp.

The phylogeny of LU-71 compared to other closely related *Burkholderia* spp., *Paraburkholderia* spp., and *Caballeronia* spp., as well as representatives from other known arsenic oxidizer species is shown in *Figure 2.4*. These three β-Proteobacteria groups were found to be closely related. Within the three groups, *Burkholderia* spp., *Paraburkholderia* spp., and *Caballeronia* spp., there are two known *Burkholderia* spp. arsenic-oxidizing bacteria, *Burkholderia* sp. *S31R* and *Burkholderia* sp. *S32*, see *Figure 2.4* (Sultana *et al*, 2012). LU-71 is a novel As-oxidizing bacterium within the *Caballeronia* spp. A neighbour-joining phylogenetic tree mapping LU-71 with other As-oxidizers was analyzed using MEGA7. The evolutionary distances were computed using the Maximum Likelihood method (Tamura *et al*, 2004).

LU-71 was a Gram-negative rod bacterium (*Figure 2.5*) and an SEM image of the bacterium highlighted its morphology; LU-71 is rod-shaped, approximately 1 µm in length, and secretes a polysaccharide matrix (determined using SEM Chemical Analysis software, Energy-Dispersive X-Ray Analysis (EDXA)). LU-71 was identified as a Gram-negative bacterium using a gram staining assay (*Figure 2.6*).

```
TGGTGGCGAG TGGCGAACGG GTGAGTAATA CATCGGAACG TGTCCTGTAG TGGGGGATAG        60
CCCGGCGAAA GCCGGATTAA TACCGCATAC GATCTACGGA AGAAAGCGGG GGATCCTTCG       120
GGACCTCGCG CTATAGGGGC GGCCGATGGC AGATTAGCTA GTTGGTGGGG TAAAGGCCTA       180
CCAAGGCGAC GATCTGTAGC TGGTCTGAGA GGACGACCAG CCACACTGGG ACTGAGACAC       240
GGCCCAGACT CCTACGGGAG GCAGCAGTGG GGAATTTTGG ACAATGGGGG AAACCCTGAT       300
CCAGCAATGC CGCGTGTGTG AAGAAGGCCT TCGGGTTGTA AAGCACTTGT TGTCCGGAAA       360
GAAAACCTTT GCACTAATAC TGTGGGGGGA TGACGGTACC GGAAGAATAA GCACCGGCTA       420
ACTACGTGCC AGCAGCCGCG GTAATACGTA GGGTGCGAGC GTTAATCGGA ATTACTGGGC       480
GTAAAGCGTG CGCAGGCGGT TCGTTAAGAC AGATGTGAAA TCCCCGGGCT TAACCTGGGA       540
ACTGCATTTG TGACTGGCGA GCTAGAGTAT GGCAGAGGGG GGTAGAATTC CACGTGTAGC       600
AGTGAAATGC GTAGAGATGT GGAGGAATAC CGATGGCGAA GGCAGCCCCC TGGGCCAATA       660
CTGACGCTCA TGCACGAAAG CGTGGGGAGC AAACAGGATT AGATACCCTG GTAGTCCACG       720
CCCTAAACGA TGTCAACTAG TTGTTGGGGA TTCATTTCCT TAGTAACGTA GCTAACGCGT       780
GAAGTTGACC GCCTGGGGAG TACGGTCGCA AGATTAAAAC TCAAAGGAAT TGACGGGGAC       840
CCGCACAAGC GGTGGATGAT GTGGATTAAT TCGATGCAAC GCGAAAAACC TTACCTACCC       900
TTGACATGGT CGGAACCCTG CTGAAAGGTG GGGGTGCTCG AAAGAGAACC GATACACAGG       960
TGCTGCATGG CTGTCGTCAG CTCGTGTCGT GAGATGTTGG GTTAAGTCCC GCAACGAGCG      1020
CAACCCTTGT CCTTAGTTGC TACGCAAGAG CACTCTAAGG AGACTGCCGG TGACAAACCG      1080
GAGGAAGGTG GGGATGACGT CAAGTCCTCA TGGCCCTTAT GGGTAGGGCT TCACACGTCA      1140
TACAATGGTC GGAACAGAGG GCTGCCAACC CGTGAGGGGG AGCTAATCCC AGAAAACCGA      1200
TCGTAGTCCG GATCGTAGTC TGCAACTCGA CTACGTGAAG CTGGAATCGC TAGTAATCGC      1260
```

Figure 2.3. The 16S ribosomal DNA sequence above was sequenced by primers 63-F and 1401-R. Numerical values listed on the right side represent the length of the sequence, not the position.

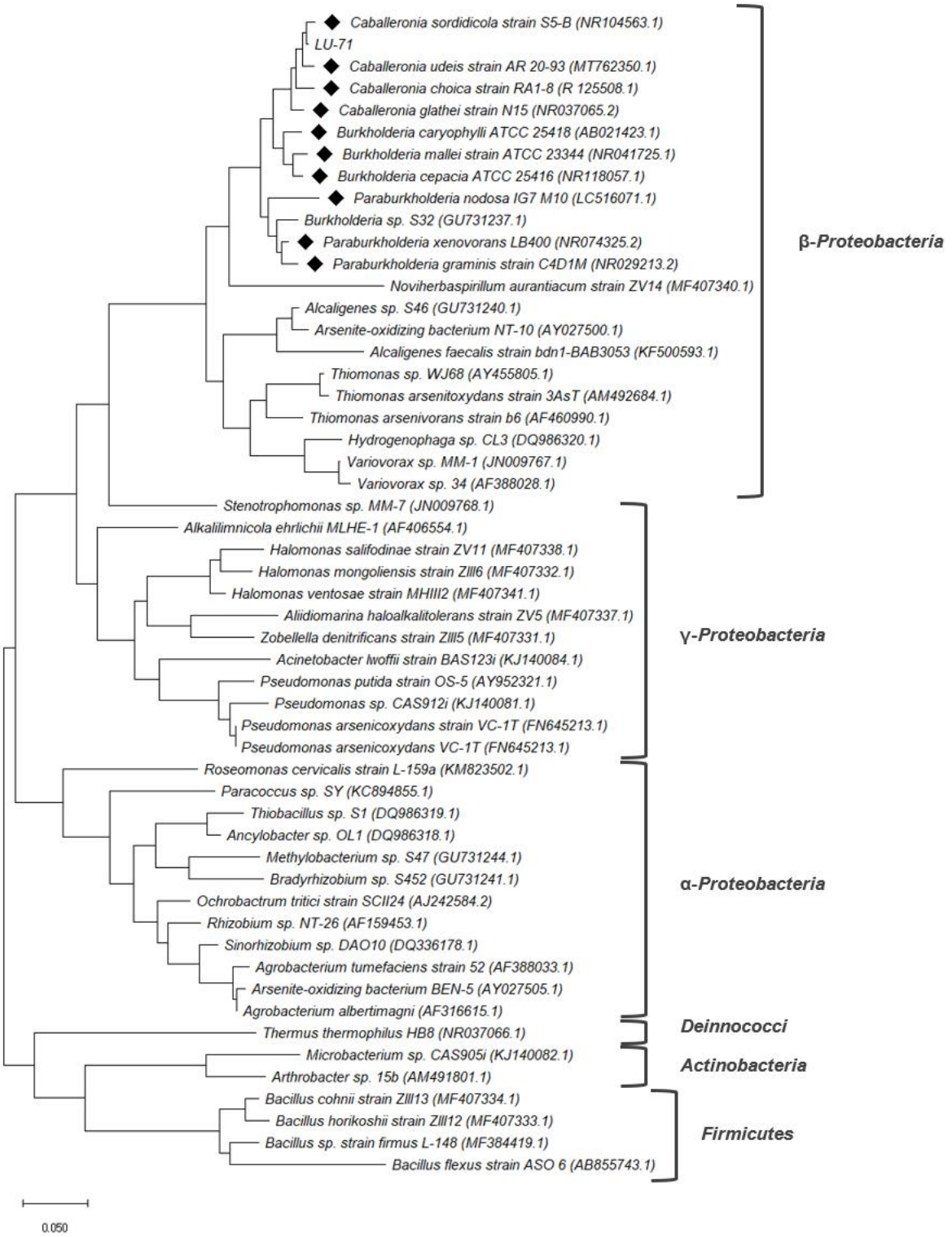

Figure 2.4. Neighbour-joining phylogenetic tree based on 16S rRNA gene sequences, showing the evolutionary history of the *Caballeronia* genus and its relation to other known arsenic-oxidizing species. NCBI Reference Sequences listed for each strain are included in the phylogeny in brackets. The bold diamond symbols (◆) indicate species that are not As-oxidizers. LU-71 is a novel arsenic-oxidizing species in the *Caballeronia* genus.

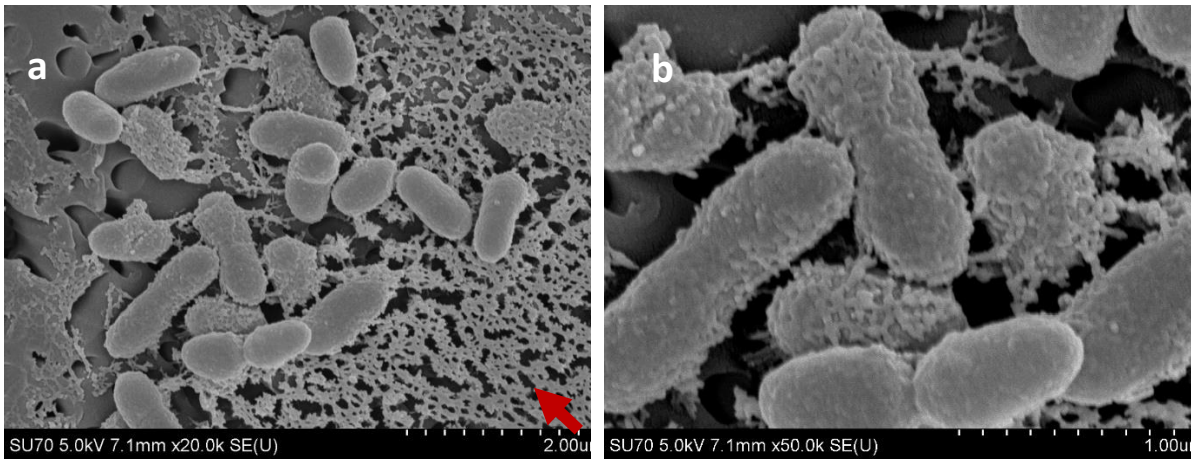

Figure 2.5. Scanning electron microscope images of the LU-71 arsenic-oxidizing bacterium. These photos were captured of a bacterial colony concentrated at OD 1. The bacterium is rod-shaped, approx. 1.00µm in length, and secretes a carbon-based matrix. **(a)** The arrow points to the polysaccharide matrix secreted by the bacteria, allowing the bacteria to adhere to surfaces using the biofilm **(b)**.

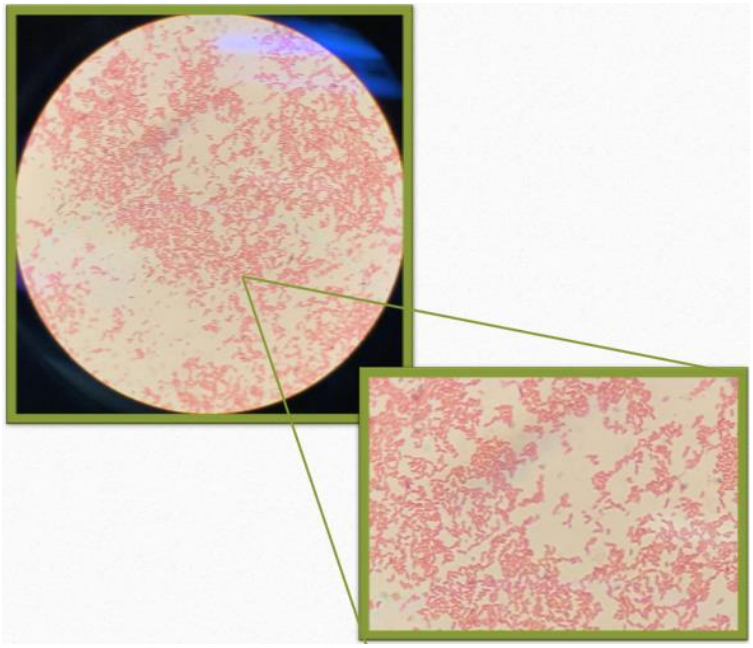

Figure 2.6. Photos taken at 20X and 40X magnification using a compound microscope. LU-71 is seen here to be a Gram negative β-proteobacterium.

2.4.4 Characterization of LU-71

2.4.4.1 Optimal Growth Temperature

The optimal growth temperature for the As-oxidizing bacterium was between 20 and 25°C in MSMG. Statistically significant difference was observed between the treatments, except pairwise between 15°C and 20°C, 15°C and 30°C, and between 20°C and 25°C (One-way repeated measures ANOVA; $p < 0.001$). Based on the growth curve shown in *Figure 2.7,* 25°C was considered the optimal temperature with a doubling time of about 7 hours and used as the constant temperature for growth in all data collection. Growth was observed at all treatments from 15-30°C, but minimal growth occurred at the upper limit, 35°C.

Depending on the temperature, LU-71 was shown to reach the stationary phase between 20-35 h. At 25°C the bacteria reached peak optical density in the least amount of time. At 30°C, the rate of growth is only slightly below the 25°C and 20°C treatments. Minimal growth was observed at 35°C (see *Figure 2.7*).

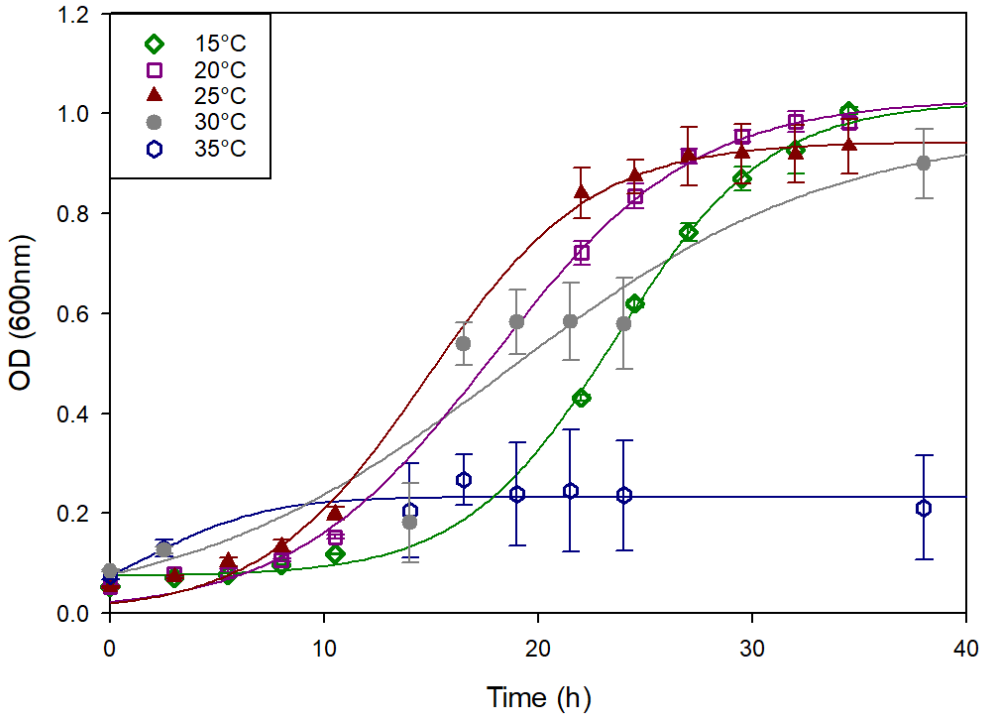

Figure 2.7. The growth of LU-71 at five different temperatures. The line of best fit representing growth at 30°C does not accurately display the rate of growth at approximately 14 h.

2.4.4.2 Optimal pH

It was determined that pH 7 optimizes growth for LU-71. At pH 7, the $OD_{500ηm}$ of LU-71 reaches approximately 0.3, while all other pH yielded OD 0.24 and lower at 500ηm. At pH 6, the growth rate is comparable to that at pH 7. A one-way repeated measures (RM) ANOVA on ranks was conducted for peak $OD_{500ηm}$ measurements collected at 51 h. The data did not pass the normality test (Shapiro-Wilk; $p < 0.001$), hence a RM ANOVA on ranks was used. A Tukey Test determined significant difference ($p < 0.05$) in the following pairwise combinations: pH 9 and pH 5, pH 9 and pH 6, pH 7 and pH 5. No significant difference was observed between pH 6 and pH 7. The bacteria had the least growth at pH 5 (see *Figure 2.8*). Large deviation may have been caused by inconsistencies in pipetting (Caraus *et al*, 2015; Henke, 2016). Randomly allocating the samples within the plate is suggested to address this systematic error in future experiments.

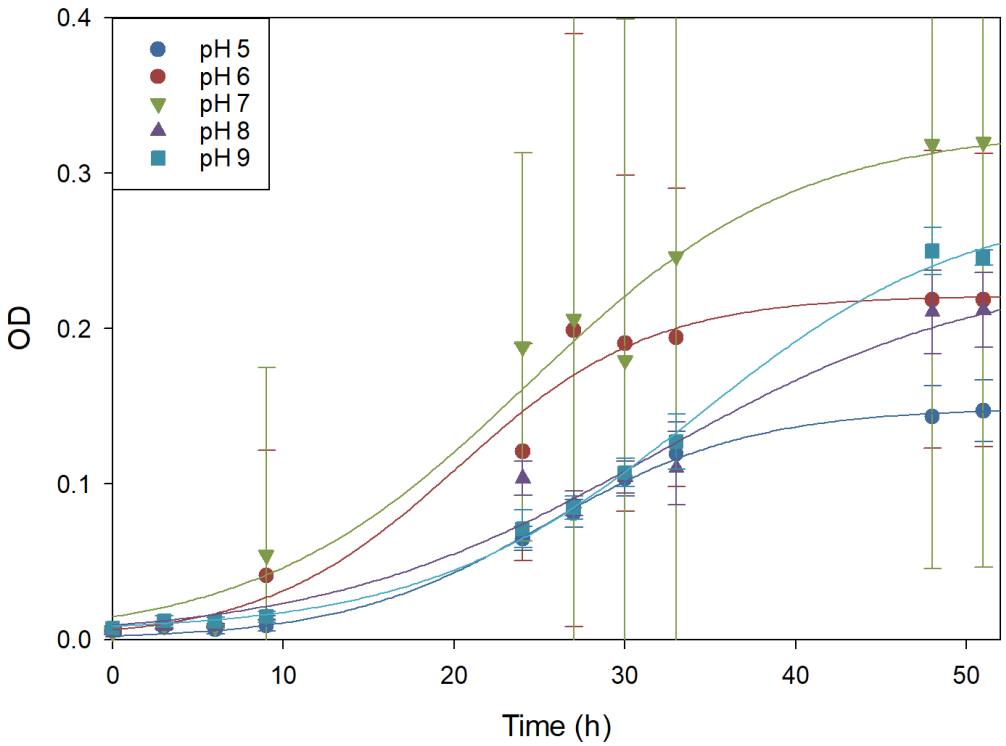

Figure 2.8. Optimal pH of the As-oxidizing bacteria. After two days of growth, pH 7 is shown to be the optimal pH. The bacteria had the least growth at pH 5. Due to the increased opportunity for random error when culturing bacteria in microtiter plates, the deviation in the graph above is explained (Caraus *et al*, 2015; Henke, 2016).

2.4.4.3 Comparing Arsenite and Glucose as Energy Source for Growth

This experiment was performed under the following conditions: 25°C, pH 7, and MSM-As(III) growth medium with or without glucose. The growth of LU-71 with As(III) as the only source of energy for growth was examined. The growth of LU-71 was only detected in the presence of glucose but not in the As(III) growth medium (without glucose); hence, LU-71 was determined to be a heterotroph (*Figure 2.9*). The doubling time of the bacteria was estimated to be about 7 hours in MSMG growth medium; from $OD_{600\eta m}$ 0.2 to a plateau of $OD_{600\eta m}$ 1.3. Exposed only to arsenite as the sole energy source, no growth was observed for the bacteria.

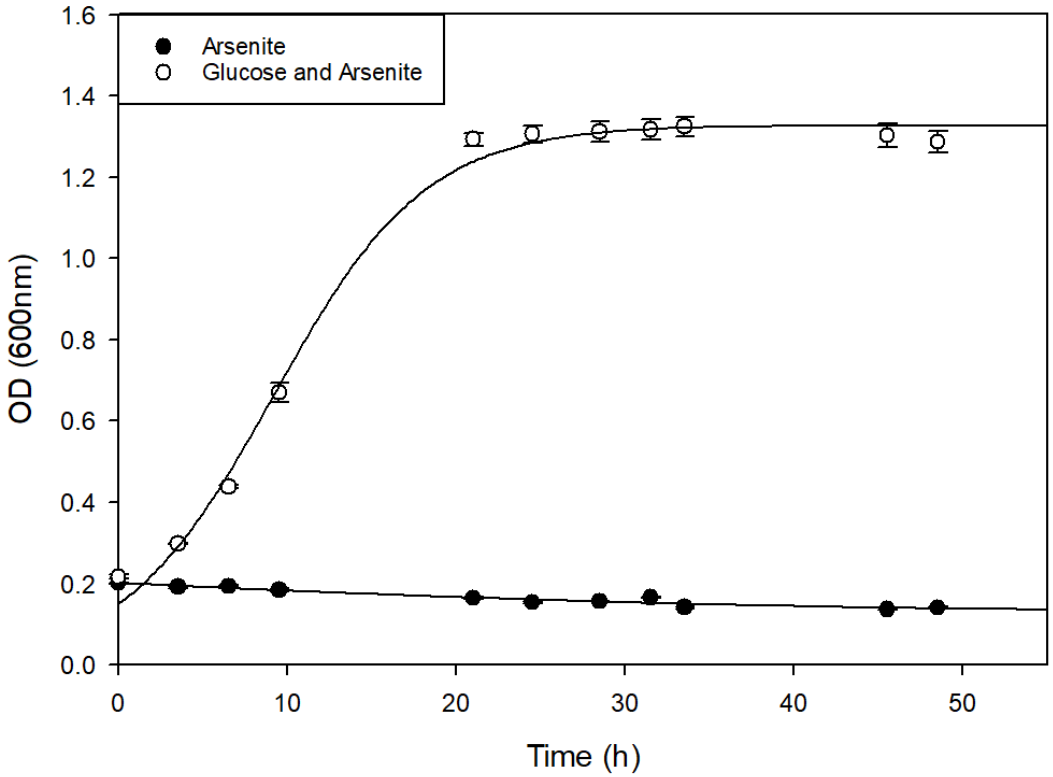

Figure 2.9. Comparative growth curves of LU-71, using two different media combinations: MSM with $NaHCO_3$ (5 mM) + $NaAsO_2$ (1 mM), and MSM with $NaHCO_3$ (5 mM) + $NaAsO_2$ (1 mM) + Glucose (0.5%), listed in the legend as "Arsenite" and "Glucose and Arsenite", respectively. Each treatment was carried out in replicates of 3, with standard deviation represented by vertical error bars.

2.4.4.4 MICs of As(III) and As(V)

Given a temperature requirement of 25°C, pH of 7, and addition of glucose to MSM growth media for optimal growth, these conditions were controlled for all remaining experiments: the minimum inhibitory concentration (MIC) of As(III) and As(V) to LU-71, the oxidation efficiency of As(III) by LU-71, and the analysis of the induction of As(III) oxidation in LU-71. The MIC of arsenite ($NaAsO_2$) was found to be 8 mM. At 8 mM sodium arsenite, LU-71 was unable to grow after 11 days. The threshold of the bacteria when exposed to arsenate (Na_3AsO_4) was significantly greater, with growth interrupted at 200 mM sodium arsenate (see Table 2.2). LU-71 was about 25 times more tolerant to As(V) than As(III).

Table 2.2. Minimum Inhibitory Concentration (MIC) of sodium arsenite and arsenate on LU-71.

	As(III)			As(V)		
Conc. (mM)	Growth (+/-)	Max. OD (600nm)	Time (h)	Growth (+/-)	Max. OD (600nm)	Time (h)
5	+	1.244	182	+		
6	+	1.370	182	+		
7	+	0.497	240	+		
8	**-**	**0.107**	**264**	+		
10	-			+	1.591	84
50	-			+	1.455	84
100	-			+	1.537	84
120	-			+	1.523	84
140	-			+	1.533	84
160	-			+	1.425	84
180	-			+	1.288	168
200	-			**-**	**0.184**	**168**

2.4.4.5 Growth and As Oxidation of LU-71

Arsenite oxidation was observed by plotting growth curves and taking aliquots every 3 hours for As fractionation and ICP-AES analysis. With reference to *Figure 2.10*, it is evident that the conversion of arsenite by LU-71 started only when the bacteria entered the exponential growth phase and As oxidation continued even after reaching the stationary phase. After 54 hours, conversion efficiency of As(III) to As(V) of 40% was reached. As-oxidation begins in conjunction with the exponential growth phase of the bacteria. Oxidation is continued in the stationary phase. In subsequent experiments, the conversion rate was shown to reach 80% (*Section 2.4.4.6*).

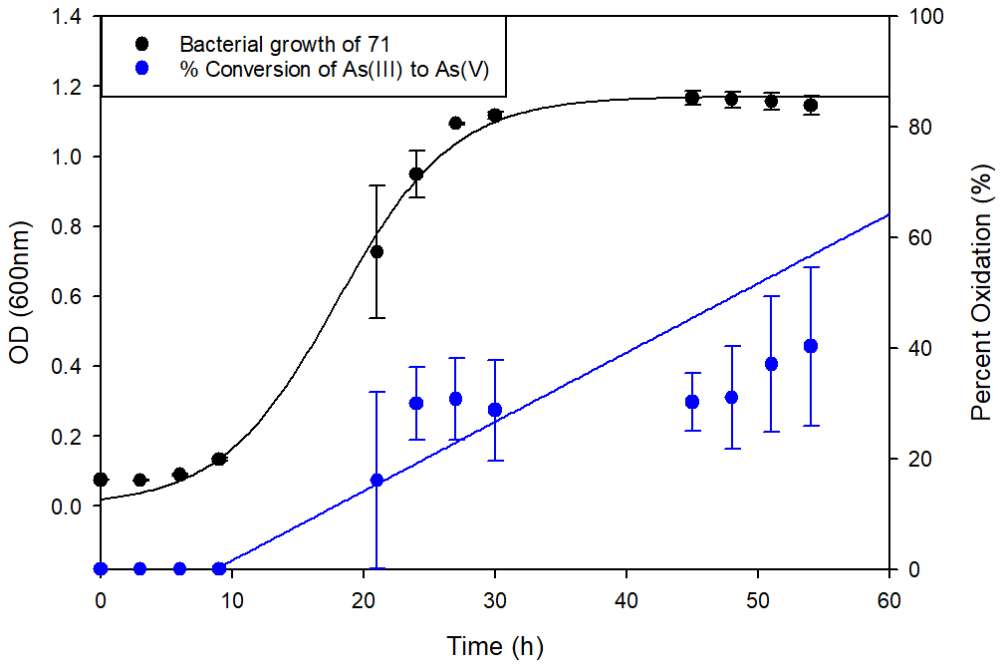

Figure 2.10. Growth of LU-71 and its oxidation of arsenite (As(III)) to arsenate (As(V)) over a 55h period. At the stationary phase, the rate of oxidation continues to increase.

2.4.4.6 Induction of As(III) Oxidation

It was found that As-oxidation by LU-71 was inducible (see *Figure 2.11*). For the bacteria pre-exposed to 0.5 mM $NaAsO_2$, As-oxidation commenced immediately. Seventy-four percent of the As(III) was oxidized in the first 18 h and 80% oxidation was reached in 57 h. For the induced culture, the bacteria rapidly oxidized the As added to the growth media. In the non-induced treatment, a lag period of about 18 hours was observed before oxidation began, and oxidation was significantly slower.

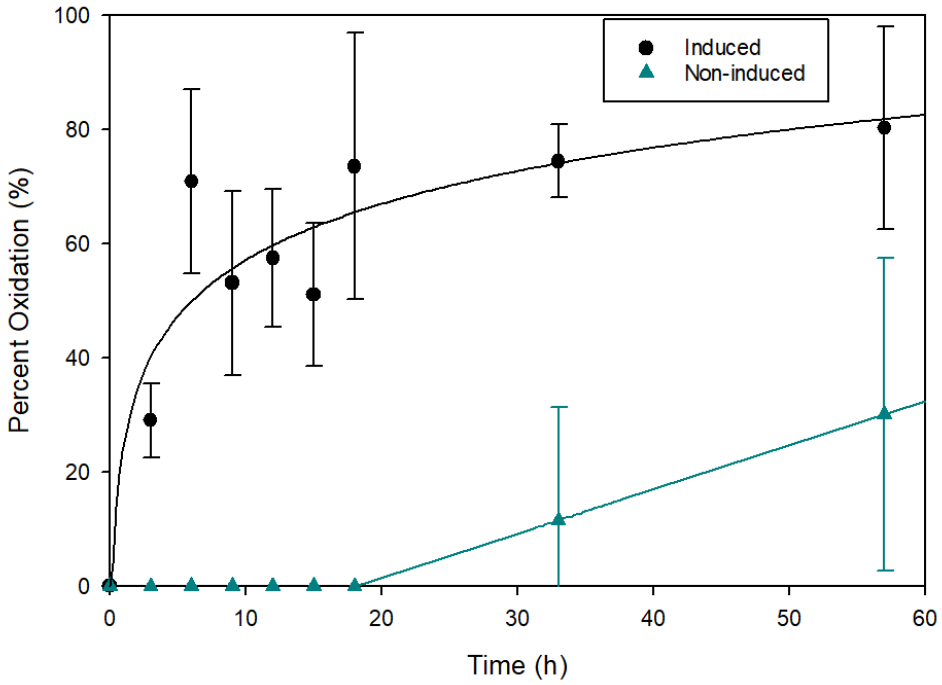

Figure 2.11. As-oxidization of As(III)-induced and non-induced LU-71.

2.5 Discussion

2.5.1 Soil Analysis

Barrick Gold Hemlo soil samples were taken from tailings that drain into the Unnamed Lake. When compared to soil quality data from other regional mines, the metal contamination in Barrick Gold tailings samples was found to be relatively low. Regional soil chemistry profiles from Premier Gold Mine in Beardmore, Ontario, and Steep Rock Mine north of Atikokan, Ontario, show levels of As at 2245.36 mg kg^{-1}, 320.65 mg kg^{-1}, respectively. Winston Lake Mine, near Schreiber, Ontario, was a former zinc mine with high levels of zinc contamination in its soil profile (787.61 mg Zn kg^{-1}), and only 2.00 mg As kg^{-1} (Mol, 2018). Soil analysis completed in 2018 at the Golden Giant Mine, within the Barrick Gold Hemlo Mine, found As averaged 23 mg kg^{-1} with some samples reaching 101 mg kg^{-1} (Mol, 2018). The sampling locations within the Barrick Gold Hemlo Mine varied between 2018 data collection and the soil analysis undertaken in this study; this allowed for a larger area of soil data to be mapped within the mine. The 2018 soil samples were taken directly from the existing mine site, whereas the soil samples for this study were collected from the tailings draining into the Unnamed Lake. Dispersion of the contaminant through runoff is suspected to have decreased levels of As surrounding the mine site, hence an average concentration of 9.85 ± 14.06 mg As kg^{-1} was recorded for the tailings soil samples.

Canadian standards of soil quality state 12 mg As kg^{-1} as the safe allowable limit in soils of all disciplines (Canadian Council of Ministers of the Environment, 2001). Past soil analysis had samples reaching 101 mg As kg^{-1} within the mine site and samples from tailings showed As concentrations as high as 38.41 mg As kg^{-1} (± 0.12 mg kg^{-1}). These soils represent a challenge for reintegrating the site to a naturalized landscape; poor soil stability, a lack of nutrient cycling, and degraded soil ecosystems are common in anthropogenic soils (Freitas *et l*, 2004). Iron and

phosphate, salts, pH, clay content, and soil moisture all affect the vailability of As within the soil matrix (Abbas *et al*, 2018). With higher soil As concentrations, microbial communities begin to adapt to the contamination, generating As-resistant strains (Dey *et al*, 2016). Since the average available concentrations of As in the tailing area were relatively low with an average of 9.85 ± 14.06 mg As kg^{-1}, it may explain the low abundance of As oxidizing bacteria at the site and why only one As-oxidizing bacteria was isolated in this study. As the concentration of As increases, soil microflora need to develop adaptation mechanisms beyond tolerance of the metal. It is predicted that isolation experiments conducted using soil samples from Premier Mine soil samples, where contamination is 2245.36 mg kg^{-1} on average, would isolate a greater number of bacteria with As-oxidization mechanisms.

Elements of the soil chemistry profile of Barrick Gold Mine tailings such as pH, phosphorous and potassium suggest suitability for a mutualistic relationship between soil communities and phytoremediation principles (Praveen *et al*, 2016). A pH range between 6-8 indicates maximum nutrient availability (Harris *et al*, 1996); pH 6.72 was observed from the tailing samples. The presence of metals such as As does not alone imply their bioavailability to plant species. Soil microbes and competition within microbial communities, temperature, As speciation, and nutrient availability all may contribute to the success of LU-71 establishment in the soil and its association with the local plant species.

2.5.2 Identification and Phylogenetic Analysis of the As-Oxidizing Isolate

Given the ubiquitous nature of As, As-resistant species are found across the world. Microorganisms play a key role in the cycling of the metal (Yamamura and Amachi, 2014). The mechanisms by which bacteria are able to oxidize As are being continuously researched, and genetic techniques mapping out the As-detoxifying genes are allowing for the discovery of more and more As-oxidizers. Well studied As-oxidizers include strains of *Alcaligenes faecalis* – with

total As(III) to As(V) conversion rates of approximately 1 mM (100 mg L^{-1}) in 2.5 hours – *Agrobacterium tumefaciens* 5A, and *Rhizobium sp* NT-26, among others (Kashyap *et al*, 2006; Santini *et al*, 2000; Wang *et al*, 2009). According to phylogenetic clustering, the genus *Burkholderia* was recently split into three genera (Dobritsa *et al*, 2017). The first of the three new genera retained the existing name *Burkholderia* and consists mainly of animal and plant pathogens. Eleven species from the original genus *Burkholderia* were moved to the new genus *Paraburkholderia*, and another new genus, *Caballeronia*, was proposed to accommodate twelve other species. The genus *Caballeronia* often includes plant-associated environmental soil bacteria (Dobritsa and Samadpour, 2016). Species within this genus are chemoorganotrophic, mesophilic, Gram negative, and rod-shaped (Dobritsa and Samadpour, 2016).

Arsenic-oxidizing bacteria are very diverse, scattered throughout distant branches of the phylogenetic tree. Within the β-Proteobacteria classification, As-oxidizers organize into numerous different clades. Two *Burkholderia* species have been identified as As-oxidizers (*Figure 2.4*. *Burkholderia* S32 and S31 were isolated by Sultana *et al* (2012) from contaminated mine sites in Germany; PCR detected arsenite oxidase genes and screening with $KMnO_4$ further demonstrated their ability to oxidize As. Another *Burkholderia* sp., *B. multivorans* ATCC 17616, was found to have the protein sequences involved in arsenite oxidation but currently no studies demonstrate this ability (Muller *et al*, 2007). While there are ample As-oxidizers in the β-Proteobacteria class, and a handful in the *Burkholderia* complex, LU-71 represents a separate phylogenetic clade from *Burkholderia* sp. and is a novel As-oxidizer within the *Caballeronia* genus; the first identified As-oxidizer within this group. Phenotypic characterization of LU-71 suggests the bacterium may have the ability to interact with plant roots, further supporting its classification as a *Caballeronia* species (Eberi and Vandamme, 2016). SEM imagery showed a polysaccharide matrix, composed of hydrogen and carbon, secreted by the bacteria (see *Figure*

2.5). This matrix suggests biofilm formation and plant root interaction. Plants support a diverse array of bacteria on and within their roots and transport vessels; root exudates from the root tip provide energy and carbon sources for soil bacteria. In turn, some bacteria have developed mutualistic relationships with plants, including plant-growth promoting traits such as auxin and siderophore production (Bogino *et al*, 2013). Based on the classification of LU-71 within the *Caballeronia* genus and observable traits, LU-71 is a good candidate for combined bioremediation and phytoremediation techniques.

2.5.3 Characterization of LU-71

LU-71 was found to be a mesophile, growing best at an optimal temperature of 25°C, at pH 7, and with an organic energy source. Compared to other soil As-oxidizing bacteria, such as the *Rhizobium* NT-26, LU-71 shares traits commonly observed in soil bacteria: Gram negative, rod-shaped, motile, and biofilm forming (Hakeem and Akhtar, 2016). The doubling times of *Rhizobium* NT-26 and LU-71 are also comparable, both requiring approximately 7 hours for the population size to double, under optimal conditions (Santini *et al*, 2000). *Rhizobium* NT-26 is an aerobic chemolithotroph, whereas *A. faecalis* strain YE56 is a heterotroph, with a doubling time of about 3 hours (Phillips and Taylor, 1976). Compared to other As-oxidizing heterotrophs, LU-71 has a long doubling time; *Burkholderia* and *Alcaligenes* strains analyzed by Sultana *et al* (2012) grew relatively fast (initial doubling times between 1.8 and 1.4 h). The isolation of a soil bacterium from a Northwestern Ontario mine, unlike the other aforementioned species, increases the transferability of the soil bacteria to other regional mine reclamation sites. LU-71 is adapted to the region, while bacteria such as *Rhizobium* NT-26, *A. tumefaciens* 5A, or *Thermus thermophilus HB8*, for example, would not so easily integrate into the climate due to the harsh winters (Kalimuthu *et al*, 2014).

Similar to the well-studied As-oxidizer *A. faecalis*, LU-71 was found to be a heterotoph, with its oxidation processes considered a detoxification mechanism rather than one that supports bacterial growth (Santini *et al*, 2000). *A. tumefaciens* 5A is another organoheterotroph As-oxidizer like *A. faecalis* and LU-71. *Rhizobium* NT-26 and *Pseudomonas arsenitoxidans*, contrastingly, are aerobic chemolithotrophs (Sultana *et al*, 2012; Gihring *et al*, 2001). While it is more common to isolate heterotrophs, bioremediation pursuits often seek lithotrophs for remediation. The preferred isolation of lithotrophs, rather than heterotrophs, for remediation of soil is two fold: (1) the bacteria are expected to stop growing when the pollutants upon which it relies are cleaned up, and (2) due to the gradual elimination of the bacterium from the environment to which it was introduced, the lithotrophs usually do not overwhelm native species (Wilson and Clarke, 1994). One drawback to using lithotrophs for remediation is their slow growing nature. By pairing a heterotrophic rhizobacterium with plant species, the obstacle of slow growth can potentially be overcome. Plant root exudates provide food for the soil bacteria and support a faster rate of growth (Ahmad *et al*, 2008). In addition, bacteria such as LU-71 isolated from within the region, pose less of a threat of being invasive, given their origin. Further study of these concepts is recommended.

Arsenite has been found to be 60 times more toxic than arsenate to microorganisms and plants (Abbas *et al*, 2017). The As-oxidizing bacteria isolated from a regional gold mine demonstrates tolerance to As(III), given the difference observed in toxicity between As(III) and As(V) (see Table 2.2). The conversion efficiency by LU-71 of As(III) to the less toxic As(V) additionally supports its potential use for soil bioremediation. LU-71 continues to oxidize the toxic metal after it reaches its stationary phase, oxidizing 80% of the total As(III) (see *Figure 2.11*). Based on the results of this study, the presence of an inducible As-oxidizing gene, “turned on” in the presence of As(III), is supported. In the non-induced treatment, LU-71 displayed a lag

period of about 18 hours before oxidation begun. The treatment with prior exposure to As(III) allowed the LU-71 culture to rapidly oxidize the As added to the growth media.

In *Agrobacterium tumefaciens* strain 52*,* the fate of As(III) after conversion to As(V) was studied under low phosphate conditions. Approximately 50% of the resulting As(V) was found associated with the periplasm, membrane or cytoplasm of the cells (Wang *et al*, 2015). Arsenic was observed to be associated with proteins and polar lipids, but not nucleic acids or sugars. *A. tumefaciens* shares characteristics such as Gram-negative, rod-shaped, and the production of extracellular polysaccharides in common with LU-71 (Subramoni *et al*, 2014). Additional studies are required to determine where the remaining As(V) is found in *A. tumefaciens* cells or surrounding environment, and whether similar processes are occurring in LU-71. Continued experiments to trace the movement of As and its speciation within LU-71 cells are recommended. This will determine the availability of As to the rhizosphere and deduce if there is any As(III) or As(V) being excreted.

2.6 Conclusion

Enhancing soil functions by promoting As-detoxifying bacteria may improve the success of direct revegetation in mine tailings. Many areas within Northwestern Ontario that have been mined represent anthropogenically extreme environments; bacteria isolated from these environments have adaptive mechanisms to support their growth, making them key species to re-introduce for remediation. In many parts of the world, surface stabilization of mine soils through revegetation is legally required after mining activities; As-oxidizing soil bacteria like LU-71 can offer solutions for soils where contamination is too high for revegetation to be successful.

3. The Effect of LU-71 (An Arsenite Oxidizing *Caballeronia* Bacterium) on the Germination and Growth of *Trifolium pratense*

3.1 Abstract

Continued understanding and advancements in the knowledge of the interaction between plants and rhizosphere bacteria unearths a novel approach to remediation. The combination of an arsenite-oxidizing soil bacterium with a fast-growing, biomass-producing ground cover species such as *Trifolium pratense* has been found to improve the success of germination and growth under controlled laboratory conditions. *T. pratense, Festuca rubra,* and *Medicago sativa* seeds were germinated on Hoagland's Nutrient Agar plates in a growth chamber with constant temperature of 20°C and a 12-hour photoperiod. All seeds were surface sterilized and half of the seeds were inoculated with the arsenite-oxidizing bacteria (LU-71); 100 µL of 1.0 x 10^9 CFU/mL was added to each seed. Mean average germination rates across all species increased by 61% with LU-71-inoculation at 0.6 mM arsenite. Total biomass production in *T. pratense* seedlings after 45 days of growth increased by 43% on average from 0.05-0.45 mM arsenite. The development of a Rifampicin-resistant LU-71 mutant (LU-71R) allowed for the analysis of the soil bacteria with and without association with *T. pratense.* The presence of *T. pratense* significantly increased LU-71R bacterial density by 42% in untreated test sand (One-way ANOVA; $p = 0.002$). This mutualistic interaction between LU-71R and *T. pratense* offers insight into the effectiveness of a combined bio-phytoremediation approach in the rehabilitation of contaminated soils.

Keywords: Arsenic, Phytoremediation, Rhizosphere, *Trifolium pratense*, *Caballeronia*

3.2 Introduction

Employing plants to remove or reduce the toxicity of hazardous substances in the environment is referred to as phytoremediation (Weis and Weis, 2004). Phytoremediation strategies include contaminant containment, known as phytostabilization, contaminant removal (phytoextraction), contaminant degradation (phytodegradation), and the removal of contaminants through the metabolic capabilities of plants into volatile compounds (phytovolatization) (Jomjun *et al*, 2011). All these processes are widely used and promoted for their low-cost implementation.

Select rhizospheric bacteria are able to convert arsenic (As) to species with different solubility, mobility, and toxicity, thus playing an important role in the biochemical cycle of the ubiquitous contaminant (Srivastava *et al*, 2013b). However, alone, the application of bioremediation in open mine sites is limited. Root exudates released in the rhizosphere by plants are integral energy sources for the cohabiting microorganisms (Ahmad *et al*, 2008). Plant-assisted bioremediation holds promise for in situ remediation of non-point source contamination. There are two main benefits of using detoxifying bacteria in combination with phytoremediating plants. First, the plant roots can provide nutrients and a suitable environment for the detoxifying bacteria to grow. This partnership will optimize the bacteria's ability to convert the toxic contaminants to their low toxicity species. Secondly, by lowering the toxicity of the contaminants, the bacteria help the plants to grow, leading to overall greater revegetation success.

Some species of soil bacteria interact with plant roots more than others. Moreover, some species have adapted evolutionary attributes such as plant growth promoting (PGP) characteristics that make them more attractive to combined bioremediation-phytoremediation efforts (Mesa *et al*, 2017). Plant growth-promoting rhizobacteria (PGPR) are bacteria that associate with plant roots and improve the growth of plants (Wang *et al*, 2011). This is

achieved through the increase of nutrient uptake and/or production of plant growth hormones and/or macronutrients such as phytohormone synthesis, ACC deaminase, phosphate solubilization, siderophore production, nitrogen fixation, and xenobiotic activity. Given the ubiquitous nature of As in soil, it is also common for bacteria to develop resistance and detoxification mechanisms in order to persist in these environments. Mechanisms include As oxidation, reduction, resistance, methylation, and volatilization (Li *et al*, 2014; Mukhopadhyay *et al*, 2002; Tripathi *et al*, 2007; Yan *et al,* 2019). Conversion of As between its inorganic forms (arsenite and arsenate) and organic forms (monomethylarsonic acid, dimethylarsinic acid, trimethylarsine, arsenobetaine, and arsenocholine) allows bacteria to alter the level of toxicity of the metalloid (Panda *et al*, 2010; Sarkar and Paul, 2016).

When exposed to elevated levels of As, normal growth and development of plants is hampered. Toxicity symptoms include inhibition of germination; a decrease in plant height; reduced root and shoot growth; wilting and necrosis of leaves; reduced leaf area and photosynthesis; reduced yield; and in some cases, plant death (Abedin and Meharg, 2002; Carbonell-Barrachina et al, 1995; Cox et al, 1996; Knauer et al, 1999; Mahdieh et al, 2011; Marin et al, 1993; Odanaka et al, 1987). Arsenic toxicity and sensitivity in plants is not only a direct effect of the concentration and speciation, but also the biological life stage. Germination and early seedling growth can indicate As tolerance at later stages of plant life (Mahdieh *et al*, 2011; Srivastava *et al*, 2013a). Specific plant metabolites involved in defense pathways such as nonprotein thiols, cysteine, glutathione, and phytochelatins have yet to establish during germination and early development; hence, As is more toxic to plants at these stages (Dixit *et al*, 2016).

Plant As absorption mechanisms are not yet fully understood and depend on a variety of environmental factors. The concentration gradient between soil and plant promotes the uptake

of arsenite (As(III)) through the roots, while arsenate (As(V)) is readily absorbed by the PHT1 family of phosphate transporters (Daiane de Souza *et al*, 2018; Rahman and Hasegawa, 2011; Coelho *et al*, 2020; Cao *et al*, 2017). Nodulin-26-like intrinsic proteins (NIPs) transport As(III) bi-directionally through plant cells. Once the As(III) enters the cells, it reacts with sulfhydryl groups of cellular proteins to inhibit enzymatic processes and biochemical reactions (Mesa et al, 2017, Coelho *et al,* 2020). The phosphate analog, As(V), interferes with oxidative phosphorylation and ATP synthesis (Abbas *et al*, 2018; Mesa *et al*, 2017). Both As(III) and As(V) accumulation leads to the overproduction of reaction oxygen species (ROS), causing oxidative stress within the affected plants (Farooq *et al*, 2016; Coelho *et al*, 2020). Damage to proteins, DNA and lipids resulting from the oxidative stress translates to impaired cellular functions and the phenotypic characteristics listed above (Campos *et al*, 2019).

A previously isolated soil bacteria native to Northwestern Ontario, LU-71, oxidizes As(III) to As(V) – reducing the toxicity of As by about 25 times to the bacteria (See Chapter 2). With oxidation efficiency of 80%, the isolate demonstrates promise in remediation settings. LU-71 is classified within the *Caballeronia* genus, a recent division from *Burkholderia* (Dobritsa *et al*, 2017). Some *Burkholderia* species have been known to demonstrate characteristics such as nitrogen fixation, phytohormone synthesis, plant defence induction and xenobiotic activity (Draghi *et al*, 2014; Suarez-Moreno *et al*, 2012). Past studies showed that LU-71 is a potential biofilm former, suggesting its potential to inhabit the surfaces of plant roots (see Chapter 2, *Section 2.4.3*). Further study of its interaction with plant roots will help understand its viability in open mine site applications.

With a long history of use in revegetation applications, *Trifolium pratense* (red clover), *Festuca rubra* (red fescue), and *Medicago sativa* (alfalfa) were selected for use in this study. *T. pratense* and *F. rubra* are part of a standard Ministry of Transportation of Ontario road mixture,

were used in seed mixtures for Sudbury's Land Reclamation Program, and have both been widely studied in phytoremediation applications (Davin *et al*, 2019; Fan *et al*, 2020; Hossner and Hons, 1992; Lautenbach, 1985; OPSS, 2014). Alfafa, red clover, and red fescue are also listed as Ontario Ministry of Agriculture, Food and Rural Affairs-approved cover crops (2020). Studies by Ndubueze *et al* (2018) and Entz *et al* (2001) also demonstrate the use of alfalfa in Ontario remediation projects.

To the best of our knowledge, the interaction between As-oxidizing soil bacteria and plants for use in remediation settings has yet to be studied. One study by Das *et al* (2016) looked at an As(III)-oxidizing bacteria exhibiting plant growth promoting traits; its effectiveness at mitigating arsenic toxicity and uptake in rice paddies was assessed. This agricultural application is less concerned with reducing the overall As in the environment, and more intent on limiting As taken up by the rice crop. The study detailed in this chapter aims to address these gaps in knowledge by analyzing As-oxidizing bacteria in partnership with plants as systems that reduce the toxicity of As in contaminated soil. The objectives of this study were to assess the difference in As(III) and As(V) toxicity to the germination of *T. pratense*, *F. rubra*, and *M. sativa* and observe any change to that relationship with inoculation by LU-71 (the As(III)-oxidizing bacteria). Secondly, effects of As(III) on entire plant growth of *T. pratense* was observed with and without inoculation of the As(III)-oxidizing bacteria. The impact of plant growth on LU-71 bacterial density in the soil was also analyzed to interpret whether the relationship between plant and soil bacteria was mutually beneficial.

3.3 Materials and Methods

3.3.1 Media Preparation

Tryptic Soy Broth and Agar (TSB and TSA), Minimal Salt Media (MSM) and Minimal Salt Media with glucose (MSMG), and the Phosphate Buffer Solution (PBS) were prepared as described in Chapter 2, *Section 2.3.2*, and autoclaved before use.

3.3.1.1 Hoagland's Agar

Hoagland Nutrient Media was prepared by adding 1.6 g of Hoagland's No. 2 Basal Salt Mixture (115.03 mg/L ammonium phosphate monobasic, 2.86 mg/L boric acid, 656.4 mg/L calcium nitrate, 0.08 mg/L cupric sulfate • $5H_2O$, 5.32 mg/L ferric tartrate • $2H_2O$, 240.76 mg/L magnesium sulfate, 1.81 mg/L manganese chloride • $4H_2O$, 0.016 mg/L molybdenum trioxide, 606.6 mg/L potassium nitrate, 0.22 mg/L zinc sulfate • $7H_2O$) to 1 L of deionized DDW (Sigma-Aldrich Canada Co, Oakville, ON, Canada). Agar (1.5%, w/v) was added before autoclaving (BD Difco Nutrient Agar 1.5%, Franklin Lakes, NJ, USA).

3.3.1.2 Lysogeny Broth (LB) Growth Medium

Lysogeny Broth (LB) growth medium was prepared by adding 25 g of Miller's Lysogeny Broth Powder (10 g peptone 140, 5 g yeast extract, 5 g sodium chloride; Fisher Scientific, Ottawa, ON, Canada) to 1 L of DDW. The broth was autoclaved before use.

3.3.2 Fractionation of As(III) and As(V) and ICP-AES Analysis

The APDC protocol as described in Chapter 2, *Section 2.3.5*, was used to fractionate As(III) and As(V) in the samples. The final samples were analyzed using ICP-AES carried out by the Lakehead University Instrument Lab (LUIL).

3.3.2.1 Inductively Coupled Plasma Atomic Electron Spectroscopy (ICP-AES) Analysis

Inductively coupled plasma atomic electron spectroscopy analysis was carried out by the LUIL, as described in Chapter 2, *Section 2.3.6*. A standard operating procedure from the LUIL is included in Appendix B.

3.3.3 Plant Growth-Promoting (PGP) Characteristics

3.3.5.1 Siderophore Production

All glassware was cleaned prior to the commencement of this experiment with 6M HCl to remove trace elements and rinsed with double distilled H_2O. Minimal media 9 (MM9) stock salt solution was prepared by dissolving 15 g KH_2PO_4, 25 g NaCl, and 50 g NH_4Cl in 500 mL of DDW. To 750 mL of DDW, 100 mL of MM9 stock salt solution was added. To this mixture, 32.24 g of piperazine-N,N'-bis(2ethanesulfonic acid) (PIPES) was dissolved at pH 6 while stirring, and adjusted to a final pH of 6.8 using NaOH. Fifteen g of Bacto agar was then added and the solution was autoclaved and cooled to 50°C. Once cooled, 30 mL of filter sterilized (0.2 µm) Casamino acid solution (3 g of Casamino acid in 27 mL of DDW, extracted with 3% 8-hydroxyquinoline in chloroform) and filter sterilized (0.2 µm) 20% glucose solution was added to the MM9+PIPES mixture. A blue dye was prepared by dissolving 0.06 g of chrome azurol S (CAS) (Fluka Chemicals, Fisher Scientific, Ottawa, ON, Canada) in 50 mL of DDW, and combining it with 9 mL of 0.0027 g $FeCl_3 \cdot 6H_2O$ dissolved in 10 mL of 10 mM HCl. To this blue dye mixture, 0.073 g of hexadecyltrimethylammonium bromide (HDTMA) dissolved in 40 mL of DDW was added, producing a blue solution, autoclaved and stored in a plastic container. To the liquid MM9-Casamino acid agar, 100 mL of the blue CAS dye was slowly added along the glass wall while agitating to thoroughly mix. Plates were then aseptically poured, allowed to set for 24 h, and LU-71 was streaked (Schwyn and Neilands, 1987). A *Pseudomonas aeruginosa* strain was used as a positive control. Siderophore production was confirmed by the appearance of an orange halo (*Figure 3.1*) (Schwyn and Neilands, 1987).

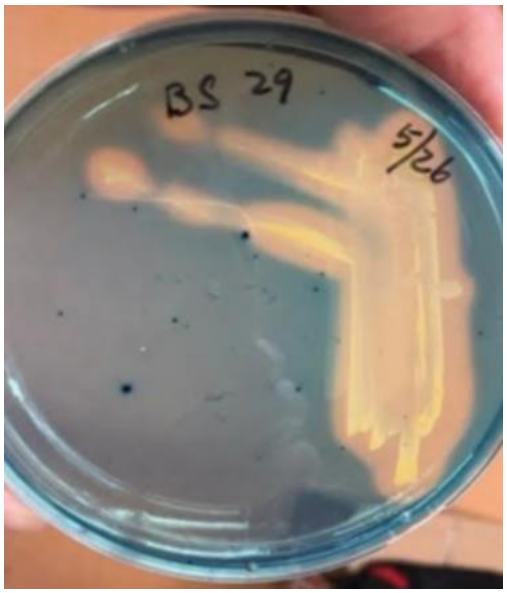

Figure 3.1. An orange halo surrounding the streaked colonies on the CAS agar was an indication of siderophore production.

3.3.5.2 Phosphate Solubilization

Following the protocol by Mehta and Nautiyal (2001), NBRI media was made in one litre of water by combining 10 g glucose, 5 g $Ca_3(PO_4)_2$, 5 g $MgCl_2 \cdot 6H_2O$, 0.25 g $MgSO_4 \cdot 7H_2O$, 0.2 g KCl, 0.1 g $(NH_4)_2SO_4$, and adjusted to pH 7. The broth was autoclaved and poured into flasks. In addition to NBRI broth, agar plates were also made by adding 1.5% (w/v) granulated agar to the NBRI media. LU-71 was grown in 10 mL of sterile TSB broth along with a positive control, *Pseudomonas aeruginosa*. The cultures were incubated at 25°C with 150 rpm shaking until the cultures reached an OD_{600nm} of about 1.0 (about 72 hours). Isolates were then transferred from the TSB to sterile NBRI broth and incubated for two days at 25°C with 150 rpm shaking. LU-71 and the positive control were then streaked on the sterile NBRI plates. Clear halos around the colonies indicated phosphate solubilization.

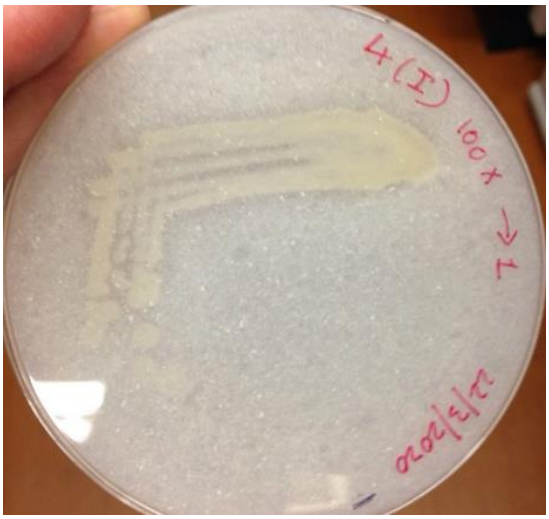

Figure 3.2. Clear halos formed around the positive control, indicating phosphate solubilization.

3.3.5.3 IAA Production

LU-71 was cultured in LB growth medium (Fisher Scientific, Ottawa, ON, Canada) for 10 hours. Following this initial culturing, the bacteria were re-inoculated in three Erlenmeyer flasks containing 10 mL LB supplemented with tryptophan at 0.5 mg/10 mL. Two biological replicates were carried out for this test, so the six flasks were incubated in the dark at 25°C with 110 rpm shaking. After 72 hours, 1.5 mL of the cell suspension was taken out and centrifuged for 10 minutes at 10,000 rpm. From the resulting supernatant, 1 mL was mixed vigorously with 2 mL of Salkowski's reagent (37.50 mL H_2SO_4, 1.88 mL 0.5 M $FeCl_3 \cdot 6H_2O$ and 60.62 mL distilled H_2O) and allowed to stand for 1 hour at room temperature. The absorbance at 530 nm was determined and compared to a IAA calibration curve. IAA production in the cultured medium was indicated by a red-pink colour (Gordon and Weber, 1951; Oller *et al*, 2012).

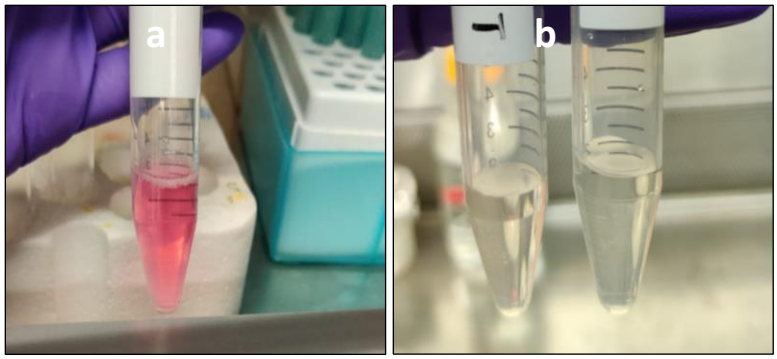

Figure 3.3. IAA production was indicated by a colour change to pink-red (a). Negative samples (b) were colourless.

3.3.4 Minimum Inhibitory Concentrations (MICs) of As(III) and As(V) on the Germination of *T. pratense, F. rubra*, and *M. sativa*

Three test species were selected to measure the difference in toxicity between As(III) and As(V). The As-oxidizing bacteria (LU-71) was added to As(III)-treated seeds to observe any change in As(III) toxicity to seed germination. Following Environment Canada's Biological Test Method (2005), one monocot and two dicots were selected from the recommended species list based on their known use in mine reclamation settings. *Trifolium pratense* L. (red clover), *Festuca rubra* L. (red fescue), and *Medicago sativa* L. (alfalfa) seeds were germinated on Hoagland's agar plates in a growth chamber with constant temperature of 20°C, constant light fluence of 12 mW/cm^2, and a 12-hour photoperiod (Environment Canada, 2007). Plates were randomly arranged, oriented upright and allowed to germinate for 10 days. Six different concentrations each of As(V) and As(III) were tested: 0.3, 0.6, 0.9, 1.2, 1.5, and 2.0 mM. A control of 0 mM was also included.

To prepare the As-spiked Hoagland's agar, stock solutions of sodium arsenite ($NaAsO_2$) and sodium arsenate (Na_2HAsO_4) were prepared and filter sterilized by sterilized 0.2 µm Isopore Membrane polycarbonate filters (Millipore Sigma, Oakville, ON, Canada). Hoagland's agar was prepared according to *Section 3.3.1.1*, divided into 500 mL flasks, and autoclaved. Stock As solution was added to the agar before it solidified (at 50°C) to final concentrations of 0.3, 0.6,

0.9, 1.2, 1.5, and 2.0 mM each of As(III) and As(V). Petri dishes 150 by 15 mm in size (Fisher Scientific, Ottawa, ON, Canada) were labelled and poured in a biosafety cabinet and allowed to set overnight.

Seeds were surface sterilized by immersion in 95% ethanol for 30 seconds, followed by immersion in 25% Clorox bleach for 5 minutes, and finally washing the seeds 7 times in sterile deionized water (Leung *et al*, 1994). All seeds were sourced from Thunder Bay Farm Co-op (Thunder Bay, ON). Using autoclaved forceps, individual seeds were placed in one row along the agar plates for a total of 10 seeds per plate (see *Figure 3.4*). Forceps were sterilized in 70% ethanol between seeds. Plates were sealed shut with parafilm and placed upright in clear containers (without lids) to hold them in the vertical orientation in the growth chamber. Percent germination was recorded daily. After 10 days at 20°C with a 12h photoperiod, final observations and percent germination was recorded. Measurements of hypocotyl and root length were also taken on the 10th day and are included in Appendix E.

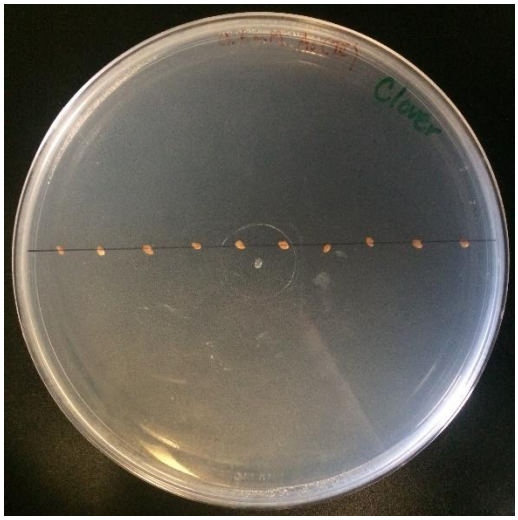

Figure 3.4 Germination experiment arrangement of seeds on Hoagland Nutrient Agar.

3.3.5 Germination of *T. pratense, F. rubra*, and *M. sativa* with LU-71

The procedure above (*Section 3.3.4*) was repeated with the addition of a bacterial suspension of soil bacterium LU-71. At each concentration were two treatments, with and without the As-oxidizing bacteria and five plate replicates of each. Each plate contained 10 seeds. The As-oxidizing bacterium was grown in TSB with 0.1 mM sodium meta-arsenite ($NaAsO_2$) to induce the As(III) oxidation genes in the bacteria. The bacterial culture was grown at 25°C for 30 hours with 150 rpm shaking. The culture was harvested at about OD of 0.92, washed three times with sterile PBS and finally suspended to a concentration of 1.0×10^9 cells/mL in sterile DDW. One hundred µL of the bacterial suspension was added to each seed before the plates were wrapped with parafilm and moved to the growth chamber. Negative controls without bacterial inoculum were treated with 100 µL of sterile DDW for each seed. The seeds were left for 10 days in the growth chamber.

3.3.6 Development of a Rifampicin-Resistant LU-71 Mutant (LU-71R)

A Rifampicin-resistant LU-71 mutant (LU-71R) was developed to determine the growth or survival of LU-71R in soil, independent of any other bacteria that may have established in the soil samples. A sterile 5% or 50,000 ppm (w:v ratio) Rifampicin (Rif) stock solution was prepared by combining 0.1 g of Rif (Sigma-Aldrich Canada Co, Oakville, ON, Canada) with 2 mL of 100% ethanol in a sterile 15 mL centrifuge tube. The solution was vortexed and sonicated to fully dissolve the Rif in ethanol. Tryptic soy agar (TSA) was prepared according to *Section 3.3.1*. While the sterile liquefied TSA was maintained at 50°C, 0.5 mL of the stock Rif solution was added to 500 mL of TSA to achieve a 50 ppm Rif concentration. The TSA+Rif was then poured into petri dishes. Once the agar had set, 100 µL of LU-71 cultured in TSB at 25°C to about OD 1 with 150 rpm shaking was spread plated onto the Rif TSA plates. After 2 days of growth at 25°C, LU-71 Rif-resistant colonies were streaked on new TSA+Rif plates to purify the LU-71 Rif mutant (LU-71R).

The As(III) oxidation ability of the LU-71R isolates was determined by comparing to that of the LU-71 wildtype. A loopful each of LU-71 and LU-71R were transferred separately to 250 mL flasks of TSB + 0.1 mM As(III). The isolates were grown for 36 hours at 25°C with 150 rpm shaking. Both the Rif-resistant As-oxidizing LU-71 (LU-71R) and the LU-71 wildtype were prepared for As fractionation and ICP-AES analysis using the protocol outlined in *Section 3.3.2*. Frozen cultures of LU-71R were prepared by mixing 1:1 with sterile 50% glycerol and stored at -80°C. Samples were preserved in replicates of ten and labelled with date and strain.

3.3.7 *T. pratense* Growth Experimental Design

Growth of one of the three test species, *T. pratense*, was investigated through an experiment set up with six levels of As(III) concentration (0, 0.05, 0.08, 0.15, 0.25, and 0.45 mM), two inoculant treatments (with and without LU-71R) and three replications for each treatment. All plants were grown in 1 L clear plastic food containers with lids. The containers and lids were disinfected with 70% ethanol prior to use. The growth substrate was a fine sand (CIL Play Sand, Rivière-du-Loup, QC, Canada), as per recommendations outlined in Environment Canada's Biological Test Method protocol (2007). The sand was moistened and autoclaved for 3 hours, twice at a 24-hour interval, and allowed to dry completely in a Biosafety cabinet before being added to the 1 L containers, 500 g per pot.

3.3.7.1 Growth of T. pratense Without LU-71R

On day 0, 50 mL of sterile Hoagland's Nutrient Solution (Sigma-Aldrich Canada Co, Oakville, ON, Canada) was added to each container and combined with the test soil using an autoclaved utensil. Seeds were surface sterilized using the protocol outlined in *Section 3.3.3*. Seeds were then soaked in sterile deionized DDW for 2 hours and added to the sterile sand using autoclaved forceps. Approximately 25 seeds were added to each container. Seeds were left to germinate in the prepared 1 L containers for 3 days. For the first 24 h, all treatments were placed in a dark

growth chamber at constant temperature of 20°C. After 24 h, seeds were exposed to 12 mW/cm^2 light intensity for a 12 h photoperiod, at 20°C. On day 3, sodium arsenite ($NaAsO_2$) was dissolved in 25 mL of DDW and filter sterilized (0.2 µm) before application to the pots. Sodium arsenite was added to the containers to reach final concentrations of 0, 0.05, 0.08, 0.15, 0.25, and 0.45 mM (3 replications of each), and *T. pratense* seedlings were thinned to 10 plants per pot. On day 15 and 30, 5 mL of sterile Hoagland's Nutrient Solution was added to each container.

3.3.7.2 Growth of T. pratense With LU-71R

The protocol for the growth of *T. pratense* seedlings without LU-71R was followed with a few minor adjustments to add in the As-oxidizing bacteria treatments. The mutant, LU-71R strain was used (*Section 3.3.6*). Each As treatment was repeated with the addition of the bacterial-71R, and there were three replicates at each concentration. Determinations of the LD_{50} for each species were assessed by analyzing the resulting graphs: the x-axis intercept of the slope of the curve at 50% germination (y-axis) was considered the concentration at which half of the seeds survived.

3.3.7.2.1 LU-71R-Treated Seeds

The Rifampicin-resistant LU-71 mutant (LU-71R) was grown on TSA at 25°C for 2 days before being cultured in TSB at 25°C with 125 rpm shaking. After 36 h, the LU-71R culture was washed 3 times in sterile DDW and resuspended to a final density of 1.8×10^9. *T. pratense* seeds were surface sterilized following the method in *Section 3.3.4* and then allowed to soak in the concentrated LU-71R cell suspension for 2 h. Seeds for the non-LU-71R treatment were submerged in sterile deionized DDW after surface sterilization for 2 h to standardize the water imbibition across all treatments.

3.3.7.2.2 Inoculation of Growth Substrate with LU-71R

At Day 0, 50 mL of LU-71R suspended in sterile Hoagland's Nutrient Solution was added to each container and combined with the sand using a sterile utensil. The bacterial suspension had final

density of 1.8 x 10^9 CFU/mL. At Day 15 and Day 30, test soil was additionally augmented with LU-71R. One litre of LU-71R was grown to $OD_{600\eta m}$ 0.871, washed and resuspended in 100 mL (concentrated 10X) of sterile Hoagland's Nutrient Solution for a final cell density of about 5.0 x 10^9 CFU/mL. Half a mL of the bacterial suspension + Hoagland's Nutrient Solution was added to the base of each seedling, for a total of 5 mL per pot. At Day 30, a repeat addition of 0.5 mL of LU-71R concentrated to approximately 5.0 x 10^9 CFU/mL and suspended in Hoagland's Nutrient Solution was added to each seed.

3.3.7.3 Dry Weight of T. pratense

The experiment was run for a total of 45 days. On Day 45, the plants were extracted from the test sand and dried at 75°C for 24-48 hours. Dried weights were determined using an Ohaus analytical scale (M & L Testing Inc, Dundas, Ontario). Measurements were recorded for root and shoot of each individual plant and the average yield per plant of each pot was calculated. Plants that did not grow beyond the phase of cotyledon leaves were considered as no growth with a yield of 0.

3.3.8 Viability of LU-71R in Sand With and Without Plants

After all plant matter was removed from the growth substrate, the sand was collected and mixed in a Ziploc bag. From each replicate, 1 g of sand was sampled and a 10X dilution series (from 10^{-1} to 10^{-8} dilutions) was made. A drop-plating assay was performed on the dilution series using sterile TSA plates containing 50 ppm Rifampicin (*Section 3.3.6*). Five 5-µl drops from each dilution were administered to the TSA-Rif plate. The plates were incubated at 25°C and the number of colonies was counted after 1 day and recounted day 2 and 3 for confirmation.

3.3.9 Moisture Content of Growth Substrate

The moisture content of the test sand was measured by placing a 3-5 g subsample into a pre-weighed aluminium weighing pan. Initial wet weight of the sand was recorded and then placed

in a drying oven at 105°C for 24 hours. The dry weight of each subsample was then measured and recorded. Soil moisture content was calculated as follows:

$$\text{Moisture content (\%)} = \frac{(\text{wet weight (g)} - \text{dry weight (g)}) \times 100}{\text{dry weight (g)}}$$

3.3.10 Statistical Analysis

All statistical analyses were conducted using SigmaPlot 12 Software integrated with SigmaStat (Systat Software Inc, 2020) and SigmaPlot 14.0. One-way analyses of variance (ANOVAs) were used to assess differences in the mean values among treatments for germination, plant yield, and soil CFU experiments. Shapiro-Wilk normality and Brown-Forsythe equal variance tests were used; when data failed to pass one of these tests, an ANOVA on ranks was conducted. Post hoc Tukey tests were applied as a follow-up to ANOVAs to compare differences between individual samples within the groups. Statistical significance was considered at $p \leq 0.05$, unless otherwise stated.

3.4 Results

3.4.1 PGP Characteristics

LU-71 was found to be able to secrete siderophores but was unable to produce IAA or solubilize phosphate. Siderophore production was observed by the formation of an orange halo surrounding the bacterial colonies. Phosphate solubilization was indicated by a clear halo appearing around colonies; for LU-71 no halo was observed (see *Figure 3.5*). IAA production was indicated by a pink-red coloration not found in LU-71 samples, indicating no IAA production.

Table 3.1. Screening of plant growth-promoting traits in As-oxidizing bacteria LU-71.

PGP Characteristic	*LU-71*
Phosphate solubilization	-
Siderophore production	+
IAA production	-

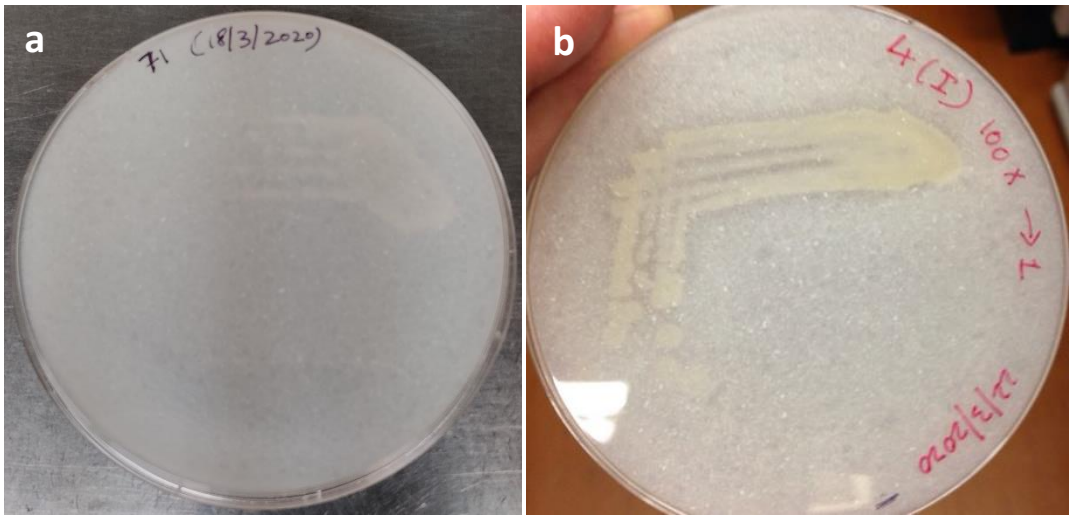

Figure 3.5. No halos were observed around the LU-71 colonies (a), while clear halos formed around the positive control that solubilized phosphate (b).

3.4.2 As(III) vs As(V) Toxicity to T. pratense, F. rubra, and M. Sativa

Significant difference was observed between As(III) and As(V) toxicity to seeds of three different plant species, *T. pratense*, *F. rubra*, and *M. sativa* (One-way ANOVA: p = 0.002, p = 0.036, and p = 0.002, respectively). Commonality was found amongst the trends for the three plant species. For *T. pratense* seeds, the LD_{50} of As(III) to seeds was 0.2 mM, while that of As(V) was 2.2 mM. Significant difference in *T. pratense* percent germination under As(III) and As(V) stress was observed (Tukey Test, p = 0.002). Mean percent germination over control (0 mM As) decreased substantially with increasing concentration of As(III) (*Figure 3.6*). Germination decreased by 49, 54, 83, and 100% at 0.1, 0.2, 0.3, and 0.6 mM As(III); whereas for As(V), decrease in percent *T. pratense* germination was 9, 22, 27, and 34 at 0.1, 0.2, 0.3, and 0.6 mM, respectively.

For *F. rubra* seeds, the LD_{50} of As(III) was 0.25 mM, and 2.5 mM for As(V). The difference in percent germination under As(III) and As(V) stress was found to be statistically significant (Tukey Test, p = 0.037). The decrease in mean germination for As(V) was less pronounced than the decrease observed in As(III)-treated seeds. Percent germination

decreased by 12, 30, 89, and 98% at 0.1, 0.2, 0.3, and 0.6 mM As(III), respectively. A decrease of 3, 3, 27, and 23% at 0.1, 0.2, 0.3, and 0.6 mM As(V), respectively, was observed in contrast. The decrease observed in percent germination correlated with increasing As concentration for *F. rubra* was similar to the trends observed in *T. pratense*.

For *M. sativa* seeds, LD_{50} for As(III) and As(V) were 0.2 and 2.2 mM, respectively, and As(V) and As(III) toxicity to seeds was statistically significant (Tukey Test, p = 0.003). Mean percent germination over control decreased by 22, 66, 98, and 100% at As(III) concentrations of 0.1, 0.2, 0.3, and 0.6 mM. Under As(V) stress, germination decreased from 3 to 12% from 0.1 to 0.6 mM As(V). Similar trends across the species were evident, with decreases in percent germination being less severe under As(V) stress than under As(III) stress in all species. For all species except *F. rubra*, no germination was observed when exposed to 0.6 mM As(III). For *F. rubra* seeds only 2% germination occurred at 0.6 mM As(III).

3.4.3 Germination of T. pratense, F. rubra, and M. Sativa with LU-71 Under As Stress

Percent germination of *T. pratense*, *F. rubra*, and *M. sativa* under As stress showed similar trends across all species. No significant difference was observed between As(V) treated *T. pratense* germination and As(III)+LU-71-treated *T. pratense* germination (Tukey Test, p = 0.350). A Rank Sum Test (Mann-Whitney) between *T. pratense* seeds grown under As(III) stress and seeds grown under As(III) stress with LU-71 inoculation showed that the LU-71 improved the germination of *T. pratense* significantly (p = 0.030). For *F. rubra* germination, again no significant difference was observed between As(V)-treated seeds and As(III)+LU-71-treated seeds (Dunn's Method, p = 0.981). A one-way ANOVA on ranks was conducted for the *F. rubra* data demonstrating significant increase in percent germination with the addition of LU-71 to As(III)-treated seeds (p = 0.036). The addition of the As-oxidizing bacteria to *M. sativa* seeds under As(III) stress significantly increased the germination rate (Tukey Test, p = 0.025). *M.*

sativa germination was found to have no significant difference between As(V) and As(III)+LU-71-treated seeds (Tukey Test, $p = 0.718$).

The LD_{50} of As(III) was around 0.2 mM for all three species of seeds. With the addition of LU-71 to As(III)-exposed seeds, the LD_{50} increased to approximately 1.2 mM for all species. The new LD_{50} for As(III)-exposed seeds treated with LU-71 is comparable to the LD_{50} of As(V) on *T. pratense*, *F. rubra*, and *M. sativa*, which was observed to be about 2.0 mM (see *Figure 3.6*). No significant difference in As(III)+LU-71-treated seeds was observed between the three species (One-way ANOVA, $p = 0.738$). Seeds exposed to As(III) without LU-71 were found to have significantly less germination success than seeds exposed to As(III) with LU-71, across all three species (One-way ANOVA: *T. pratense*, $p = 0.002$; *F. rubra*, $p = 0.036$; and *M. sativa*, $p = 0.002$). At 0 mM As, prior to data correction for 100% germination in the control treatments, LU-71-treated seeds showed a 2% lower germination rate, on average, than seeds without LU-71 ($p = 0.846$). While no germination occurred in the seeds without LU-71 at 0.6 mM As(III), 61% germination, on average, occurred in LU-71-treated seeds at the same concentration (see *Figure 3.6*). Seeds were considered to have germinated when the radicle protruded from the seed coat by 2 mm. At higher concentrations of As(III) (0.6 and 0.8 mM) phenotypic observations such as chlorosis of cotyledons and stunted growth were recorded.

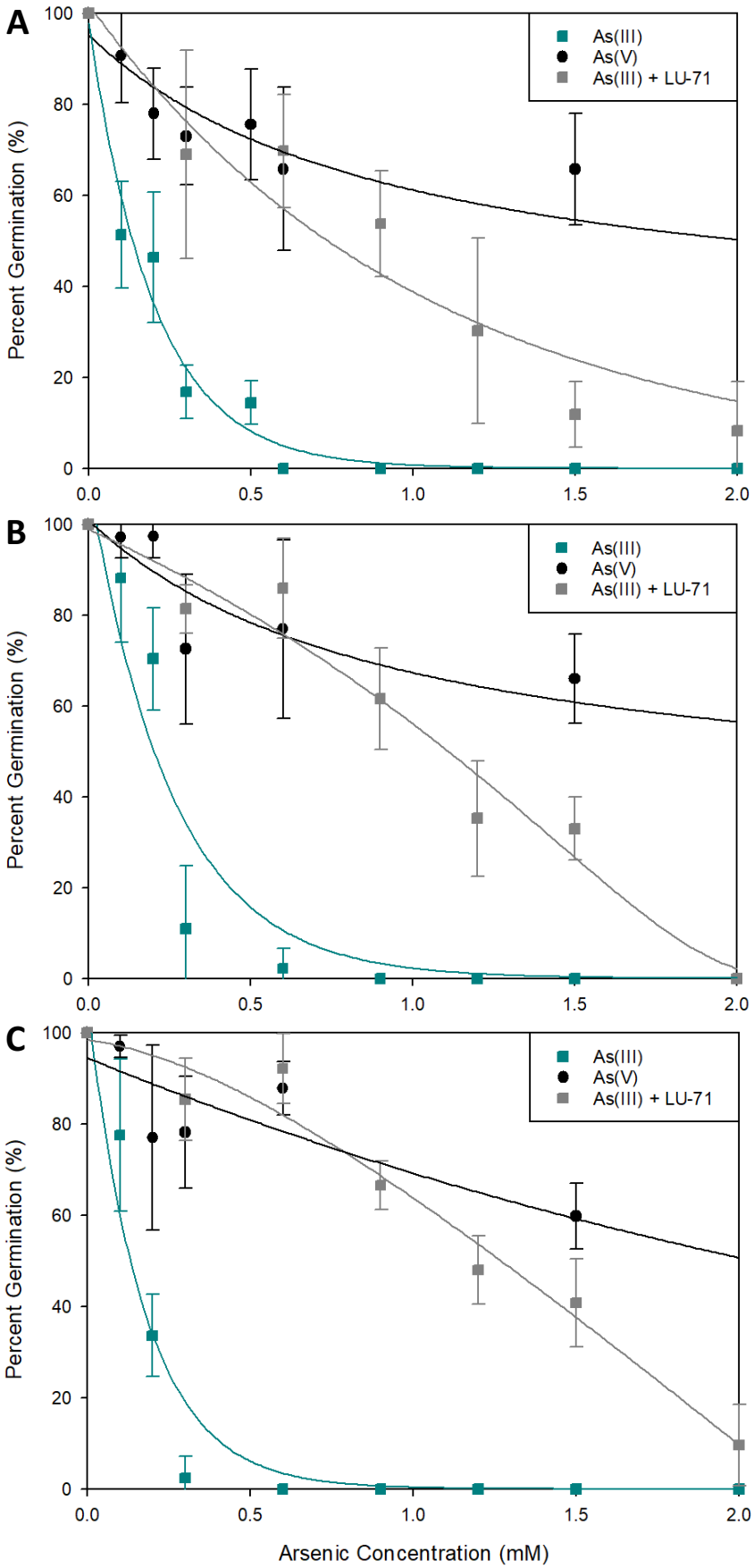

Figure 3.6. Effect of arsenite (As(III)) (green), arsenite+LU-71 (grey), and arsenate (As(III)) (black) on the germination of *T. pratense* (A)*, F. rubra* (B)*,* and *M. sativa* (C).

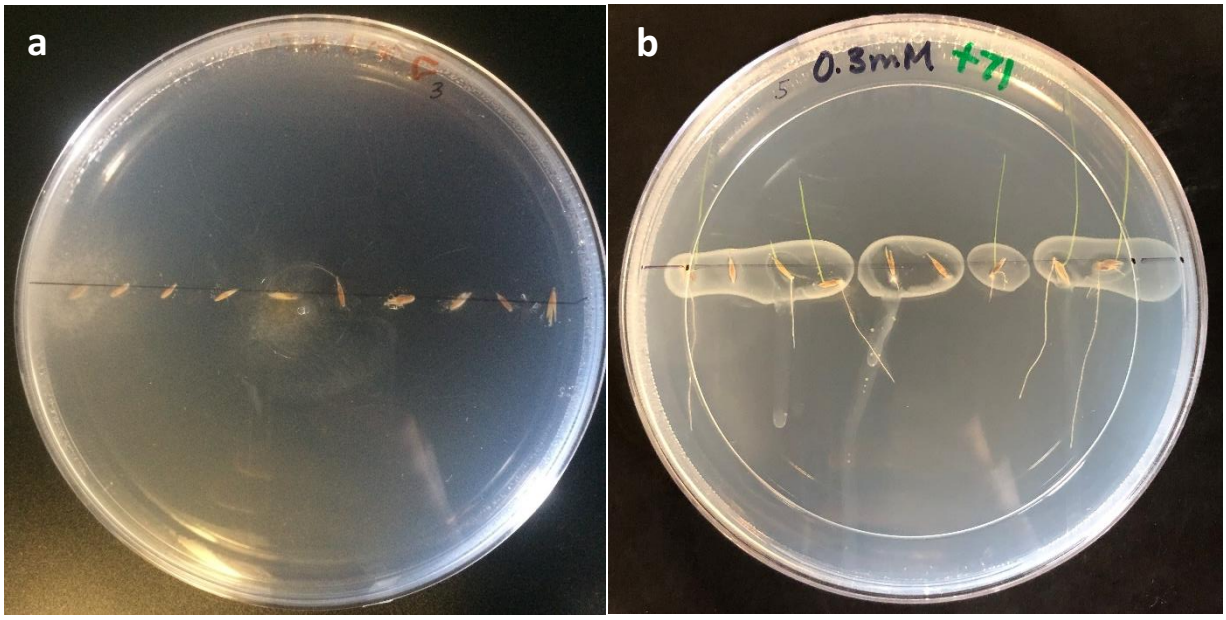

Figure 3.7. Germination of *F. rubra* on Hoagland's Nutrient Agar spiked with 0.3 mM As(III), with (b) and without (a) As-oxidizing LU-71 seed inoculation. At 0.3mM As(III), between 0 and 20% germination occurred and growth was stunted. The addition of the As-oxidizing bacteria increased germination rates by about 70%.

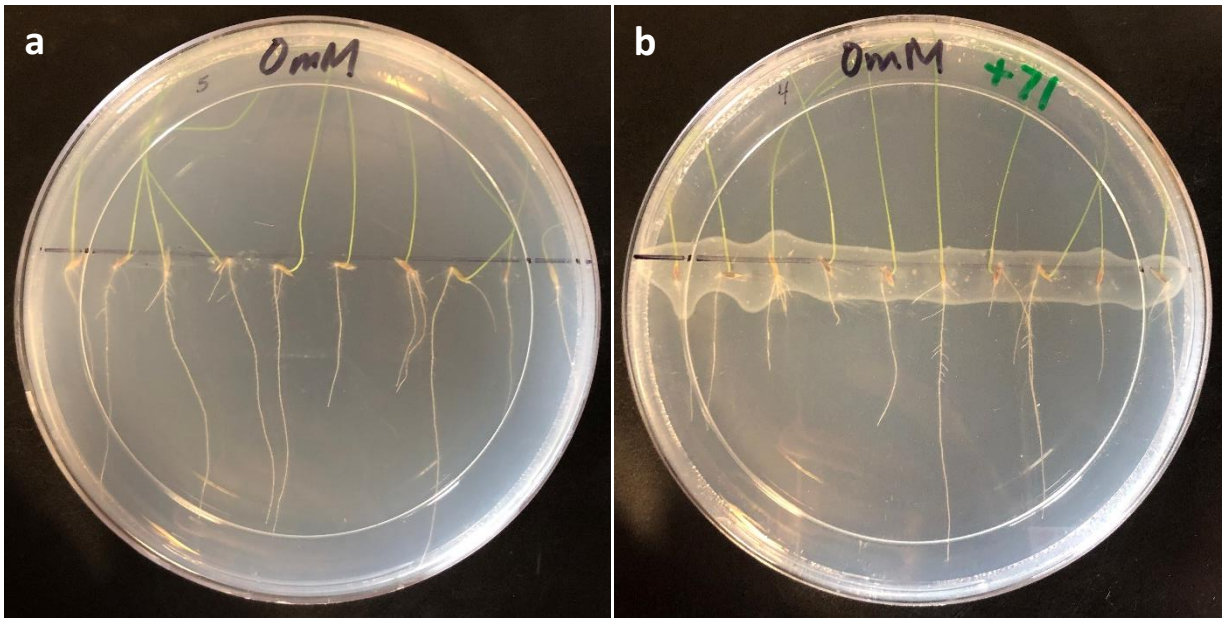

Figure 3.8. Comparison of experimental set-up with (b) and without (a) the As-oxidizing bacteria. 100% germination is observed in the above control plates, with 0 mM As(III), germinated on Hoagland's Nutrient Agar. The cream film observed on the right (b) is the concentrated LU-71 suspension.

3.4.4 Rif-resistant LU-71

To ensure the mutant strain exhibited the same oxidation rates as LU-71, percent conversion of As(III) to As(V) was assessed. The wildtype demonstrated 79.4 ± 8.5% As(III) oxidation and the mutant sample showed 76.4 ± 2.8% oxidation (see *Figure 3.9*). No significant difference was found between LU-71 and LU-71R percent oxidation (T-test, p = 0.665).

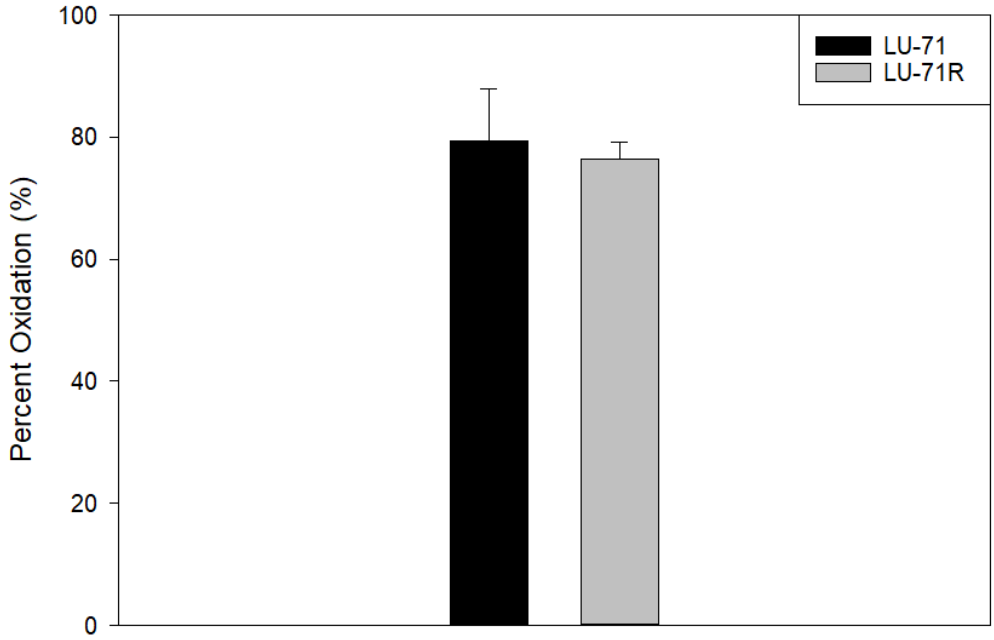

Figure 3.9. Percent oxidation of As(III) to As(V) by the LU-71 wildtype (black) and the LU-71R Rifampicin mutant (grey).

3.4.5 Growth of T. pratense with LU-71R

Significant differences among the mean values of the two different treatments (with and without LU-71R) and across the levels of As toxicity were observed (p < 0.001) (*Figure 3.10*). Growth of *T. pratense* was significantly reduced with the addition of As(III) to the growth substrate; without inoculation, yields at 0.05-0.45 mM As(III) were on average 47% less than the healthy control plants (no As(III) and no LU-71R-inoculation), which had a total average yield of 9.36 mg per plant (One-way ANOVA, p < 0.001). The inoculated treatment at 0 mM As(III) yielded 10.02 mg total dry weight, and was found not to be significantly different from the untreated 0 mM As control plants (p = 0.546). Although inoculation by LU-71R did not increase

plant yield at 0 As(III) significantly, it improved the yields of the As(III)-treated plants at all exposure levels significantly ($p < 0.05$). In addition, the yields of the inoculated plants exposed to 0.05-0.45 mM of As(III) were not significantly different from each other or the control treatment (without exposure to either As(III) and LU-71R) ($p < 0.05$). However, the insignificant loss of yield observed in inoculated seedlings was not consistent across all As concentrations. When compared to the LU-71R inoculated treatment without exposure As(III), the yields at 0.05 and 0.15 mM As(III) were significantly lower. The other three of the five As(III) treatments, 0.08, 0.25 and 0.45 mM, were not significantly lower than the 0 mM treatment (*Figure 3.10).* Moisture content was maintained at 20%, or 0.8 grams of dry soil per 1 gram of wet soil.

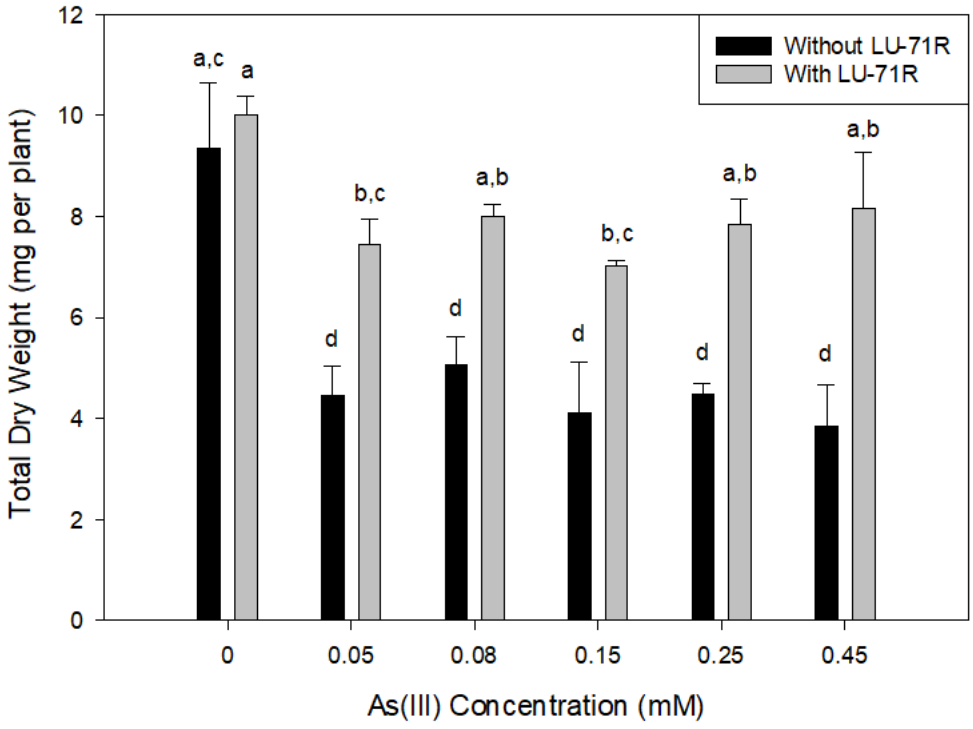

Figure 3.10. Growth of *T. pratense* at five different concentrations of As(III), with and without LU-71R inoculation. Significant differences between treatments are identified with a, b, c, d.

3.4.6 Growth of LU-71R with and without T. pratense

Bacterial densities of LU-71R demonstrated tolerance of As(III) at high concentrations, and a preference for plant-associated growth (*Figure 3.11*). After harvesting plants for dry

weight analysis, the remaining soil was mixed and sampled to provide representation of LU-71R density in the bulk soil. The use of the Rifampicin-resistant mutant ensured only LU-71R was being observed on the TSA-Rifampicin plates. Bacteria grown in soil without *T. pratense* showed significantly reduced cell densities as compared to the bacteria grown in soil with *T. pratense* seedlings (One-way ANOVA, $p = 0.002$). At 0 mM As(III) without *T. pratense*, there was 2.6×10^7 LU-71R CFU per g of dry soil, whereas bacteria grown with plants at the same concentration had CFUs per g of dry soil of 6.2×10^7. As the As(III) concentration increased, a decrease in cell density was observed ($p < 0.05$). At 0.05 and 0.08 mM As(III) bacterial density was not significantly different from the control, while growth of LU-71R colonies at higher As(III) concentrations was significantly reduced (0.15, 0.25, and 0.45 mM; $p = 0.023$, $p = 0.004$, and $p = 0.010$, respectively). The average CFUs per g of dry soil at 0.05, 0.08, 0.15, 0.25 and 0.45 were 4.9, 4.1, 3.1, 2.3, and 2.7×10^7, respectively.

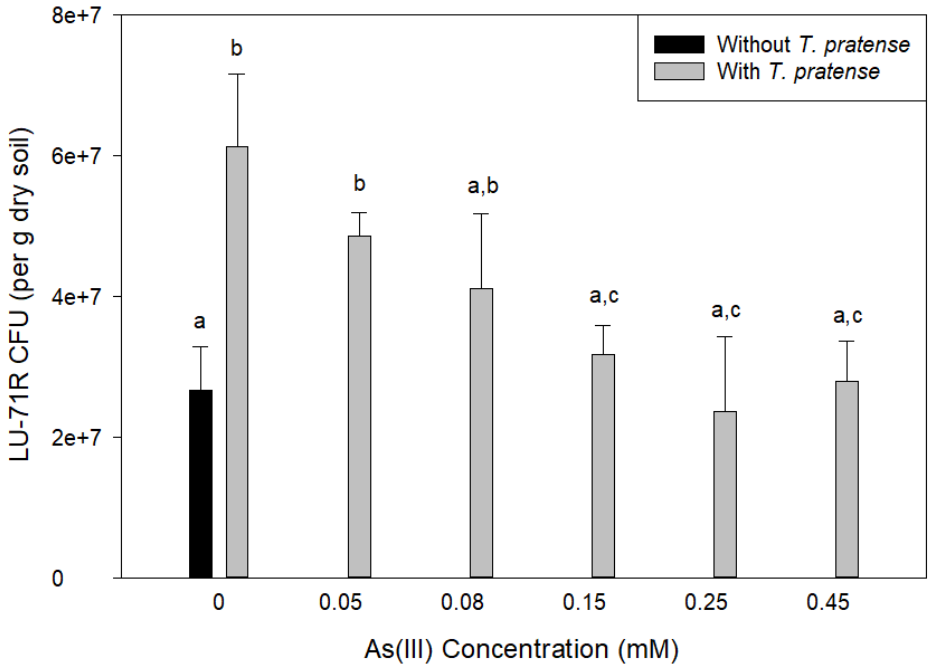

Figure 3.11. LU-71R bacterial colonies per g of dry soil inoculated in sand with and without *T. pratense* seedlings. Bacteria grew significantly better in association with plants ($p = 0.007$). Significant differences between treatments are identified with a, b, c, d. Data was not collected for bacterial growth without *T. pratense* at concentrations 0.05-0.45 mM.

3.5 Discussion

3.5.1 As(III) vs As(V) Toxicity to T. pratense, F. rubra, and M. Sativa

A large discrepancy in acute toxicity was demonstrated by the two inorganic species of As on *T. pratense, F. rubra* and *M. Sativa* germination, supporting the statement by Canada Health Services Drinking Water Quality Guideline (2008): "oxidation of As(III) to As(V) is the preferred method of removing inorganic arsenic [in combination with other treatment technologies], as it ensures that total arsenic is reduced in an efficient manner". Across all species, the LD_{50} of As(III) was observed to be about 11 times less than the concentration of As(V) required to inhibit germination in half the seeds. Similar differences in As(III) vs As(V) toxicity were also observed in mesquite (*Prosopis juliflora x p. velutina*), wheat (*Triticum aestivum*), lettuce (*Lactuca sativa*), Indian mustard (*Brassica juncea* L.), and rice (*Oryza sativa* L.), among others (Abedin and Meharg, 2002; Chaturvedi, 2006; Gusman *et al*, 2013; Liu *et al*, 2005; Mokgalaka-Matlala *et al*, 2008).

The mean percent germination of *T. pratense, F. rubra,* and *M. sativa* decreased significantly ($p < 0.001$) with increasing concentration of As(III) (*Figure 3.6*). This was more prominent with As(III) than As(V) ($p < 0.001$). Germination decreased by 28, 50, 90, and 95% at 0.1, 0.2, 0.3, and 0.6 mM As(III), respectively. The decrease was 5, 16, 25, and 25% at 0.1, 0.2, 0.3, and 0.6 mM, respectively, for As(V). *T. pratense* demonstrated the highest tolerance to As(III) at 0.6 mM, with just under 15% greater germination than *M. sativa* and *F. rubra*, which experienced 0 and 2% germination, respectively, at this concentration. Members of the *Fabaceae* family, such as *T. pratense and M. sativa*, are considered good candidates for phytoremediation in industrial and contaminated soils due to their ability to colonize poor quality soils by fixing nitrogen in association with symbiotic nitrogen fixing bacteria and by other mechanisms not yet fully understood (Davin *et al*, 2019; Hall *et al,* 2011). Based on the

tolerance demonstrated by *T. pratense* to high As(III) concentration, combined with its known use in remediation, *T. pratense* was selected for the study of plant growth and yield under As stress.

Different vegetative response end points including root and shoot length, root and shoot biomass, and total biomass (root and shoot) are generally used to assess metal resistance in plants (Abedin and Meharg, 2002). While not as commonly used, Karataglis (1980) described germination as one of the best indicators for plant development on variable soil types. Germination was found to be a determining factor in the ability of *T. pratense*, *F. rubra*, and *M. sativa* to tolerate As stress. From preliminary germination trials, the decision to separate the germination and plant yield experiments was made. With germination approximately 2.5 times more sensitive to As than plant growth (see *Figures 3.6* and *3.10*), it was important to study both phases as independent events. Implications in mining applications include the recommendation to transplant germinated seedlings in areas of high soil As concentration, or alternatively to provide seeds with a protective seed coat to foster higher rates of germination in these environments.

3.5.2 Germination of T. pratense, F. rubra, and M. Sativa with LU-71 Under As Stress

The addition of the As-oxidizing bacteria, LU-71, altered the observed relationship between As(III) and As(V). Mean percent germination of all three species decreased by only 17% at 0.6 mM with LU-71 inoculation, much less than the 95% decrease observed without LU-71 at 0.6 mM As(III). With the addition of LU-71, the decrease in percent germination from the control became comparable to trends observed in As(V) treated seeds. At 0.6 mM, percent decrease was 17% for As(III)+LU-71 and 23% for As(V) without LU-71. The oxidation capability of LU-71 is hypothesized to be responsible for the increase in germination observed. It is also possible that other PGP traits may contribute to the detoxification effect of LU-71 on *T.*

pratense, F. rubra, and *M. sativa* germination. The average percent germination (uncorrected for 100% germination in the control treatment) for all three species without LU-71 inoculation at 0 mM As(III) is about 86.7%; with LU-71 it's 84.7%. While there is a slight difference observed in the control treatments with and without LU-71, the difference is not significant. Had this difference been significantly higher for the bacterial treatment, the difference may have been attributable to the PGP characteristics of LU-71. Given that the difference at 0 mM As(III) with and without LU-71 is not significant under controlled conditions, the majority of the impact of LU-71 is expected to be due to the conversion of As(III) to As(V) by the bacteria.

The rhizospheric effect is the well-acknowledged concept of the provision of conditions favourable to microorganisms by plant roots (Martin *et al*, 2014). These plant-microbe associations can also be of benefit to the involved plants (Uroz *et al*, 2019). Das *et al* (2016) similarly observed improved seed germination and seedling vigor under As stress in rice with inoculation by an As-oxidizing and tolerant bacterium (32 and 280 mM tolerance for arsenite and arsenate, respectively). *Bacillus flexus* ASO-6, a PGP bacteria isolated from the rhizosphere surrounding *Oryza sativa* roots also significantly improved seed germination and seedling vigor compared to un-inoculated seeds, measured by increases in root biomass, rice straw and grain yield, chlorophyll and carotenoid production (Das *et al*, 2016). Germination of *Oryza sativa* cultivar *cv* TN 11 was increased by 20.6% by the PGP bacteria without any exposure to As, likely as a result of its phosphate solubilization and ACC deaminase and siderophore production (Das *et al*, 2016). In contrast, germination of *T. pratense, F. rubra* and *M. sativa* decreased by 2% with LU-71 inoculation at 0 mM As (prior to corrections for 100% control germination). The decrease was not significant thus indicating a minimal role of PGP activity in LU-71's toxicity reduction, if any. That said, based on the presence of PGP characteristics in other known As-

oxidizing bacteria, it was predicted that LU-71 possessed other PGP characteristics in addition to its As-oxidizing capabilities.

3.5.3 Plant Growth-Promoting Characteristics of LU-71

The As(III)-oxidizing bacterium, LU-71, was found to secrete siderophores into the surrounding environment. Siderophores are secreted by bacteria to solubilize iron from the surrounding soil. Ferric-siderophore complexes, once formed, move by diffusion with eventual return to the cell surface where they are actively transported across the membrane (Beneduzi *et al*, 2012). Plants able to recognize bacterial ferric-siderophore complexes demonstrate enhanced iron uptake, satisfying one of many nutritional requirements in plants (Beneduzi *et al*, 2012). Not only does siderophore production support plant health and function, siderophores are also known to alter metal bioavailability and complexation in soil, resultantly reducing metal toxicity (Kamaludeen and Ramasamy, 2008; Oller *et al*, 2012). It is important to consider that siderophore production by LU-71 was observed under controlled settings. Ahmad *et al* (2008) found that in iron-rich soils siderophore production is not an expressed biochemical trait. In many gold mine soils, iron has been observed in elevated concentrations (Ding *et al*, 2016; Fashola *et al*, 2016). Given this knowledge and the observation of minimal difference between *T. pratense, F. rubra* and *M. sativa* seeds germinated at 0 mM with and without LU-71 inoculation, it can be theorized that most of the benefit to the plant under As stress is a result of As oxidation. IAA production and phosphate solubilization were also tested for in LU-71 but concluded negative results. Additional PGP traits such as ACC deaminase and ethylene production, nitrogen fixation, and xenobiotic activity should be screened for in future experiments to further test this hypothesis and accreditation of As-oxidation as the main benefit to plant germination under As stress.

3.5.4 Growth of T. pratense with LU-71R

Biomass production in the As(III)-treated *T. pratense* was significantly increased with the addition of LU-71R. While the average yield of inoculated *T. pratense* seedlings was not significantly different from the healthy control plants (untreated and unexposed to As(III) seedlings) ($p = 0.546$). At all As(III) concentrations, plant yield increased by 43% in LU-71R-inoculated specimens compared to non-inoculated (*Figure 3.10*). Standard deviation in this experiment was relatively high, as is common in determinations of plant biomass; increasing the number of replicates is one way to mitigate this in future studies (Poorter and Garnier, 1996). As the concentration of As increased in the growth substrate, the distribution of As(III) within the soil was of greater consideration. Application via a spray bottle to the surface of the growth substrate could provide a more evenly distributed toxin application than the pouring of the As solution down the side wall of the container (Environment Canada, 2005). This is proposed as another method by which to decrease the deviation encountered in this experiment. Nevertheless, the results collected provide insight into the feasibility of this combined bioremediation- phytoremediation technique in applied mine soil rehabilitation.

While other studies on the impact of As-oxidizing bacteria on As-stressed plants are limited, a study looking at the effect of *Pseudomonas fluorescens* and pyoverdine on the phytoextraction of cesium by *T. pratense* found that cesium accumulated primarily in plant roots (Hazotte *et al*, 2018). Another study by Dong *et al* (2008) observed improved plant phosphorous nutrition, resulting in better plant growth and enhanced tolerance to As contamination in white clover in symbiosis with arbuscular mycorrhizae. In a study by Das *et al* (2016), *Bacillus flexus* ASO-6-inoculated rice seeds demonstrated 32.2% greater root biomass at 20 mg kg^{-1} As. For comparison, LU-71R-inoculated red clover plants increased root biomass by 49.5% at 0.15 mM or 20 mg kg^{-1} As, and by 45.9% at 0.45 mM or about 60 mg kg^{-1} As (see *Appendix E*). Das *et al* (2016) also found that in addition to the enhancement of plant growth, inoculation by *Bacillus*

flexus ASO-6 significantly decreased As accumulation in straw and grain and concentrated the As accumulation in the roots at all treatment levels. Additional research on As-uptake in *T. pratense* is encouraged to identify the plant's suitability as a phytostabilizer and the potential benefits of LU-71R to this interaction.

T. pratense is a high biomass-producing crop, with known tolerance to high levels of zinc, chromium, copper, nickel and lead, and nitrogen-fixing capabilities, all of which are important attributes for the remediation of mining soils (Jin *et al*, 2013; Mikalajune and Jasulaityte, 2011). Along with applications by Transportation Canada in roadside vegetation mixes, and in agriculture as a ground cover crop, it has also been used as an indicator plant for biological monitoring of metals in polluted soils (Shahbaz *et al*, 2018). Perhaps the most important factor for selecting a species for soil cleaning and remediation is accounting for the characteristics of the site in question (Mikalajune and Jasulaityte, 2011).

3.5.5 Mutualistic relationship between T. pratense and LU-71R

Increased contact between soil and microorganisms, soil aeration, and the release of exudates by plant roots are all factors contributing to the accessibility of food to the microbiota, thus increasing microbial communities and in this case, the effectiveness of these communities at detoxifying soil As for enhanced plant germination and growth (Ouvrard *et al*, 2014; Alagić *et al*, 2015; Davin *et al*, 2019). Root exudates are composed of organic acids, sugars and amino acids. But it is also known that plant roots release a large diversity of secondary plant metabolites into the environment, some of which exhibit surfactant properties (the reduction in surface tension of a liquid). Surfactants possess the ability to place themselves at the interface between a hydrophobic and hydrophilic phase and have been studied in soil remediation washing technologies, as well as for the enhancement of transfer of contaminants towards degrading microorganisms (Kobayashi *et al*, 2012; Von Lau *et al*, 2014). The release of these

saponins has been studied in the *Fabaceae* family, and could provide additional insight into the activities occurring between plant roots and LU-71 (Vincken et al, 2007).

Phytoremediation effectiveness relies on the successful establishment of plants with sufficient shoot and root biomass growth and root activities supportive of a flourishing microbial consortium assisting phytoremediation of the contaminated environment (Wenzel, 2009). In reciprocation, a healthy microbial community surrounding plant roots will benefit the plant through plant growth-promoting activities. That said, in soils with severely impacted nutrient availability resource competition can become a limiting factor for microbial growth and biodegradation (Joner *et al*, 2006). It has been found that plants and microorganisms adapted to toxic pollutant concentrations are less impacted by this resource competition (Belimov *et al*, 2005; Burd *et al*, 2000; Wenzel, 2009).

With respect to LU-71R and *T. pratense*, it was found that the bacteria grow best when in combination with *T. pratense*. Even in association with plants, however, bacterial densities decreased as the concentration of As increased. The highest three As(III) concentrations, 0.15, 0.25, and 0.45 mM, showed significantly lower LU-71R densities than at 0, 0.05, and 0.08 mM ($p < 0.05$). A closer look at the survival of LU-71R at the three highest concentrations finds only minor difference in bacterial density among the As levels. Additional tests extending the experiment to higher As concentrations is recommended to determine the concentration at which LU-71R density is further reduced. *T. pratense* yield at 0.15, 0.25, and 0.45 mM As(III), *Figure 3.10*, does not parallel the decrease in LU-71R densities observed between low and high As. Many soil factors may have influenced this relationship, such as altered pH and nutrient availability in the presence of As (Abbas *et al*, 2018). The decrease in bacterial density at 0.15-0.45 mM but not in plant yield at the same As(III) concentrations may also be an indication that the bacterial densities determined for bulk soil did not accurately depict the rhizosphere

densities of the bacteria; it is predicted that analysis of the soil adhering to plant roots provide a more reliable representation of LU-71R density in the rhizosphere (Bulgarelli *et al*, 2012; Han *et al*, 2020).

3.5.6 Conclusion

The germination rate and growth of *T. pratense* under As stress was significantly improved with the addition of LU-71. Given its isolation from a regional gold mine, the bacterium presents a valuable option in soil rehabilitation settings in Ontario; non-invasive and adapted to the climate, it is much more practical to use LU-71 over alien As-oxidizing species that may not survive in a new environment or can disrupt existing bacterial communities. *T. pratense*, a phytoremediator commonly used in Ontario, is also a good candidate for provincial remediation efforts. The combined effect of *T. pratense* and LU-71 can be an effective method of As remediation in open mine sites, with a 40-50% increase in *T. pratense* biomass production and 70% increase in germination at 0.6 mM As(III). While there is still much more to understand with reference to the way As moves once inside *T. pratense*, the compatibility of the plant with beneficial rhizobacteria is an advancement to the existing literature.

3.5.7 Future Direction

Continued research is recommended to determine As uptake in root and shoot, and speciation of As within dried plant matter. Such conclusions could not be achieved from these experiments as 0.5 g of pulverized plant material is required for digestion and consequent ICP-AES analysis (Costa *et al*, 2016). The total sum dry weight of the ten plants per pot was around 0.1 g from the experiments conducted in this study. Experiments should be repeated with a higher density of plants per pot, or the plants should be left to grow for a longer period of time to produce enough mass for ICP-AES analysis. Further analysis investigating the movement of As throughout the plant would provide valuable insights into the success of these species at

detoxifying the contaminant. There are many different proposed routes a plant may take to store or further detoxify As, including degradation, vacuolar sequestration, extrusion, translocation and volatilization (Verbruggen *et al,* 2009; Mateo *et al,* 2019; Fayiga and Saha, 2016; Pilon-Smits, 2005). Ideally, secondary metabolism and further degradation by the plant would allow for the removal inorganic As from the environment. Vacuolar sequestration and translocation would also be beneficial end points of the phytoremediation component of the proposed bioremediation-phytoremediation technique; translocated As from plant roots to shoots can be followed by harvesting and incineration, whereas sequestration of As within plant root would allow As to be unavailable to the surrounding environment, promoting the growth of more plant species which overtime will return the soil to its natural state.

Additional study of LU-71R populations in the rhizosphere, as opposed to bulk soil, would allow for further interpretation of the data collected in this chapter. Further analysis of the growth of both LU-71R and *T. pratense* in various types of soils is also recommended. Higher clay content in soils provides increased adsorption sites of As compared to sandy soils, and is another factor that should be considered in future studies, and prior to applications in mines (Silva Gonzaga *et al*, 2012; Bergqvist *et al*, 2014).

References

Abbas G, Murtaza B, Bibi I, Shahid M, Niazi NK, Khan MI, Amjad M, Hussain M, and Natasha. 2018. Arsenic uptake, toxicity, detoxification, and speciation in plants: physiological, biochemical, and molecular aspects. *Int J Environ Res Public Health* 15(59). https://doi.org/10.3390/ijerph15010059.

Acosta JA, Arocena JM, Faz A. 2015. Speciation of arsenic in bulk and rhizosphere soils from artisanal cooperative mines in Bolivia. *Chemosphere* 138: 1014-1020.

Ahmad I, Pitchel J, Hayat S. *Plant-Bacteria Interactions*. Wiley-VCH Verlag GmbH & Co. KGaA, Weinheim, 2008.

Alagić S, Maluckov BS, Radojičić VB. 2015. How can plants manage polycyclic aromatic hydrocarbons? May these effects represent a useful tool for an effective soil remediation? A review. *Clean Technol Environ Policy* 17(3): 597-614.

Andres J, Arsène-Ploetze F, Barbe V, Brochier-Armanet C, Cleiss-Arnold J, Coppée J-Y, Dillies M-A, Geist L, Joublin A, Koechler S, Lassalle F, Marchal M, Médigue C, Muller D, Nesme X, Plewniak F, Proux C, Ramírez-Bahena MH, Schenowitz C, Sismeiro O, Vallenet D, Santini JM, Bertin PN. 2013. Life in an arsenic-containing gold mine: Genome and physiology of the autotrophic arsenite-oxidizing Rhizobium sp NT-26. *Genome Biol Evol* 5(5): 943-953.

Ascar L, Ahumada I, Ritcher P. 2008. Influence of redox potential (Eh) on the availability of arsenic species in soils and soils amended with biosolid. *Chemosphere* 72(1): 1548-1552.

Basta N, McGowen S. 2004. Evaluation of chemical immobilization treatments for reducing heavy metal transport in a smelter-contaminated soil. *Environ Pollut* 127: 73-82.

Begum MC, Islam MS; Islam M, Amin R; Parvez MS, Kabir AH. 2016. Biochemical and molecular responses underlying differential arsenic tolerance in rice (*Oryza sativa* L.). *Plant Physiol Biochem* 104: 266-277.

Belimov AA, Hontzeas N, Safronova VI, Demchinskaya SV, Piluzza G, Bullitta S, et al. 2005. Cadmium-tolerant plant growth-promoting bacteria associated with roots of Indian mustard (*Brassica juncea* L Czem). Soil Biol Biochem 37: 241-250.

Belval Challan S, Garnier F, Michel C, Chautard S, Breeze D, Garrido F. 2009. Enhancing pozzolana colonization by As(III)-oxidizing bacteria for bioremediation purposes. *Appl Microbiol Biot* 84(3): 565-573.

Beneduzi A, Ambrosini A, Passaglia LMP. 2012. Plant growth-promoting rhizobacteria (PGPR): Their potential as antagonists and biocontrol agents. *Genet Mol Biol* 35(4 Suppl): 1044-1051.

Bergqvist C, Herbert R, Persson I, Greger M. 2014. Plants influence on arsenic availability and speciation in the rhizosphere, roots and shoots of three different vegetables. *Environ Pollut* 184: 540-546.

Bogino PC, Olivia M, Sorroche FG, Giordano W. 2013. The role of bacterial biofilms and surface components in plant-bacterial associations. *Int J Mol Sci* 14(8): 15838-15859.

Brown S, Chaney R, Hallfisch J, Ryan JA, Berti WR. 2004. In situ soil treatments to reduce the phyto-and bioavailability of lead, zinc, and cadmium. *J Environ Qual* 33: 522-531.

Bulgarelli D, Rott M, Schlaeppi K, Ver Loren van Themaat E, Ahmadinejad N, Assenza F. 2012. Revealing structure and assembly cues for Arabidopsis root-inhabiting bacterial microbiota. *Nature* 488(7409): 91+.

Burd GI, Dixon DG, Glick BR. 2000. Plant growth-promoting bacteria that decrease heavy metal toxicity in plants. *Can J Microbiol* 46: 237-245.

Caballero-Mellado J, Matinez-Aquilar L, Paredes-Valdez G, Estrada-de los Santos L. 2004. *Burkholderia unamae* sp nov, an N_2-fixing rhizospheric and endophytic species. *Int J Syst Evol* 54: 1165-1172.

Campos FV, Oliveira JA, Silva AA, Ribeiro C, Farnese FS. 2019. Phytoremediation of arsenite-contaminated environments: is *Pistia stratiotes* L. a useful tool? *Ecol Indic* 104:794–801.

Canadian Council of Ministers of the Environment. 2001. Canadian soil quality guidelines for the protection of environmental and human health: Arsenic (inorganic) (1997). Updated In: Canadian environmental quality guidelines, 1999, Canadian Council of Ministers of the Environment, Winnipeg.

Canada Health Services. 2008. Guidelines for Canadian Drinking Water Quality: Guideline Technical Document – Arsenic. Retrieved from < https://www.canada.ca/en/health-canada/services/publications/healthy-living/guidelines-canadian-drinking-water-quality-guideline-technical-document-arsenic/page-8-guidelines-canadian-drinking-water-quality-guideline-technical-document-arsenic.html#a7>, accessed 23/08/2020.

Canadian Water Network. 2015. Arsenic in Canadian Drinking Water. University of Alberta, Alberta, Canada.

Cao Y, Sun D, Ai H, Mei H, Liu X, Sum S, Xu G, Liu Y, Chen Y, Ma LQ. 2017. Knocking out OsPT4 gene decreases arsenate uptake by rice plants and inorganic arsenic accumulation in rice grains. *Environ Sci Technol* 51: 12131-12138.

Caraus I, Alsuwailem AA, Nadon R, Makarenkov V. 2015. Detecting and overcoming systematic bias in high-throughput screening technologies: a comprehensive review of practical issues and methodological solutions. *Brief Bioinformatics* 16(6): 974-986.

Catarecha P, Segura MD, Franco-Zorrilla JM, García-Ponce B, Lanza M, Solano R, *et al*. 2007. A Mutant of the Arabidopsis Phosphate Transporter PHT1;1 Displays Enhanced Arsenic Accumulation. *The Plant Cell* 19(3) 1123–1133. https://doi.org/10.1105/tpc.106.041871.

Cavalca L, Zanchi R, Corsini A, Colombo M, Romagnoli C, Canzi E, et al. 2010. Arsenic-resistant bacteria associated with roots of the wild *Cirsium arvense* (L.) plant from an arsenic polluted soil, and screening of potential plant growth-promoting characteristics. *Syst Appl Microbiol* 33: 154-164.

Chandrakar V, Dubey A, Keshavkant S. 2016. Modulation of antioxidant enzymes by salicylic acid in arsenic exposed *Glycine max* L. *J Soil Sci Plant Nutr* 16: 662-676.

Chen Z, Zhu Y-G, Liu W-J, Meharg AA. 2005. Direct evidence showing the effect of root surface iron plaque on arsenite and arsenate uptake into rice (*Oryza sativa*) roots. *New Phytol* 165: 91-97.

Chibuike GU, Obiora SC. 2014. Heavy metal polluted soils: Effect on plants and bioremediation methods. *Appl Environ Soil Sci*, 752708.

Coelho DG, Marinato CS, de Matos LP, de Andrade HM, da Silva VM, Santos-Neves PH, *et al*. 2020. Is arsenite more toxic than arsenate in plants? *Ecotoxicology* 29(2): 196-202.

Costa BES, Coelho LM, Araujo CST, Rezende HC, Coelho NMM. 2016. Analytical strategies for the determination of arsenic in rice. *Journal of Chemistry*, Article ID: 1427154. https://doi.org/10.1155/2016/1427154.

Daiane de Souza T, Borges AC, Teixeira de Matos A, Veloso RW, Braga AF. 2018. Optimization of arsenic phytoremediation using *Eichhornia crassipes. Int J Phytoremediat* 20(11): 1129-1135.

Das S, Jean J-S, Chou M-L, Rathod J, Liu C-C. 2016. Arsenite-oxidizing bacteria exhibitin plant growth promoting traits isolated from the rhizosphere of *Oryza sativa* L.: Implications for mitigation of arsenic contamination in paddies. *J Hazard Mat* 302: 10-18.

Davin M, Starren A, Marit E, Lefébure K, Fauconnier M-L, Colinet G. 2019. Investigating the effect of *Medicago sativa* L. and *Trifolium pratense* L. root exudates on PAHs bioremediation in an aged-contaminated soil. *Water Air Soil Pollut* 230(296), doi: https://doi-org.ezproxy.lakeheadu.ca/10.1007/s11270-019-4341-4.

Dey U, Chatterjee S, Mondal NK. 2016. Isolation and characterization of arsenic-resistant bacteria and possible application in bioremediation. *Biotechnol Rep* 10: 1-7.

Ding H, Ji H, Tang L, Zhang A, Guo X, Li C, Gao Y, Briki M. 2016. Heavy metals in the gold mine soil of the upstream area of a metropolitan drinking water source. *Environ Sci Pollut Res*, 23: 2831-2847.

Dobritsa AP, Linardopoulou EV, Samadpour M. 2017. Transfer of 13 species of the genus *Burkholderia*to the genus *Caballeronia* and reclassification of *Burkholderia jirisanensis* as *Paraburkholderia jirisanensis* comb. nov. *Int J Syst Evol* 67: 3846-3853.

Dong Y, Zhu Y-G, Smith A, Wang Y, Chen B. 2008. Arbuscular mycorrhiza enhanced arsenic resistance of both white clover (*Trifolium repens* Linn) and ryegrass (*Lolium perenne* L) plants in an arsenic-contaminated soil. *Environ Pollut* 155(1): 174-181.

Eberi L, Vandamme P. 2016. Members of the genus *Burkholderia*: good and bad guys. *F1000 Faculty Reviews* 5: 1007.

Egamberdieva D, Wirth SJ, Alqarawi AA, Allah EF, Hashem A. 2017. Phytohormones and beneficial microbes: Essential components for plants to balance stress and fitness. *Frontiers in Microbiol*, *8*. <https://doi.org/10.3389/fmicb.2017.02104>.

Elias M, Wellner A, Goldin-Azulay K, Chabriere E, Vorholt JA, Erb TJ, and Tawfik DS. 2012. The molecular basis of phosphate discrimination in arsenate-rich environments. *Nature* 491(7422).

El Mehdawi AF, Jiang Y, Guignardi ZS, Esmat A, Pilon M, Pilon-Smits EAH, Schiavon M. 2018. *New Phytol*, 217(1): 194-205.

Entz M, Bullied JW, Forster DA, Gulden RH. 2001. Extraction of subsoil nitrogen by alfalfa, alfalfa-wheat, and perennial grass systems. *Agronomy Journal* 93(3), doi: 10.2134/agronj2001.933495x.

Environment Canada. (2007). *Biological Test Method: Test for Measuring Emergence and Growth of Terrestrial Plants Exposed to Contaminants in Soil*. Environmental Technology Centre, Ottawa ON.

Fan M, Haibo L, Yinghua L, Weina C, Mingshuai W, Zhe L, Rui C, Hongxuan W. 2020. Toxicity of Ag+ on microstructure, biochemical activities and genetic material of *Trifolium pratense* L. seedlings with special reference to phytoremediation. *Ecotoxicol Environ Saf* 195: 110499.

Fashola MO, Ngole-Jeme VM, Babalola OO. 2016. Heavy metal pollution from gold mines: environmental effects and bacterial strategies for resistance. *Int J Environ Res Public Health* 13(11): 1047.

Fatnassi IC, Chiboub M, Saadani O, Jebara M, Jebara SH. 2015. Impact of dual inoculation with *Rhizobium* and PGPR on growth and antioxidant status of *Vicia faba* L under copper stress. *CR Biologies* 338: 241-254.

Farooq MA, Islam F, Ali B, Najeeb U, Mao B, Gill RA, Yan G, Siddique KHM, Zhou W. 2016. Arsenic toxicity in plants: cellular and molecular mechanisms of its transport and metabolism. *Environ Exp Bot* 132: 42-52.

Fayiga AO, and Saha UK. 2016. Arsenic hyperaccumulating fern: Implications for remediation of arsenic contaminated soils. *Geoderma* 284: 132-143. https://doi.org/10.1016/j.geoderma.2016.09.003.

Freitas H, Prasad M, Pratas J. 2004. Plant communities tolerant to trace elements growing on the degraded soils of São Domingos mine in the south east of Portugal: environmental implications. *Environ Int* 30: 65-72.

Funes Pinter MI, Salomon MV, Berli F, Gil R, Bottini R, Piccoli P. 2018. Plant growth promoting rhizobacteria alleviate stress by As(III) in grapevine. *Agric Ecosyst Environ* 267: 100-108.

Garbinski LD, Rosen BP, Chen J. 2019. Pathways of arsenic uptake and efflux. *Environ Int* 126: 585-597.

Genrich I, Burd D, Dixon G, Glick BR. 1999. Plant growth-promoting bacteria that decrease heavy metal toxicity in plants. *Can J Microbiol* 46: 237-245.

Glick BR. 2012. Plant growth-promoting bacteria: mechanisms and applications. *Scientifica* 963401.

Ghosh P, Rathinasabapathi B, Ma LQ. 2011. Arsenic-resistant bacteria solubilized arsenic in the growth media and increased growth of arsenic hyperaccumulator *Pteris vittata* L. *Bioresour Technol* 102: 8756-8761.

Gihring TM, Druschel GM, McCleskey RB, Hamers RJ, Banfield JF. 2001. Rapid arsenite oxidation by *Thermus aquaticus* and *Thermus thermophilus*: Field and laboratory investigations. *Environ Sci Technol,* 35: 3856-3862.

Gordon SA, Weber RP. 1951. Colorimetric estimation of indoleacetic acid. *Plant Physiol* 26(1): 192-195.

Gunes A, Pilbeam DJ, Inal A. 2008. Effect of arsenic-phosphorous interaction on arsenic-induced oxidative stress in chickpea plants. *Plant and Soil* 314: 211-220.

Hall J, Soole K, Bentham R. 2011. Hydrocarbon phytoremediation in the family Fabaceae – a review. *Int J Phytorem* 13(4): 317-332.

Han Q, Ma Q, Chen Y, Tian B, Xu L, Bai Y, Chen W, Li X. 2020. Variation in rhizosphere microbial communities and its association with the symbiotic efficiency of rhizobia in soybean. *ISME J* 14: 1915-1928.

Harris J. 2003. Measurements of the soil microbial community for estimating the success of restoration. *Eur J Soil Sci* 54(4): 801-808.

Hazotte A, Péron O, Gaudin P, Abdelouas A, Lebeau T. 2018. Effect of *Pseudomonas fluorescens* and pyoverdine on the phytoextraction of cesium by red clover in soil pots and hydroponics. *Environ Sci Pollut Res* 25: 20680-20690.

Hossner LR, Hons FM. 1992. Reclamation of mine tailings. *Advances in Soil Science* 17: 311-350.

Henke HA. 2016. Five challenges in plate assays that can be mastered by the right choice of pipetting tool. Eppendorf, *White Paper* 35: 1-9.

Hu Y, Li J, Lou B, Wu R, Wang G, Lu C, Wang H, Pi J, Xu Y. 2020. The role of reactive oxygen species in arsenic toxicity. *Biomolecules* 10(2): 240.

Jin ZM, Sha W, Zhang YF, Zhao J, Ji H. 2013. Isolation of Burkholderia cepacian JB12 from lead- and cadmium- contaminated soil and its potential in promoting phytoremediation with tall fescue and red clover. *Can J Microbiol* 59(7): 449+.

Jomjun N, Siripen T, Maliwan S, Jintapat N, Prasak T, Somporn C, Petch P. 2011. Phytoremediation of arsenic in submerges soil by wetland plants. *Int J Phytoremediation* 13:35-46. https://doi.org/10.1080/15226511003671320.

Joner EJ, Leyval C, Colpaert JV. 2006. Ectomycorrhizas impede phytoremedation of polycyclic aromatic hydrocarbons (PAHs) both within and beyond the rhizosphere. *Environ Poll* 142: 34-38.

Kapahi M, Sachdeva S. 2019. Bioremediation options for heavy metal pollution. *J Health Pollut* 9(24): 191-203.

Kashyap DR, Botero LM, Franck WL, Hassett DJ, McDermott TR. 2006. Complex regulation of arsenite oxidation in *Agrobacterium tumefaciens*. *J Bacteriol* 188(3): 1081-1088.

Kaushik P, Rawat N, Mathur M, Raghuvanshi P, Bhatnagar P, Swarnkar H, Flora S. 2012. Arsenic hyper-tolerance in four *Microbacterium* species isolated from soil contaminated with textile effluent. *Toxicol Int* 19(2): 188-194.

Ko M-S, Park H-S, Lee U-J. 2017. Influence of indigenous bacteria stimulation on arsenic immobilization in field study. *Catena* 148: 46-51.

Kobayashi T, Kaminaga H, Navarro RR, Iimura Y. 2012. Application of aqueous saponin on the remediation of polycyclic aromatic hydrocarbons-contaminated soil. *J Environ Sci Heal A* 47: 1138-1145.

Kruger MC, Bertin PN, Heipieper HJ, Arsène-Ploetze F. 2013. Bacterial metabolism of environmental arsenic – mechanisms and biotechnological applications. *Applied Microbiol Biotechnol* 97(9): 3827-2841.

Kumari N, Jagadevan S. 2016. Genetic identification of arsenate reductase and arsenite oxidase in redox transformations carried out by arsenic metabolising prokaryotes – A comprehensive review. *Chemosphere* 163: 400-412.

Lautenbach WE. 1985. Land Reclamation Program 1978 - 1984. Vegetation Enhancement Technical Advisory Committee, Regional Municipality of Sudbury, Sudbury, Ontario, Canada.

Lett M-C, Muller D, Lièvremont D, Silver S, Santini J. 2012. Unified nomenclature for genes involved in prokaryotic aerobic arsenite oxidation. *J Bacteriol* 194(2): 207-208.

Leung K, Wanjage FN, Bottomley PJ. 1994. Symbiotic characteristics of *Rhizobium leguminosarum* bv. trifolii isolates which represent major and minor nodule-occupying chromosomal types of field-grown subclover (*Trifolium subterraneum* L.). *Appl Environ Microbiol* 60(2): 427-433.

Ma Y, Rajkumar M, Zhang C, Freitas H. 2016. Beneficial role of bacterial endophytes in heavy metal phytoremediation. *J Environ Management 174*: 14-25. <https://doi.org/10.1016/j.jenvman.2016.02.047>.

Mallick I, Tofajjen Hossain SK, Sinha S, Mukherjee SK. 2014. *Brevibacillus* sp KUMAs2, a bacterial isolate for possible bioremediation of arsenic in rhizosphere. *Ecotoxicol Environ Saf* 107: 236-244.

Mandal SM, Gouri SS, De D, Das BK, Mondal KC, Pati BR. 2011. Effect of arsenic on nodulation and nitrogen fixation of blackgram (*Vigna mungo*). *Indian Journal of Microbiology 51*(1): 44-47. <https://doi.org/10.1007/s12088-011-0080-y>.

Marques APGC, Rangel AOSS, Castro PML. 2009. Remediation of heavy metal contaminated soils: phytoremediation as a potentially promising clean-up technology. *Crit Rev Environ Sci Technol* 39(8): 622-654.

Martin BC, George SJ, Price CA, Ryan MH, Tibbett M. 2014. The role of root exuded low molecular weight organic anions in facilitating petroleum hydrocarbon degradation: Current knowledge and future directions. *Sci Total Environ* 472: 642-653.

Masscheleyn PH, Delaune RD, Patrick WH Jr. 1991. Effect of redox potential and pH on arsenic speciation and solubility in a contaminated soil. *Environ Sci Technol* 25: 1414-1419.

Meharg AA, Hartley-Whitaker J. 2002. Arsenic uptake and metabolism in arsenic resistant and non resistant plant species. *New Phytol* 154: 29-43.

Meng Y-L, Liu Z, Rosen BP. 2004. As(III) and Sb(III) uptake by GlpF and efflux by ArsB in Escherichia coli. *J Biol Chem* 279(18): 18334-18341.

Mesa V, Navazas A, Gonzalez-Gil R, Gonzalez A, Weyens N, Lauga B, Gallego JLR, Sanchez J, Pelaez AI. 2017. Use of endophytic and rhizosphere bacteria to improve phytoremediation of arsenic-contaminated industrial soils by autochthonous *Betula celtiberica*. *Appl Environ Microbiol* 83:e03411-16. https://doi.org/10.1128/AEM.03411-16.

Mikalajune A, Jasulaityte G. 2011. Cleaning of soil contaminated with heavy metals using red clovers. *Environmental Engineering,* the 8th International Conference, ISSN 2029-7092. Ministry of the Environment. 2011. Soil, ground water and sediment standards for use under Part XV.1

of the Environmental Protection Act. Ministry of the Environment, Conservation and Parks, Ontario.

Mol C, Lee P, Meyer L, Leung K. 2016. Bioremediation of contaminated soils from mine sites using native plants in Northwestern Ontario. Dissertation, Lakehead University.

Muller D, Médigue C, Koechler S, Barbe V, Barakat M, Taila E, Bonnefoy V, Krin E, Arsène-Ploetze F, Carapito C, Chandler M, Cournoyer B, Cruveriller S, Dossat C, Duval S, Heymann M, Leize E, Lieutaud A, Lièvrement D, Makita Y, Mangenot S, Nitschke W, Ortet P, Perdial N, Schoepp B, Siguier P, Simeonova DD, Rouy Z, Sergurens B, Turlin E, Vallenet D, Van Dorsselaer A, Weiss S, Weissenbach J, Lett M-C, Danchin A, Bertin PN. 2007. A tale of two oxidation states: Bacterial colonization of arsenic-rich environments. *PLoS Genet* 3(4): e53.

Navari-Izzo F, Quartacci MF. 2001. Phytoremediation of metals: Tolerance mechanisms against oxidative stress. *Minerva Biotec* 13(2): 73-83.

Ndubueze EU, Yanful EK, Macfie S. 2018. Potential of five plant species for phytoremediation of metal PAH-pesticide contaminated soil. *Electronic Thesis and Dissertation Repository* 5342: https://ir.lib.uwo.ca/etd/5342.

Nussaume L, Kanno S, Javot H, Marin E, Pochon N, Ayadi A, *et al*. 2011. Phosphate Import in Plants: Focus on the PHT1 Transporters. *Frontiers in plant science* 2. https://doi.org/10.3389/fpls.2011.00083.

Olanrewaju OS, Glick BR, Babalola OO. 2017. Mechanisms of action of plant growth promoting bacteria. *World J Microbiol Biotechnol* 33(11).

Oller ALW, Talano MA, Agostini E. 2012. Screening of plant growth-promoting traits in arsenic-resistant bacteria isolated from the rhizosphere of soybean plants from Argentinean agricultural soil. *Plant Soil* 369: 93-102.

Ontario Open For Business. 2020. 'Mining', https://www.investinontario.com/mining#secure.

Ontario Provincial Standard Specification (OPSS). 2014. Construction Specification for Seed and Cover. OPSS PROV 804.

Ouvrard S, Leglize P, Morel JL. 2014. PAH phytoremediation: rhizodegradation of rhizoattenuation? *Int J Phytorem* 16(1): 46-61.

Ozturk F, Duman F, Leblebici Z, Temizgul R. 2010. Arsenic accumulation and biological responses of watercress (*Nasturtium officinale* R. Br.) exposed to arsenite. Environ Exp Bot 69: 167-174.

Pajuelo E, Rodríguez-Llorente ID, Dary M, Palomares AJ. 2008. Toxic effects of arsenic on Sinorhizobium– Medicago sativa symbiotic interaction. *Environ Pollut* 154(2): 203-211.

Pandey S, Ghosh PK, Ghosh E, De TK, Maiti TK. 2013. Role of heavy metal resistant *Ochrobactrum* sp. and *Bacillus* spp. strains in bioremediation of a rice cultivar and their PGPR like activities. *J Microbiol* 51: 11-17.

Phillips SE, Taylor ML. 1976. Oxidation of arsenite to arsenate by *Alcaligenes faecalis. Appl Environ Microbiol,* 32(3): 392-399.

Pivetz BE. 2001. Phytoremediation of contaminated soil and ground water at hazardous waste sites. United States Environmental Protection Agency, Office of Research and Development, Office of Solid Waste and Emergency Response, Washington DC, USA.

Plewniak F, Koechler S, Navet B, Dugat-Bony E, Bouchez O, Peyret P, et al. 2013. Metagenomic insights into microbial metabolism affecting arsenic dispersion in Mediterranean marine sediments. *Mol Ecol* 22: 4870-4883.

Porter H, Garnier E. 1996. Plant growth analysis: an evaluation of experimental design and computational methods. *J Exp Bot* 47(302): 1343-1351.

Punchun T, Jackson BP, Meharg AA, Warczack T, Scheckel K, Guerinot ML. 2018. *Sci Total Environ,* 28043702.

Rahman S, Kim K-H, Saha SK, Swaraz AM, Paul DK. 2014. Review of remediation techniques for arsenic (As) contamination: A novel approach utilizing bio-organisms. *J Environ Manage* 134: 175-185.

Ronzan M, Piacentini D, Fattorini L, Della Rovere F, Eiche E, Riemann M, et al. 2018. Cadmium and arsenic affect root development in Oryza sativa L. negatively interacting with auxin. *Environmental and Experimental Botany* 151, 64-75.

Rusch A, Islam S, Savalia P, Amend JP. 2014. Burkholderia insulsa sp. nov., a facultatively chemolithotrophic bacterium isolated from an arsenic-rich shallow marine hydrothermal system. *Int J Syst Evol Microbiol* 65(1): 189-194.

Saleem M, Arshad M, Hussain S, Bhatti AS. 2007. Perspective of plant growth promoting rhizobacteria (PGPR) containing ACC deaminase in stress agriculture. *J Ind Microbiol Biot* 34(10): 635-648.

Salles JF, Antonius van Veen J, Dirk van Elsas J. 2004. Multivariate analyses of *Burkholderia* species in soil: Effect of crop and land use history. *Appl Environ Microbiol* 70(7): 4012-4020. https://doi.org/10.1128/AEM.70.7.4012-4020.2004.

Santini JM, Sly LI, Schnagl RD, Macy JM. 2000. A new chemolithoautotrophic arsenite-oxidizing bacterium isolated from a gold mine: Phylogenetic, physiological, and preliminary biochemical studies. *Appl Environ Microbiol* 66(1): 92-97.

Sarkar A, Paul B. 2016. The global menace of arsenic and its conventional remediation – A critical review. *Chemosphere* 158: 37-49.

Segura A, Ramos JL. 2013. Plant-bacteria interactions in the removal of pollutants. *Curr Opin Biotechnol* 24(3): 467-473.

Shahbaz AK, Iqbal M, Jabbar A, Hussain S, Ibrahim M. 2018. Assessment of nickel bioavailability through chemical extractants and red clover (*Trifolium pratense* L) in an amended soil: Related changes in various parameters of red clover. *Ecotoxicol Environ Safety* 149: 116-127.

Sher S, Rehman A. 2019. Use of heavy metals resistant bacteria – a strategy for arsenic bioremediation. *Appl Microbiol Biotechnol* 103: 6007-6021.

Siciliano SD, Fortin N, Mihoc A, Wisse G, Labelle S, Beaumier D, Ouellette D, Roy R, Whyte LG, Banks MK, *et al*. 2001. Selection of specific endophytic bacterial genotypes by plants in response to soil contamination. *Appl Environ Microbiol*, 67: 2469-2475.

Silva Gonzaga MI, Ma LQ, Pacheco EP, dos Santos WM. 2012. Predicting arsenic bioavailability to hyperaccumulator *Pteris* ferns. *Int J Phytorem* 14: 939-949.

Simeonova DD, Lievremont D, Lagarde F, Muller DAE, Groudeva VI, Lett M-C. 2004. Microplate screening assay for the detection of arsenite-oxidizing and arsenate-reducing bacteria. *FEMS Microbiol Lett*, 237(2): 249-253.

Simmler M, Suess E, Christl I, Kotsev T, Kretzschmar R. 2016. Soil-to-plant transfer of arsenic and phosphorous along a contamination gradient in the mining-impacted Ogosta River floodplain. *Sci Total Environ* 572: 742-754.

Singh N, Ma LQ. 2006. Arsenic speciation, and arsenic and phosphate distribution in arsenic hyperaccumulator *Pteris vittata* L. and non-hyperaccumulator *Pteris ensiformis* L. *Environ Pollut* 141(2): 238-246.

Singh NK, Rai UN, Tewari A, Singh M. 2010. Metal accumulation and growth response in *Vigna radiata* L. inoculated with chromate tolerant rhizobacteria and grown on tannery sludge amended soil. *Bull Environ Contam Toxicol* 84: 118-124.

Sizova OI, Kochetkov VV, Boronin AM. 2006. The arsenic-phytoremediation potential of genetically modified *Pseudomonas* spp. In J-L Morel, G Echevarria, N Gonchavora (Eds) *Phytoremediation of Metal-Contaminated Soils* (Vol 68, pp 327-334). Dordrecht: Kluwer Academic Publishers.

Srivastava S, Akkarakaran JJ, Suprasanna P, D'Souza SF. 2013a. Response of adenine and pyridine metabolism during germination and early seedling growth under arsenic stress in *Brassica juncea*. *Acta Physiol Plant* 35: 1081-1091.

Srivastava S, Verma PC, Chaudhry V, Singh N, Abhilash PC, Kumar KV, Sharma N, Singh N. 2013b. Influence of inoculation of arsenic-resistant *Staphylococcus arlettae* on growth and arsenic uptake in *Brassica juncea* (L.) Czern. Var. R-46. *J Hazard Mat* 262: 1039-1047.

Suárez-Moreno ZR, Caballero-Mellado J, Coutinho BG, Mendonça-Previato L, James EK, Venturi V. 2012. Common features of environmental and potentially beneficial plant-associated *Burkholderia*. *Microb Ecol* 63: 249-266.

Subramoni S, Nathoo N, Klimov E, Yuam Z-C. 2014. *Agrobacterium tumefaciens* responses to plant-derived signaling molecules. *Front Plant Sci* <https://doi.org/10.3389/fpls.2014.00322>.

Sultana M, Vogler S, Zargar K, Schmidt A-C, Saltikov C, Seifert J, Schlömann, M. 2012. New clusters of arsenite and unusual bacterial groups in enrichments from arsenic-contaminated soil. *Arch Microbiol*, 194: 623-635.

Thunder Bay CEDC (Community Economic Development Commission). 2020. Mining. Retrieved from <https://www.thunderbay.ca/en/mining.aspx#>.

Toussaint J-P, Pham TTM, Barriault D, Sylvestre M. 2012. Plant exudates promote PCB degradation by rhodococcal rhizobacteria. *Appl Microbiol Biotechnol* 95: 1589-1603.

Tsuchiya T, Ehara A, Kasahara Y, Hamamura N, Amachi S. 2019. Expression of genes and proteins involved in arsenic respiration and resistance in dissimilatory arsenate-reducing *Geobacter* sp. Strain OR-1. *Appl Environ Microbiol* 85(14): e00763-19.

Tu S, Ma LQ. 2003. Interactive effects of pH, arsenic and phosphorous on uptake of As and P and growth of the arsenic hyperaccumulator *Pteris vittata* L. under hydroponic conditions. *Environ Exp Bot* 50(3): 243-251.

Tu S, Ma LQ, Luongo T. 2004. Root exudation and its role in arsenic hyperaccumulation of *Pteris vittata. Plant Soil* 258: 9-19.

Ullah A, Heng S, Munis MFH, Fahad S, Yang X. 2015. Phytoremediation of heavy metals assisted by plant growth promoting (PGP) bacteria: A review. *Environ Exp Bot* 117: 28-40.

Uroz S, Courty PE, Oger P. 2019. Plant symbionts are engineers of the plant-associates microbiome. *Trends Plant Sci* 24(10): 905-916.

Valenzuela C, Moraga R, Leon C, Smith CT, Mondaca M-A, Campos VL. 2015. Arsenite oxidation by Pseudomonas arsenicoxydans immobilized on zeolite and its potential biotechnological application. *Bull Environ Contam Toxicol* 94(5): 667-673.

Vincken JP, Heng L, de Groot A, Gruppen H. 2007. Saponins, classification and occurrence in the plant kingdom. *Phytochem* 68: 275-297.

Von Lau E, Gan S, Ng HK, Poh PE. 2014. Extraction agents for the removal of polycyclic aromatic hydrocarbons (PAHs) from soil in soil washing technologies. *Environ Pollut* 184: 640-649.

Wang Q, Xiong D, Zhao P, Yu X, Yu B, Wang G. 2011. Effect of applying an arsenic-resistant and plant growth-promoting rhizobacterium to enhance soil arsenic phytoremediation by

Populus deltoides LH05-17. *J Appl Microbiol* 111: 1065-1074.

Wang Y-T, Suttigarn A, Dastidar A. 2009. Arsenite oxidation by immobilized cells of *Alcaligenes faecalis* strain 01201 in a fluidized-bed reactor. *Water Environ Res* 81(2): 173-177.

Weeger W, Lievremont D, Perret M, Lagarde F, Leroy M, Lett M-C. 1998. Oxidation of arsenite to arsenate by a bacterium isolated from an aquatic environment. *Biometals* 12: 141-149.

Weis JS, Weis P. 2004. Metal uptake, transport and release by wetland plants: implications for phytoremediation and restoration. *Environ Int* 30: 685–700.

Wilson D, Clarke A. Hazardous Waste Site Soil Remediation: Theory and Application of Innovative Technologies. Marcel Dekker, Inc., New Yok, 1994.

Wu F, Wang J-T, Yang J, Li J, Zheng Y-M. 2016. Does arsenic play an important role in the soil microbial community around a typical arsenic mining area. *Environ Pollut* 213: 949-956.

Yamamura S, Amachi S. 2014. Microbiology of inorganic arsenic: From metabolism to bioremediation. *J Biosci Bioeng* 118(1): 1-9.

Yan G, Chen X, Du S, Deng Z, Wang L, Chen S. 2019. Genetic mechanisms of arsenic detoxification and metabolism in bacteria. *Curr Genet* 65(2): 329-338.

Yang Q, Tu S, Wang G, Liao X, Yan X. 2012. Effectiveness of applying arsenate reducing bacteria to enhance arsenic removal from polluted soils by *Pteris vittata* L. *Int J Phytorem* 14: 89-99.

Appendix A

Figure A.1 Map of Barrick Gold Hemlo Mine in relation to Thunder Bay

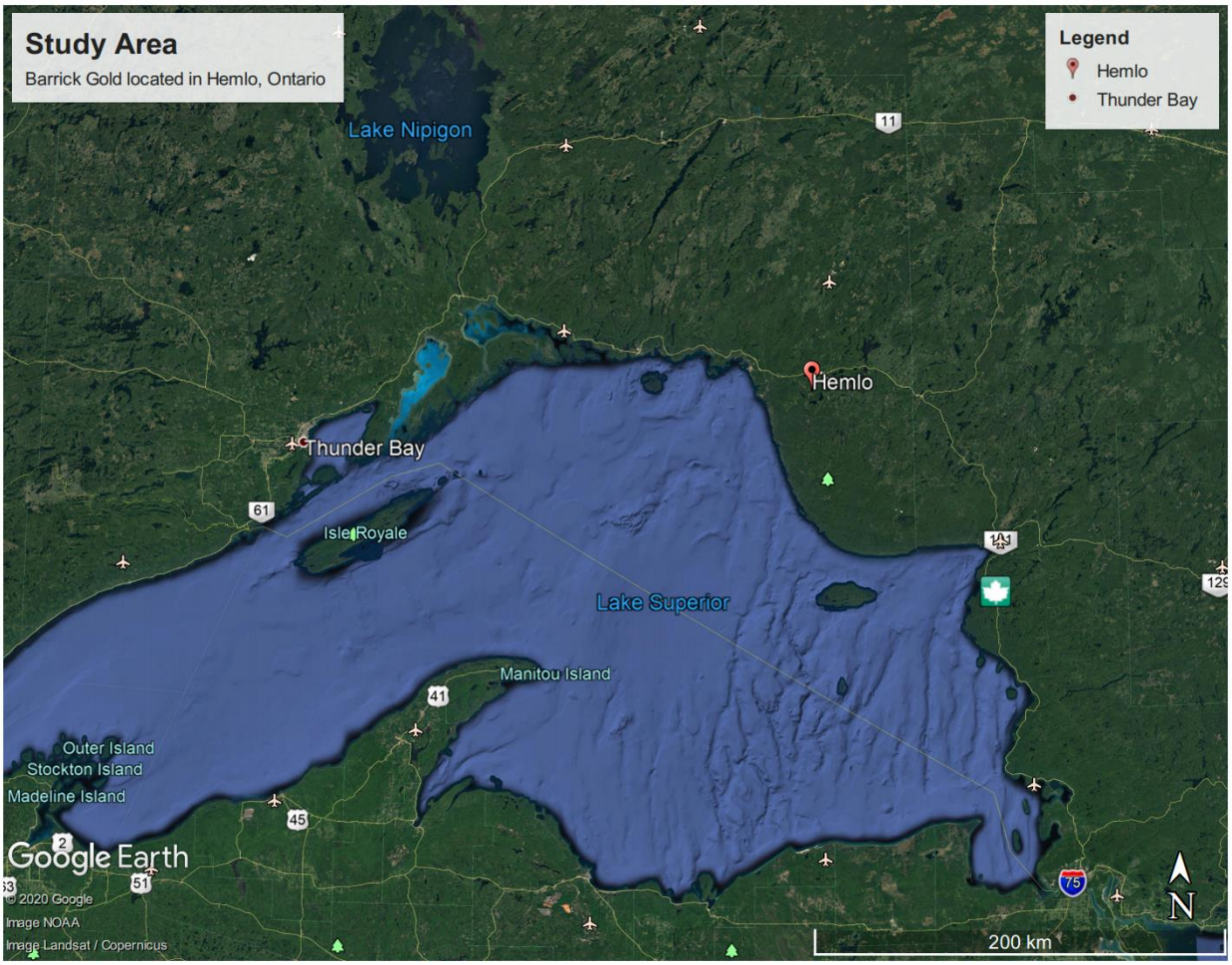

Figure A.2 Map of Barrick Gold Hemlo Mine soil sampling area

Appendix B

Lakehead UNIVERSITY | Instrumentation Laboratory Centre for Analytical Services

INSTRUMENTATION LABORATORY EXTERNAL SERVICES

Varian Vista Pro Basic Operating Procedures

SOP #IL-002

Authorized by: **Dr Francis Appoh**

Written by: A. Raitsakas, J.Joncas, Grezgorz Kepka

Revision number: 1.0.3
Original Date: October 3, 2002
Rev. September 2, 2004, March 2005, August 2005, June 2019
Filename: LUCDATA\QAQC\SOPS\ILES_ICP\Varian Vista Standard Operating Procedures.wpd (xx.doc in 0805)

Table of Contents

ICP OPERATOR'S GUIDE

1. Scope

The objective of this document is to provide detailed instructions in the operation of the Instrument Lab Varian Vista Pro ICP-AES.
This document is to be used every day during the operation of the aforementioned ICP. Herein are described the permissible tasks of the ICP operator and any others involved in the operation of the ICP.

All ICP operators should meet the minimum qualifications defined in the LUCAS Quality Assurance Manual, Section 3.4.

1. General Cautions:

1.1 Leave the computer on at all times with the VistaPro software program (ICP Expert) running. **Do not exit the program unless a complete shutdown is desired**.
Program can be minimized and monitor turned off.
1.2 Do not change the supplied worksheets and templates. Always save the worksheet under a new name before any modification.
1.3 **Leave the instrument on at all times**, even when there is no argon supply. The only exception is before expected power outages or during periods of unstable power
1.4 Multi-tasking during an analytical run should be avoided. Running other applications (such as Excel) during a run can cause an "unexpected system error" and crash.
1.5 Always ensure that the nebulizer has sample or rinse solution flowing through it whenever the plasma is on. Running the nebulizer in a dry condition can damage the torch.
1.6 Keep the ICP area clean and free of dust.
1.7 Calibration standards used for instrument standardization should ideally be no more than 6 months old.

2. Startup:

2.1 Routine ICP START-UP CHECKS:

1. Check argon gas pressure @ 80 psi absolute maximum, 65 minimum. Dewar pressure should be >100 psi – adjust pressure builder if necessary. Water chiller on
2. Check Exhaust vent on and drawing air properly. Close Fume hood door.
3. Torch and snout properly positioned and relatively clean? If not, go to 2.2.
4. Gas lines well connected
5. Inspect injector tube
6. Inspect top of torch
7. Snout must rest on bonnet and be well aligned.

8. Close door securely.
9. Ensure that the nebulizer and spray chamber used are appropriate for the sample type.
10. Check condition of pump lines and replace if necessary (blue-blue for waste line, grey-grey for sample feed line). Attach sample feed and waste lines to the peristaltic pump and clamp in position.
11. Position the autosampler in the rinse station or, preferably, a bottle of water on the rack.
12. Check rinse station on the autosampler. Fill rinse bottle with rinse solution and empty waste bottle. Solution in the rinse station should be the same as the sample matrix - eg. 2%HNO3.
13. Peristaltic Pump on. Check for proper sample flow. Raise and lower autosampler arm several times to introduce a series of bubbles in the sample feed line. Adjust pump clamp tensioner knob 1 1/2 to 2 turns past the point where sample flow just starts.
14. Start plasma. (Peristaltic pump will stop during this operation) Check torch and related components for persistent arcing or orange glow. Turn off the plasma if these conditions last for more than a few seconds.
15. Turn off autosampler rinse if A/S sampler tube is in a bottle of rinse solution. **Ensure that there is ALWAYS a flow of rinse solution to the nebulizer when the plasma is on.**
16. Load worksheet and set up standards and samples. **See section 5.**
15. **Check that Polychromator boost and snout purge are on during warmup**. If analytical lines $\lambda < 210$ nm are used, poly boost and snout purge should be left on; otherwise it can be turned off after ½ hour warmup period. Note that selection of deep UV lines < 190 nm in a method will require that poly boost be on for 3 hours prior to analysis.

2.2 Non-Routine startup (under supervision only):

2.2.1 If spray chambers or torches have been changed or adjusted, alignment checks should be performed.
2.2.2 After all adjustments, perform horizontal torch alignment test, then dark current followed by wavelength calibration checks. Note results in the maintenance logbook.
2.2.3 Go to 2.1

3. Shutdown:

3.1 There are two types of shutdown - a standby mode for nightly shutdowns and shutdown mode for extended periods.

3.2 Nightly Shutdown by operator:
Post analysis:
- Cap the standards and QC samples and store them. Cap customer samples if desired.
- Rinse for 5-10 minutes with water or low acid blank
- Torch off, unclamp peristaltic pump tubing. Release tubing from pump rollers.
- Release peristaltic pump tubing at bottom of pump

- Poly purge boost off (Analyze tab). If deep UV lines <190nm are to be used in an analysis the next day, leave the polyboost ON.
- Check snout purge is off
- **Turn off the water chiller.** Note that turning off the chiller automatically turns off the peltier and gives a warning.
- turn off computer monitor. Always leave computer and instrument on.

3.3 Extended shutdown:
Do not turn off the instrument unless there are compelling reasons to do so.

3.4 If the argon supply is about to run out or be changed, turn off the peltier and chiller first.

4. Power Outages:

4.1 When there is no immediate risk of another power failure, turn off instrument switch, press the reset button on electrical panel, turn on instrument switch.
4.2 Logon to the computer and start the ICP program. The instrument will go through startup procedures. Load an existing worksheet to enable control of the autosampler.

5. Setting up Worksheets and Sample Runs:

It is more convenient to load an existing worksheet or method template, rename and edit it than to create a new method ab initio.

5.1 Choose an analytical method which is applicable to the sample type. There are methods created for different analyte concentration ranges and different matrix composition.
5.2 Load an appropriate worksheet or worksheet template (preferred), rename and save in an appropriate directory. The new worksheet's name should include client name, date and job number (eg - "ATRC IL02-666 June 6 2002")
5.3 Delete any old analysis data in the newly named worksheet only. Using the sequence editor, enter the customer's job label in the xxx field and the Instrument Lab job number in the xxxx field. Enter sample names. Save the worksheet regularly. In sequence parameters, ensure that "prompt on reuse of sample rack" is unchecked.
5.4 QC samples appropriate to the method (posted on method list on wall and in individual method SOP binders) should be placed in the sequence at start and end and every 10-20 samples. Note that if the QC (or any other sample repeatedly used) is in the 'S' row of the autosampler, its location will have to be manually edited.
5.4.1 Always check the QC check table in the worksheet against the latest QC reports to ensure that the correct values are being used.
5.4.2 Elements with no valid QC information and high concentration elements (eg Ca-hi) should have the QC failure flag unselected (column properties in the worksheet)
5.5 Always insert a rinse before and after QC's.
5.4 **Always** double-check all of the worksheet for errors. This is to be done with the following procedure:

- goto the worksheet sequence. Click on 'Tube', 'special copy ' , paste into Excel spreadsheet, edit for clarity, print sheet
- random checks to confirm the correct identities and locations of at least 10% of the samples will be made and initialed by another person.
- this sheet will be stored along with the copy of the analysis data.

Always have the worksheet checked by someone other than the operator prior to initiating an analysis run.

5.5 Ensure that the proper autosampler trays have been selected in the autosampler setup page.

5.6 After the instrument has warmed up - approximately ½ hour - select all samples (click upper left corner of Analysis page in worksheet) or just the ones required. Press green arrow to start analysis.

5.7 Observe the performance of the standards and QC samples at the start of the analysis. If a QC is flagged, stop the analysis and consult with the ICP supervisor (or delegate) as to the action to be taken.

5.8 Examine the response of the calibration blank to ensure that there is no significant amount of any analyte present. If necessary, restandardize the blank, using fresh solution.

5.9 Ensure that calibration standards used are (ideally) less than 6 months old. QC standards can be used until exhausted.

Procedure to create a new worksheet:

1. Click: **File\New\Method**.

2. Choose the appropriate method from the Method template list. Do not edit worksheets or templates without supervisor's approval.

2.1 Type the job name, date in the "*File name*" box, then save it.

2.2 Alternatively, load an earlier worksheet from the selected method. SAVE AS "new filename" . Delete all data in the newly named worksheet.

3. In the worksheet, click **Method** icon, then choose **Edit Method**.

4. Click the **Sequence** icon in the worksheet.

4.1 Input the **Batch Label,** which should be the Method, e.g.: CATALAN, ATRC

4.2 Input the **Customer ID,** e.g.: CATALAN, ATRC, HS02-102, and NIRDOSH.

4.3 Input the **Customer Label,** which should be the Instrument Lab ID, eg, IL02-122).

4.4 Click the **Sequence Editor** box.

In the *Samples and Calibrations* window, set the *sample count* number as required.

In the *Manually inserted QC* window, set the *Error Action* to **Flag and continue**.

Click **OK** to close the window.

4.5 Go to the **Sequence Parameters** box.

Uncheck the *Prompt on reuse of sample rack*. Click **OK**.

4.6 Click the **Autosampler Setup** box

Select the appropriate *Standard Rack Type*

Choose the **Calib/QC** for the *Rack Use*, and *starting tube* from **1**. Click **OK**.

4.7 In the Sequence window, edit the tube position for each row of the tube. Input the Sample

Label for each solution.

5. Go to **Window/Autosampler Setup**, set the *Down height* according to how deep the solution is - 5 mm is good unless there is very little sample. Note that the calibration standards sit lower in their rack than samples in their racks – problems can occur with small volumes of cal standards or samples with deposits at the bottom of the tube.
Click OK to close the window

6. Click the **Analysis** icon in the worksheet.
Click **Tube** in the left corner to select all the samples.
Check that the polyboost and snout purge are on.
7. Click the triangle icon (Shift + F8) to **Start Analysis**.
8. Check the graphics of the blank calibration standard for non-zero peaks and rerun fresh blanks if necessary. This can be done at any time.

6. QC Sample Protocol:

6.1 See QC Protocol in SOP#001 for details such as frequency and actions.

6.2 All non-normal QC failures must be reported to the ICP supervisor as they occur and noted in the sample logbook on the left-hand page opposite the details of the run. “Xx-hi” analytical lines and elements missing from the QC solution normally have a failure flag and should be ignored.

6.2 For certain methods where high analyte levels are expected, at least one rinse should precede a QC analysis. For these analyses, use an appropriate concentration calibration standard for QC (actually CCV) checks later in the run.

7. Instrument Maintenance:

7.1 Run 0.1% Triton-X through the SIS for a few minutes occasionally, especially after any new components have been installed. Rinse with water for 10 minutes afterwards.

7.2 Keep the ICP area clean. Regularly - once a week or as needed - wipe the surfaces of the computer, ICP, autosampler and argon dewar with a damp cloth to reduce the circulation of contaminating dust. Use only approved cleaners and cloths for the computer monitor’s screen.
7.3 Changing the argon dewar:

7.3.1 Turn off the peltier cooler (Analyze:Peltier off) - water chiller can be left on
7.3.2 Turn off the gas feed valve on the dewar. Remove the gas regulator carefully.
7.3.3 Install regulator on new dewar. Use two large wrenches to prevent lateral forces on the long tube for the gas outlet.

NOTE: Exercise great caution when maneuvering the dewar so that it does not contact the ICP

or its table.

7.4 If the computer's response seems to be slowing (eg. - multiple worksheets loading slowly, software errors, etc), it may be necessary to exit the Varian software and restart the computer. Defragmentation and other computer maintenance may also need to be done in administrator mode.

7.5 At least once a week, perform a torch scan by running a 5ppm Mn solution (or "Vista Test Solution"). Note the response in the maintenance logbook and compare to previous data. If response has dropped significantly or has gradually declined (> 10-20 %), notify supervisor immediately.

8. Data Export:

There are two basic data export methodologies besides printouts:

8.1 Export to LUIL LIMS for LUEL data:

8.1.1 On the Analysis tab, highlight the rows of data to be exported. Use Ctrl key as needed.

8.1.2 Go to File, Export Settings. Check appropriate boxes and enter file name. Export to the Exported data folder. Click export now.

8.1.3 Minimize ICP software window and open exported data folder on desktop. Open the exported file in Excel. Use the macro 'shift-Ctrl-l' (that's a lower case 'L'). Arrange data further as needed. Save as "filename".csv . Ignore error message. Delete original exported "txt" file and change extension of "csv" file to "txt".

8.1.4 Copy file to "tempdata on UILSERV1/ ICP/LUEL subdirectory

8.2 Creation of an Excel spreadsheet: Cust/SolutionLabel/Element/Conc/BatchLabel

Appendices:

Maintenance checklist (from Varian help pages)

To keep the ICP-OES in peak operating condition it is recommended that you perform regular maintenance on the individual components of your spectrometer.

Below is a check-list of recommended times for cleaning or attending to the instrument components. The recommended times are based on assumed daily use of the instrument.

Things to do…

Frequently

Empty the drain vessel

Daily

Clean the surface of your instrument <CleanVista.htm> (This is a link on the help pages to detailed instructions and videos)
Rinse with water for 10 minutes at the end of each analysis.

Check the pump tubing and replace if necessary <ReplaceTubing.htm>

Weekly (recommended)

Clean the torch <CleanTorch.htm>

Clean the snout <Snout.htm> (radial instruments)

Clean the bonnet <CleanBonnet.htm> (radial instruments)

- After these adjustments, always perform a torch scan and wavelength calibration using the "Varian test solution". Note the results in the maintenance logbook

Monthly

Clean the spraychamber <SprayChamber.htm>

Clean the nebulizer <Nebulizer.htm>

Clean the cooling air intake filter <Filters.htm>

Inspect the state of the induction coil. <InductionCoil.htm> Contact your local Varian office or representative <../Contacts/ContactsHome.htm> if maintenance is required.

Check the water level in the water cooler (refer to manual supplied with the water cooler for details).

Perform a Wavelength Calibration <../HowTo/PerformWLCalib_vista.htm>

Warning This instrument contains electrical circuits, devices and components operating at dangerous voltages. Contact with these circuits, devices and components can result in death, painful electrical shock or serious injury.

Operators and other unauthorized personnel must NEVER remove the main covers. The main covers of this instrument must be opened only by Varian-trained, Varian-qualified, or Varian-approved customer service representative (unless otherwise specified).

Appendix C

Table C.1 Total recoverable soil chemistry analysis of Barrick Gold Hemlo site samples.

Parameter	MDL	Units	Average	STD	Site 1 (n=3)		Site 2 (n=2)		Site 3 (n=2)	
					Avg	STD	Avg	STD	Avg	STD
% Moisture	1.00	%	48.07	23.12	32.0563	2.690587	81.74282	0.358965	65.7539	8.295099
Conductivity	0.50	us/cm	474.99	254.89	236	35.22565	408	33.6	418.8	13.2
Bulk Density	0.05	g/cm3	0.45	0.3	0.541883	0.077554	0.115725	0.019675	0.28245	0.1061
Organic Matter			29.1	27.52	5.557658	0.784473	77.26738	1.233404	33.13735	13.4745
pH 1:1 water to soil ratio	0.00	unit	6.72	1.2	6.966667	0.075719	7.33	0.04	7.41	0.03
Total Recoverable Aluminum	0.10	ug/g PPM	9414.541	3605.96	9127.999	612.0852	9470.861	870.8609	13035.63	1364.368
Total Recoverable Arsenic	2.00	ug/g PPM	9.146748	14.11291	<DL	<DL	38.40944	0.107115	28.75523	3.681549
Total Recoverable Barium	0.10	ug/g PPM	199.8712	242.1333	57.72926	4.493501	126.1227	21.02965	114.5988	42.87247
Total Recoverable Beryllium	0.04	ug/g PPM	<DL	<DL	<DL	<DL	<DL	<DL	<DL	<DL
Total Recoverable Calcium	0.06	ug/g PPM	14502.62	12481.59	6136.376	534.7483	31468.33	683.6993	17228.97	5514.46
Total Recoverable Cadmium	0.25	ug/g PPM	<DL	<DL	<DL	<DL	<DL	<DL	<DL	<DL
Total Recoverable Cobalt	0.20	ug/g PPM	11.05847	5.958621	12.2064	1.384529	23.30025	1.048591	11.06146	0.601694
Total Recoverable Chromium	0.03	ug/g PPM	23.61912	13.29709	36.77059	3.729878	10.88688	0.21246	18.0761	1.018633
Total Recoverable Copper	0.05	ug/g PPM	21.99792	8.460573	23.23955	3.136055	16.14616	1.867088	16.09328	4.872232
Total Recoverable Iron	0.10	ug/g PPM	10898.01	4749.801	16729.38	2101.229	8071.731	153.8503	10283.98	764.4404
Total Recoverable Potassium	1.00	ug/g PPM	1134.976	447.1013	1012.546	51.47363	1327.952	234.6966	1257.205	321.4156
Total Recoverable Magnesium	0.20	ug/g PPM	4051.829	2236.062	4743.294	167.9888	2800.177	193.2004	3577.108	20.78645
Total Recoverable Manganese	0.05	ug/g PPM	801.155	884.7822	694.2947	143.7438	3122.563	105.3442	638.3581	69.85239
Total Recoverable Molybdenum	0.01	ug/g PPM	35.79425	47.90863	14.95401	0.295133	160.0541	5.643539	49.35523	17.08155
Total Recoverable Sodium	0.20	ug/g PPM	291.6757	182.9685	180.7225	5.319963	544.9877	22.42954	349.1095	69.74108
Total Recoverable Nickel	0.20	ug/g PPM	20.27521	11.05663	20.76675	0.930633	33.78931	5.045126	35.16394	11.47973
Total Recoverable Phosphorous	3.20	ug/g PPM	481.1575	205.7225	450.1249	51.8147	727.5266	41.48006	630.4392	147.4918
Total Recoverable Lead	1.00	ug/g PPM	19.11575	11.74115	12.9277	1.574932	38.77468	5.132296	26.12377	6.56588
Total Recoverable Sulphur	1.00	ug/g PPM	1218.752	814.6164	483.5565	73.85464	2761.073	372.7014	1957.048	872.8373
Total Recoverable Silicon	0.05	ug/g PPM	276.1278	108.0999	226.2441	12.75477	420.254	76.85862	311.123	0.049365
Total Recoverable Strontium	0.20	ug/g PPM	147.273	150.2224	64.48911	2.465624	493.4091	4.339288	268.3126	81.11264
Total Recoverable Titanium	2.00	ug/g PPM	690.9854	351.7776	901.8909	38.98346	303.2805	41.88511	751.5172	140.4828
Total Recoverable Vanadium	0.40	ug/g PPM	23.09187	9.975327	33.07449	3.612081	16.28592	0.588249	23.94362	1.782698

Total Recoverable Zinc	0.03	ug/g PPM	96.37419	101.6487	79.87052	7.058908	102.6407	19.66395	98.28651	20.51809

Table C.1 cont.

			Site 4 (n=2)		Site 5 (n=2)		Site 6 (n=2)		Site 7 (n=2)	
Parameter	MDL	Units	Avg	STD	Avg	STD	Avg	STD	Avg	STD
% Moisture	1.00	%	70.97461	1.26538	49.11806	2.736391	21.30106	1.789848	47.04478	1.964396
Conductivity	0.50	us/cm	812.4	84.9	315.8	122.7	461.4	110.9	210.5	53.1
Bulk Density	0.05	g/cm3	0.11415	0.00565	0.5408	0.02675	1.03645	0.06355	0.54335	0.05445
Organic Matter			74.07505	2.330478	11.5973	1.09602	3.384742	0.521106	11.51675	1.471588
pH 1:1 water to soil ratio	0.00	unit	4.36	0.17	6.975	0.285	8.335	0.045	7.22	0.16
Total Recoverable Aluminum	0.10	ug/g PPM	6023.115	147.9377	14495.48	1959.26	10206.69	451.5382	12223.62	271.9746
Total Recoverable Arsenic	2.00	ug/g PPM	<DL	<DL	<DL	<DL	<DL	<DL	15.15606	0.338448
Total Recoverable Barium	0.10	ug/g PPM	126.1013	9.846025	260.9616	84.11949	63.29336	6.25094	833.0997	15.95687
Total Recoverable Beryllium	0.04	ug/g PPM	<DL	<DL	<DL	<DL	<DL	<DL	<DL	<DL
Total Recoverable Calcium	0.06	ug/g PPM	14558.59	495.0701	7575.114	471.1349	39575.27	4442.641	7270.855	428.2395
Total Recoverable Cadmium	0.25	ug/g PPM	<DL	<DL	<DL	<DL	<DL	<DL	<DL	<DL
Total Recoverable Cobalt	0.20	ug/g PPM	4.12458	0.045633	15.98634	2.975818	9.739394	0.260606	10.69424	0.228834
Total Recoverable Chromium	0.03	ug/g PPM	13.64427	3.433744	43.69872	4.996017	35.41926	0.631377	25.51441	0.15592
Total Recoverable Copper	0.05	ug/g PPM	33.12402	2.06019	22.72603	0.347653	34.23705	1.509781	20.21508	1.797498
Total Recoverable Iron	0.10	ug/g PPM	6399.599	192.5065	15126.46	795.6472	14923.53	671.4077	12552.97	128.7926
Total Recoverable Potassium	1.00	ug/g PPM	1048.235	35.1857	894.936	23.80085	1666.069	168.6145	1799.818	112.2704
Total Recoverable Magnesium	0.20	ug/g PPM	1786.884	43.90538	4964.808	279.4026	9052.175	249.6433	4968.927	156.3481
Total Recoverable Manganese	0.05	ug/g PPM	278.187	48.6551	564.2248	156.8563	251.3117	9.954124	1177.178	72.27244
Total Recoverable Molybdenum	0.01	ug/g PPM	48.743	0.572788	6.994595	6.994595	<DL	<DL	31.31177	0.116801
Total Recoverable Sodium	0.20	ug/g PPM	171.5614	9.77193	186.6856	1.422475	622.3537	145.7476	275.2353	14.57599
Total Recoverable Nickel	0.20	ug/g PPM	7.050579	0.892684	26.05917	2.361878	19.15098	0.823705	21.33126	1.306103
Total Recoverable Phosphorous	3.20	ug/g PPM	749.7144	33.96976	452.1394	62.45519	425.4937	33.49367	475.7039	11.08853
Total Recoverable Lead	1.00	ug/g PPM	34.65043	1.402202	20.24211	4.557895	11.41458	2.129728	14.80945	0.435828
Total Recoverable Sulphur	1.00	ug/g PPM	1798.592	41.14502	639.7468	157.01	628.2447	57.57806	772.9373	129.2011
Total Recoverable Silicon	0.05	ug/g PPM	440.709	3.659388	255.5818	0.965576	292.7923	69.13172	253.4395	28.47246
Total Recoverable Strontium	0.20	ug/g PPM	229.3887	7.374487	62.65292	4.568706	51.48516	1.957883	99.55415	10.43327
Total Recoverable Titanium	2.00	ug/g PPM	450.7419	4.784434	1198.651	253.138	1019.258	77.19755	825.715	44.83447
Total Recoverable Vanadium	0.40	ug/g PPM	13.89856	0.338279	30.37838	2.421622	34.60061	2.285462	27.79847	0.553183
Total Recoverable Zinc	0.03	ug/g PPM	27.27697	0.013811	66.61451	7.288193	77.47			

*Sediment samples

Table C.1 cont.

Parameter	MDL	Units	*Site 8 (n=1) Avg	STD	*Site 9 (n=1) Avg	STD	*Site 10 (n=1) Avg	STD
% Moisture	1.00	%	88.68445		68.68471		64.18791	
Conductivity	0.50	us/cm	789.8		1009		789.3	
Bulk Density	0.05	g/cm3	0.0944		0.2713		0.3583	
Organic Matter			42.74364		20.08846		22.32766	
pH 1:1 water to soil ratio	0.00	unit	4.75		7.02		4.99	
Total Recoverable Aluminum	0.10	ug/g PPM	2083.117		4423.246		4660.581	
Total Recoverable Arsenic	2.00	ug/g PPM	<DL	<DL	<DL	<DL	<DL	<DL
Total Recoverable Barium	0.10	ug/g PPM	10.55411		349.6593		15.92531	
Total Recoverable Beryllium	0.04	ug/g PPM	<DL	<DL	<DL	<DL	<DL	<DL
Total Recoverable Calcium	0.06	ug/g PPM	1032.372		4160.633		2090.78	
Total Recoverable Cadmium	0.25	ug/g PPM	<DL	<DL	<DL	<DL	<DL	<DL
Total Recoverable Cobalt	0.20	ug/g PPM	1.030303		4.320641		7.26971	
Total Recoverable Chromium	0.03	ug/g PPM	3.402597		7.639279		9.311203	
Total Recoverable Copper	0.05	ug/g PPM	5.679654		8.128257		27.3527	
Total Recoverable Iron	0.10	ug/g PPM	2439.827		3793.988		5025.726	
Total Recoverable Potassium	1.00	ug/g PPM	347.9654		754.9499		300.5809	
Total Recoverable Magnesium	0.20	ug/g PPM	721.9913		1800.401		1880.498	
Total Recoverable Manganese	0.05	ug/g PPM	24.05195		162.3246		87.88382	
Total Recoverable Molybdenum	0.01	ug/g PPM	<DL	<DL	6.517034		<DL	<DL
Total Recoverable Sodium	0.20	ug/g PPM	44.67532		285.3707		78.08299	
Total Recoverable Nickel	0.20	ug/g PPM	3.168831		7.647295		6.746888	
Total Recoverable Phosphorous	3.20	ug/g PPM	92.46753		142.8457		153.112	
Total Recoverable Lead	1.00	ug/g PPM	2.588745		5.851703		4.829876	
Total Recoverable Sulphur	1.00	ug/g PPM	885.7143		1329.86		1156.017	
Total Recoverable Silicon	0.05	ug/g PPM	132		102.0922		109.6763	
Total Recoverable Strontium	0.20	ug/g PPM	3.515152		37.11423		7.211618	
Total Recoverable Titanium	2.00	ug/g PPM	97.48918		238.1563		298.0913	
Total Recoverable Vanadium	0.40	ug/g PPM	4.034632		8.841683		9.742739	

*Sediment samples

Total Recoverable Zinc	0.03	ug/g PPM	10.5368	38.31663	496.6805

Table C.2 Average and standard deviation values for total extractable soil chemistry parameters for Barrick Gold Hemlo site samples.

Parameter	MDL	Units	Average	STD	Site 1 (n=3)		Site 2 (n=2)		Site 3 (n=2)	
					Avg	STD	Avg	STD	Avg	STD
Bulk Density	0.05	g/cm3	0.423083	0.285082	0.541883	0.077554	0.115725	0.019675	0.28245	0.1061
Total Extractable Aluminum	0.10	ug/g PPM	77.05816	56.53012	111.4547	13.39237	15.00581	4.240933	76.06041	39.73627
Total Extractable Arsenic	2.00	ug/g PPM	0.086784	0.086591	0.129723	0.023717	0.049334	0.010224	0.219534	0.029542
Total Extractable Barium	0.10	ug/g PPM	3.839817	4.112305	2.715435	0.427654	0.628451	0.052775	1.583449	0.296581
Total Extractable Beryllium	0.04	ug/g PPM	0.004266	0.004402	0.006652	0.000768	0.001922	0	0.00509	0.002279
Total Extractable Calcium	0.06	ug/g PPM	719.4255	1007.585	282.2652	37.21274	406.9674	35.19321	543.3614	37.69222
Total Extractable Cadmium	0.25	ug/g PPM	0.027303	0.053922	0.009537	0.001659	0.011869	0.000167	0.019899	0.001504
Total Extractable Cobalt	0.20	ug/g PPM	0.198677	0.152188	0.296428	0.047159	0.094817	0.001431	0.133487	0.051223
Total Extractable Chromium	0.03	ug/g PPM	0.027851	0.024157	0.069456	0.008841	0.002864	0.000218	0.022704	0.01485
Total Extractable Copper	0.05	ug/g PPM	0.377108	0.345313	0.794355	0.085817	0.003179	0.000694	0.027841	0.018415
Total Extractable Iron	0.10	ug/g PPM	28.98405	25.72368	61.83253	9.782202	0.644869	0.166807	10.50713	4.16973
Total Extractable Potassium	1.00	ug/g PPM	10.6348	5.22962	7.68334	1.385925	11.66966	1.431486	17.75558	1.844397
Total Extractable Magnesium	0.20	ug/g PPM	37.58714	66.4666	14.71709	2.858293	16.70671	2.364197	19.81358	0.570474
Total Extractable Manganese	0.05	ug/g PPM	23.34242	18.74119	39.71031	12.17481	26.88333	4.072159	19.66353	8.113559
Total Extractable Molybdenum	0.01	ug/g PPM	0.003069	0.008731	<DL		0.030443	0	0.024797	0
Total Extractable Sodium	0.20	ug/g PPM	16.78008	20.5377	5.759582	0.138272	9.872465	1.669772	11.51661	1.277476
Total Extractable Nickel	0.20	ug/g PPM	0.249786	0.155026	0.253855	0.031996	0.108027	0.032486	0.472479	0.054133
Total Extractable Phosphorous	3.20	ug/g PPM	4.321621	3.292284	8.840873	1.081287	0.457219	0.033207	1.548808	0.646389
Total Extractable Lead	1.00	ug/g PPM	0.199583	0.158678	0.428377	0.045304	0.011339	0.000343	0.095311	0.059843
Total Extractable Sulphur	1.00	ug/g PPM	11.77549	15.94734	2.709788	0.30282	7.508607	0.531075	2.919961	0.373766
Total Extractable Silicon	0.05	ug/g PPM	18.35135	13.19218	19.95149	1.991179	3.73602	0.47603	16.90258	6.227745
Total Extractable Strontium	0.20	ug/g PPM	4.383826	2.19022	3.726503	0.460698	5.957426	0.518927	8.440069	0.850322
Total Extractable Titanium	2.00	ug/g PPM	0.173834	0.227931	0.24094	0.036663	<DL		0.072834	0
Total Extractable Vanadium	0.40	ug/g PPM	0.094011	0.090529	0.19135	0.032141	<DL		0.065384	0.05104
Total Extractable Zinc	0.03	ug/g PPM	4.764816	12.99383	2.224185	0.309239	0.640065	0.182493	1.279535	0.004656

Table C.2 cont.

			Site 4 (n=2)		Site 5 (n=2)		Site 6 (n=2)		Site 7 (n=2)	
Parameter	MDL	Units	Avg	STD	Avg	STD	Avg	STD	Avg	STD
Bulk Density	0.05	g/cm3	0.11415	0.00565	0.5408	0.02675	1.03645	0.06355	0.54335	0.05445
Total Extractable Aluminum	0.10	ug/g PPM	18.13627	1.209237	159.3186	10.40637	4.686222	3.503072	128.415	2.193618
Total Extractable Arsenic	2.00	ug/g PPM	<DL		0.07657	0	<DL		0.166554	0.038341
Total Extractable Barium	0.10	ug/g PPM	1.356855	0.126006	9.166219	2.021055	2.820121	0.260729	12.33353	3.502318
Total Extractable Beryllium	0.04	ug/g PPM	0.001311	0	0.011629	0.0002	<DL		0.010082	0.000508
Total Extractable Calcium	0.06	ug/g PPM	238.0636	14.8463	511.4006	106.5801	3489.569	590.6316	436.989	31.6649
Total Extractable Cadmium	0.25	ug/g PPM	0.005301	0.000525	0.019664	0.007192	0.009717	0	0.027391	0.000664
Total Extractable Cobalt	0.20	ug/g PPM	0.028717	0.004008	0.367799	0.264421	0.193006	0.010664	0.204775	0.083621
Total Extractable Chromium	0.03	ug/g PPM	0.001713	2.56E-05	0.045409	0.007695	0.020978	0.008161	0.032097	0.004866
Total Extractable Copper	0.05	ug/g PPM	0.06041	0.004187	0.355851	0.005858	0.165298	0.015	0.530672	0.093587
Total Extractable Iron	0.10	ug/g PPM	6.546172	0.105808	7.477286	0.12318	32.96277	6.132057	18.60942	8.515618
Total Extractable Potassium	1.00	ug/g PPM	11.07461	0.673596	12.55027	2.843802	7.838636	1.224674	9.689781	0.939252
Total Extractable Magnesium	0.20	ug/g PPM	9.216357	0.348155	17.17682	3.920143	216.2692	60.88617	14.18819	0.612571
Total Extractable Manganese	0.05	ug/g PPM	4.175958	1.121715	25.09952	9.837134	10.98457	1.317587	52.78447	22.56546
Total Extractable Molybdenum	0.01	ug/g PPM	<DL		<DL		<DL		<DL	
Total Extractable Sodium	0.20	ug/g PPM	3.077771	0.301212	8.922636	2.150353	68.2822	15.27713	13.26932	1.530051
Total Extractable Nickel	0.20	ug/g PPM	0.037382	0.000834	0.236167	0.078914	0.180707	0.01325	0.487922	0.106686
Total Extractable Phosphorous	3.20	ug/g PPM	3.098802	0.253036	4.32715	0.723066	0.158699	0.015225	7.462782	0.419243
Total Extractable Lead	1.00	ug/g PPM	0.083982	0.002421	0.27954	0.073941	<DL		0.248223	0.091896
Total Extractable Sulphur	1.00	ug/g PPM	2.598886	0.259387	2.837156	1.277872	16.30355	6.651664	2.663201	0.509606
Total Extractable Silicon	0.05	ug/g PPM	0.917592	0.028487	30.54438	0.24719	16.07162	2.598632	43.93316	4.229893
Total Extractable Strontium	0.20	ug/g PPM	3.481651	0.184326	4.342426	0.987786	3.265375	0.364868	6.135698	0.377086
Total Extractable Titanium	2.00	ug/g PPM	0.024151	0.002131	0.093261	0.035319	<DL		0.142218	0.033293
Total Extractable Vanadium	0.40	ug/g PPM	0.015679	0.00015	0.062001	0.003369	<DL		0.0969	0.034999
Total Extractable Zinc	0.03	ug/g PPM	0.194016	0.050769	1.495748	0.633365	1.996844	0.062621	3.324662	0.646932

Table C.2 cont.

Parameter	MDL	Units	*Site 8 (n=1) Avg	*Site 8 (n=1) STD	*Site 9 (n=1) Avg	*Site 9 (n=1) STD	*Site 10 (n=1) Avg	*Site 10 (n=1) STD
Bulk Density	0.05	g/cm3	0.0944		0.2713		0.3583	
Total Extractable Aluminum	0.10	ug/g PPM	21.58904		102.4983		125.3508	
Total Extractable Arsenic	2.00	ug/g PPM	<DL	<DL	0.22553		<DL	<DL
Total Extractable Barium	0.10	ug/g PPM	0.530002		3.952789		0.710357	
Total Extractable Beryllium	0.04	ug/g PPM	<DL	<DL	<DL		<DL	<DL
Total Extractable Calcium	0.06	ug/g PPM	118.5543		512.6592		218.9488	
Total Extractable Cadmium	0.25	ug/g PPM	0.009429		0.028539		0.246906	
Total Extractable Cobalt	0.20	ug/g PPM	0.020234		0.210519		0.410948	
Total Extractable Chromium	0.03	ug/g PPM	<DL	<DL	0.025388		0.016025	
Total Extractable Copper	0.05	ug/g PPM	0.467926		0.430674		1.219772	
Total Extractable Iron	0.10	ug/g PPM	58.73731		44.6806		79.30206	
Total Extractable Potassium	1.00	ug/g PPM	2.131402		23.01624		2.07161	
Total Extractable Magnesium	0.20	ug/g PPM	11.67674		22.1825		11.81629	
Total Extractable Manganese	0.05	ug/g PPM	1.696478		14.45835		5.695082	
Total Extractable Molybdenum	0.01	ug/g PPM	<DL	<DL	<DL	<DL	<DL	<DL
Total Extractable Sodium	0.20	ug/g PPM	5.671297		40.6194		8.590064	
Total Extractable Nickel	0.20	ug/g PPM	0.08447		0.310404		0.294348	
Total Extractable Phosphorous	3.20	ug/g PPM	2.414279		6.132105		8.613257	
Total Extractable Lead	1.00	ug/g PPM	0.196639		0.356177		0.317752	
Total Extractable Sulphur	1.00	ug/g PPM	36.72435		39.87017		57.57219	
Total Extractable Silicon	0.05	ug/g PPM	9.737658		29.56345		6.958078	
Total Extractable Strontium	0.20	ug/g PPM	0.362044		3.604395		0.517639	
Total Extractable Titanium	2.00	ug/g PPM	0.525091		0.394167		0.894851	
Total Extractable Vanadium	0.40	ug/g PPM	0.144385		0.184945		0.308897	
Total Extractable Zinc	0.03	ug/g PPM	0.828595		2.208966		58.19484	

*Sediment samples

Table C.3 Total recoverable soil chemistry parameters from First Quantum soil sample sites.

Parameter	MDL	Units	Average	STD	Site 1 (n=1)	Site 2 (n=1)	Site 3 (n=1)	Site 4 (n=1)	Site 5 (n=1)	Site 6 (n=1)
% Moisture	1.00	%	20.86406	13.9433	15.610202	19.173296	17.897011	12.205002	22.454071	17.628338
Conductivity	0.50	us/cm	85.11491	144.2799	41.62	22.38	25.06	20.6	36.27	37.93
Bulk Density	0.05	g/cm3	0.710739	0.258311	0.78415	0.75185	0.912	1.18115	0.51285	1.1906
Organic Matter			8.69701	14.35437	2.7099407	1.9950788	2.7467105	1.0117259	8.0042898	2.8473039
pH 1:1 water to soil ratio	0.00	unit	5.390541	1.184401	6.28	6.38	5.7	5.7	5.34	5.59
Total Recoverable Aluminum	0.10	ug/g PPM	11783.4	3799.563	14364.767	9509.6774	14737.209	13254.237	19895.652	23435.028
Total Recoverable Arsenic	2.00	ug/g PPM	20.69475	70.71828	<DL	<DL	<DL	<DL	<DL	<DL
Total Recoverable Barium	0.10	ug/g PPM	35.94578	19.42942	27.336788	17.698925	27.44186	32.79096	35.543478	23.864407
Total Recoverable Beryllium	0.04	ug/g PPM	<DL	<DL	<DL	<DL	<DL	<DL	<DL	<DL
Total Recoverable Calcium	0.06	ug/g PPM	4760.702	3301.505	5869.4301	3604.3011	4106.9767	6092.6554	15802.174	16442.938
Total Recoverable Cadmium	0.25	ug/g PPM	2.359382	2.72758	2.4870466	<DL	<DL	<DL	3.5869565	2.4632768
Total Recoverable Cobalt	0.20	ug/g PPM	11.20989	5.360022	11.937824	6.4516129	11.744186	12.067797	15.434783	17.60452
Total Recoverable Chromium	0.03	ug/g PPM	36.97357	19.61072	37.554404	19.268817	36.534884	39.096045	52.956522	56.180791
Total Recoverable Copper	0.05	ug/g PPM	418.9098	611.1146	65.305699	10.258065	32.813953	69.265537	167.45652	139.63842
Total Recoverable Iron	0.10	ug/g PPM	31487.96	33002.95	18841.451	15030.108	22630.233	21475.706	22130.435	23322.034
Total Recoverable Potassium	1.00	ug/g PPM	934.2936	465.8668	1200.4145	826.88172	951.16279	1357.7401	770.86957	760.90395
Total Recoverable Magnesium	0.20	ug/g PPM	6047.037	2468.024	7239.3782	3602.1505	6623.2558	8757.0621	8876.087	8738.9831
Total Recoverable Manganese	0.05	ug/g PPM	204.2899	83.16118	230.67358	123.16129	241.62791	300.11299	261.73913	303.27684
Total Recoverable Molybdenum	0.01	ug/g PPM	0.400927	2.337784	<DL	<DL	<DL	<DL	<DL	<DL
Total Recoverable Sodium	0.20	ug/g PPM	382.1411	409.3171	507.35751	132.27957	180.04651	276.61017	1556.9565	2019.435
Total Recoverable Nickel	0.20	ug/g PPM	21.39527	9.01319	33.512953	12.451613	24.232558	24.836158	29.630435	35.050847
Total Recoverable Phosphorous	3.20	ug/g PPM	429.4326	132.0727	289.74093	313.33333	359.76744	661.01695	436.95652	381.9209
Total Recoverable Lead	1.00	ug/g PPM	17.4195	24.05245	9.761658	<DL	7.0465116	<DL	23.586957	26.485876
Total Recoverable Sulphur	1.00	ug/g PPM	1951.049	4050.688	364.55959	<DL	<DL	<DL	1177.6087	290.16949
Total Recoverable Silicon	0.05	ug/g PPM	193.0955	47.1458	275.02591	247.31183	213.23256	195.72881	217.3913	183.50282
Total Recoverable Strontium	0.20	ug/g PPM	17.99962	7.017537	16.953368	18.860215	13.837209	20.248588	29.369565	30.259887
Total Recoverable Titanium	2.00	ug/g PPM	11240.72	13372.43	28107.772	18159.14	28311.628	25152.542	38269.565	45062.147
Total Recoverable Vanadium	0.40	ug/g PPM	37.44888	11.53813	39.336788	26.623656	44.534884	42.259887	45.847826	52.384181
Total Recoverable Zinc	0.03	ug/g PPM	951.0738	931.6973	1200.6218	533.33333	233.72093	354.35028	1273.2609	677.06215

Table C.3 cont.

Parameter	MDL	Units	Site 7 (n=1)	Site 8 (n=1)	Site 9 (n=1)	Site 10 (n=1)	Site 11 (n=1)	Site 12 n=1)	Site 13 (n=1)
% Moisture	1.00	%	19.77701	21.69519	2.8785798	41.129832	55.980861	6.8647288	12.691604
Conductivity	0.50	us/cm	522.3	33.99	56.11	35.6	42.32	16.36	18.26
Bulk Density	0.05	g/cm3	0.8922	0.77095	0.99025	0.3861	0.1288	0.9436	0.69205
Organic Matter			8.041919	3.249238	0.8987629	14.257964	67.779503	1.8598983	1.8134528
pH 1:1 water to soil ratio	0.00	unit	2.82	5.95	8.68	4.17	3.91	6.04	5.64
Total Recoverable Aluminum	0.10	ug/g PPM	7548.315	12825.67	10914.595	11804.651	6636.4641	14876.836	17576.331
Total Recoverable Arsenic	2.00	ug/g PPM	<DL	<DL	<DL	<DL	<DL	<DL	<DL
Total Recoverable Barium	0.10	ug/g PPM	41.73034	24.59893	20.086486	37.976744	114.96133	30.124294	39.810651
Total Recoverable Beryllium	0.04	ug/g PPM	<DL	<DL	<DL	<DL	<DL	<DL	<DL
Total Recoverable Calcium	0.06	ug/g PPM	2802.247	4209.626	4847.5676	1961.6279	2200.884	3688.1356	9363.3136
Total Recoverable Cadmium	0.25	ug/g PPM	1.05618	1.625668	<DL	1.9069767	6.1657459	<DL	<DL
Total Recoverable Cobalt	0.20	ug/g PPM	10.26966	8.941176	12.562162	3.6046512	2.8508287	13.672316	16.662722
Total Recoverable Chromium	0.03	ug/g PPM	37.86517	33.09091	45.47027	22.046512	12.39779	50.59887	52.449704
Total Recoverable Copper	0.05	ug/g PPM	659.1011	165.4332	69.297297	308.37209	2304.9724	29.446328	126.60355
Total Recoverable Iron	0.10	ug/g PPM	165280.9	15824.6	21487.568	9941.8605	8702.7624	21887.006	32000
Total Recoverable Potassium	1.00	ug/g PPM	1495.056	770.2674	838.48649	474.18605	696.1326	1179.435	1419.4083
Total Recoverable Magnesium	0.20	ug/g PPM	5802.247	5764.706	8451.8919	1589.7674	974.80663	7288.1356	9777.5148
Total Recoverable Manganese	0.05	ug/g PPM	102.9438	184.2353	305.08108	91.069767	149.63536	268.0226	433.37278
Total Recoverable Molybdenum	0.01	ug/g PPM	<DL	<DL	<DL	<DL	<DL	<DL	<DL
Total Recoverable Sodium	0.20	ug/g PPM	568.9888	237.6471	105.03784	118.27907	52.928177	111.38983	699.1716
Total Recoverable Nickel	0.20	ug/g PPM	22.20225	21.96791	26.572973	6.7906977	5.9668508	31.118644	33.988166
Total Recoverable Phosphorous	3.20	ug/g PPM	363.8202	392.7273	384.64865	199.5814	562.65193	319.32203	680.71006
Total Recoverable Lead	1.00	ug/g PPM	30.42697	<DL	<DL	12.139535	40.066298	<DL	9.6094675
Total Recoverable Sulphur	1.00	ug/g PPM	15413.48	226.9519	263.35135	278.83721	1326.4088	127.88701	242.13018
Total Recoverable Silicon	0.05	ug/g PPM	216.1348	198.1818	206.24865	284.4186	310.05525	206.0791	186.3432
Total Recoverable Strontium	0.20	ug/g PPM	24.51685	18.97326	21.254054	13.883721	20.044199	16.813559	40.047337
Total Recoverable Titanium	2.00	ug/g PPM	13074.16	23512.3	19450.811	20818.605	10400	26589.831	31602.367
Total Recoverable Vanadium	0.40	ug/g PPM	31.10112	29.7754	50.118919	32.697674	16.729282	43.00565	60.591716
Total Recoverable Zinc	0.03	ug/g PPM	1493.708	771.7647	52.475676	143.86047	1182.5414	69.853107	301.77515

Table C.3 cont.

Parameter	MDL	Units	Site 14 (n=1)	Site 15 (n=1)	Site 16 (n=1)	Site 17 (n=1)	Site 18 (n=1)	Site 19 (n=1)	Site 20 (n=1)
% Moisture	1.00	%	9.883155	10.29205	15.928562	11.834709	9.2780499	17.000182	27.033481
Conductivity	0.50	us/cm	17.26	51.91	35.02	109.1	15.22	127.3	130.6
Bulk Density	0.05	g/cm3	0.64785	0.76485	0.63785	0.8705	0.77785	0.9125	0.7181
Organic Matter			1.682488	1.941557	3.7077683	1.217691	1.2855949	5.0027397	4.3447988
pH 1:1 water to soil ratio	0.00	unit	5.32	5.93	4.89	5.32	5.38	5.42	7.28
Total Recoverable Aluminum	0.10	ug/g PPM	14447.83	14566.04	14056.216	10360.694	10649.438	6421.6216	11010.127
Total Recoverable Arsenic	2.00	ug/g PPM	<DL	<DL	69.513514	<DL	<DL	101.05946	<DL
Total Recoverable Barium	0.10	ug/g PPM	33.26087	36.62893	41.72973	16.462428	28.449438	27.027027	27.594937
Total Recoverable Beryllium	0.04	ug/g PPM	<DL	<DL	<DL	<DL	<DL	<DL	<DL
Total Recoverable Calcium	0.06	ug/g PPM	6610.87	8815.094	4557.8378	5858.9595	4029.2135	2177.2973	4746.8354
Total Recoverable Cadmium	0.25	ug/g PPM	<DL	2.993711	<DL	<DL	<DL	4.0648649	2.0253165
Total Recoverable Cobalt	0.20	ug/g PPM	8.804348	20.40252	12.821622	9.0404624	9.5505618	31.091892	7.443038
Total Recoverable Chromium	0.03	ug/g PPM	28.28261	42.7673	35.891892	28.369942	27.078652	118.16216	31.443038
Total Recoverable Copper	0.05	ug/g PPM	40.69565	177.0566	283.02703	71.745665	85.168539	1391.5676	27.468354
Total Recoverable Iron	0.10	ug/g PPM	19206.52	26389.94	73448.649	14906.358	23033.708	76302.703	13653.165
Total Recoverable Potassium	1.00	ug/g PPM	1370.217	1305.66	1919.7838	647.63006	944.04494	650.16216	392.40506
Total Recoverable Magnesium	0.20	ug/g PPM	7747.826	8296.855	9176.2162	6094.7977	8310.1124	3902.7027	5349.3671
Total Recoverable Manganese	0.05	ug/g PPM	246.9565	359.2453	246.05405	198.63584	214.42697	162.63784	148.98734
Total Recoverable Molybdenum	0.01	ug/g PPM	<DL	<DL	<DL	<DL	<DL	14.032432	<DL
Total Recoverable Sodium	0.20	ug/g PPM	636.7391	729.0566	409.94595	373.4104	217.66292	488.43243	178.40506
Total Recoverable Nickel	0.20	ug/g PPM	20.21739	26.38994	14.378378	14.890173	16.853933	30.118919	21.468354
Total Recoverable Phosphorous	3.20	ug/g PPM	502.6087	483.0189	530.81081	489.24855	507.19101	266.59459	202.32911
Total Recoverable Lead	1.00	ug/g PPM	7.043478	9.006289	42.097297	<DL	10.067416	33.362162	8.3037975
Total Recoverable Sulphur	1.00	ug/g PPM	<DL	552.4528	2268.1081	120.16185	417.07865	8105.9459	297.97468
Total Recoverable Silicon	0.05	ug/g PPM	188.1304	225.9623	177.83784	166.0578	147.91011	145.05946	193.49367
Total Recoverable Strontium	0.20	ug/g PPM	30.34783	27.57233	18.205405	21.803468	13.685393	11.87027	15.341772
Total Recoverable Titanium	2.00	ug/g PPM	25417.39	24855.35	-1869.459	907.51445	1022.4719	690.59459	767.08861
Total Recoverable Vanadium	0.40	ug/g PPM	43.69565	47.34591	70.010811	31.722543	37.52809	29.708108	27.797468
Total Recoverable Zinc	0.03	ug/g PPM	65.3913	1702.39	471.35135	294.33526	203.88764	1962.1622	327.8481

Table C.3 cont.

Parameter	MDL	Units	Site 21 (n=1)	Site 22 (n=1)	Site 23 (n=1)	Site 24 (n=1)	Site 25 (n=1)	Site 26 (n=1)	Site 27 (n=1)
% Moisture	1.00	%	31.10785	46.83506	14.123693	44.025465	55.131155	33.862163	9.6428176
Conductivity	0.50	us/cm	94.91	60.67	394.2**	30.11	20.78	641.7	7.454
Bulk Density	0.05	g/cm3	0.6346	0.1768	0.7269	0.2286	0.195	0.3877	0.8171
Organic Matter			5.357706	43.41063	4.360985	32.589676	43.948718	14.418365	1.3707013
pH 1:1 water to soil ratio	0.00	unit	6.81	4.07	3.17	4.35	4.62	2.67	5.61
Total Recoverable Aluminum	0.10	ug/g PPM	9798.883	9210.989	8954.5455	9869.0476	6203.5088	4515.3374	11782.857
Total Recoverable Arsenic	2.00	ug/g PPM	<DL	<DL	152.20455	<DL	<DL	389.44785	<DL
Total Recoverable Barium	0.10	ug/g PPM	28.96089	55.16484	31.204545	69.666667	82.105263	51.95092	29.462857
Total Recoverable Beryllium	0.04	ug/g PPM	<DL	<DL	<DL	<DL	<DL	<DL	<DL
Total Recoverable Calcium	0.06	ug/g PPM	3955.307	2698.901	4340.9091	1607.619	2008.1871	2180.3681	4155.4286
Total Recoverable Cadmium	0.25	ug/g PPM	8.648045	4.461538	7.0454545	4.5714286	7.0409357	<DL	<DL
Total Recoverable Cobalt	0.20	ug/g PPM	20.6257	7.494505	7.8636364	5.8809524	6.7134503	6.1104294	11.68
Total Recoverable Chromium	0.03	ug/g PPM	39.17318	24.17582	35	15.714286	19.812865	17.423313	31.885714
Total Recoverable Copper	0.05	ug/g PPM	742.5698	586.3736	1624.3182	1065.7143	444.44444	2397.546	86.057143
Total Recoverable Iron	0.10	ug/g PPM	29944.13	15639.56	77522.727	11897.619	10542.69	124883.44	20002.286
Total Recoverable Potassium	1.00	ug/g PPM	461.2291	495.3846	1683.6364	604.7619	476.95906	2483.4356	984
Total Recoverable Magnesium	0.20	ug/g PPM	6616.76	2336.264	6254.5455	1664.0476	1352.5146	4041.7178	8123.4286
Total Recoverable Manganese	0.05	ug/g PPM	167.2179	72.72527	158.45455	73.452381	77.871345	93.349693	281.37143
Total Recoverable Molybdenum	0.01	ug/g PPM	<DL	<DL	<DL	<DL	<DL	<DL	<DL
Total Recoverable Sodium	0.20	ug/g PPM	226.5922	223.7363	852.5	78.452381	58.502924	489.07975	179.40571
Total Recoverable Nickel	0.20	ug/g PPM	37.81006	15.58242	12.022727	10.166667	11.391813	4.3190184	20.114286
Total Recoverable Phosphorous	3.20	ug/g PPM	415.419	643.2967	406.36364	475	336.14035	383.06748	580.8
Total Recoverable Lead	1.00	ug/g PPM	11.62011	27.45055	45.340909	25.5	28.631579	133.25153	<DL
Total Recoverable Sulphur	1.00	ug/g PPM	1445.587	1525.055	10484.091	1201.6667	1011.2281	16397.546	<DL
Total Recoverable Silicon	0.05	ug/g PPM	150.3017	244.6154	179.59091	258.57143	227.53216	160.51534	135.38286
Total Recoverable Strontium	0.20	ug/g PPM	11.3743	11.23077	14.113636	10.214286	10.783626	6.9447853	20.48
Total Recoverable Titanium	2.00	ug/g PPM	662.3464	548.5714	1012.7273	540.95238	472.04678	1002.6994	1015.3143
Total Recoverable Vanadium	0.40	ug/g PPM	31.62011	21.64835	39.181818	22.642857	17.192982	58.257669	38.285714
Total Recoverable Zinc	0.03	ug/g PPM	3166.48	1230.33	3009.0909	1377.8571	1901.0526	833.37423	280.91429

Table C.3 cont.

Parameter	Site 28 (n=1)	Site 29 (n=1)	Site 30 (n=1)	Site 31 (n=1)	Site 32 (n=1)	Site 33 (n=1)	Site 34 (n=1)	Site 35 (n=1)
% Moisture	10.09538	10.97074	19.19856	16.27278	23.020662	46.56081	19.302139	10.067873
Conductivity	7.306	9.942	19.13	11.03	81.54	249.4**	34.74	67.42
Bulk Density	0.75875	0.8034	0.6513	0.66605	0.842	0.3904	1.0546	0.7155
Organic Matter	1.429984	1.73637	4.053432	3.303055	3.4976247	11.885246	2.8446804	2.3759609
pH 1:1 water to soil ratio	5.98	5.17	5.61	5.5	4.95	4.5	6.38	7.08
Total Recoverable Aluminum	11054.75	8953.684	8871.429	13615.14	12108.235	11504.865	15275.269	11809.091
Total Recoverable Arsenic	<DL	<DL	<DL	<DL	<DL	<DL	<DL	12.090909
Total Recoverable Barium	21.8324	20.71579	38.47619	16.28108	25.882353	20.627027	36.107527	44.545455
Total Recoverable Beryllium	<DL	<DL	<DL	<DL	<DL	<DL	<DL	<DL
Total Recoverable Calcium	4294.972	3362.105	2368.571	2614.054	2877.6471	4285.4054	2987.0968	5100
Total Recoverable Cadmium	<DL	0.905263	4.214286	<DL	<DL	3.4378378	<DL	9.1590909
Total Recoverable Cobalt	9.608939	10.06316	7.619048	9.232432	8.5176471	15.632432	9.5268817	12.818182
Total Recoverable Chromium	25.85475	25.6	27.09524	34.24865	34.729412	87.632432	34.473118	33.75
Total Recoverable Copper	59.68715	59.13684	252.619	73.25405	37.552941	614.05405	44.731183	349.09091
Total Recoverable Iron	18677.09	15909.47	14392.86	19809.73	17444.706	33102.703	13154.839	33659.091
Total Recoverable Potassium	843.352	577.4737	757.381	329.7297	515.76471	606.27027	739.13978	1170.9091
Total Recoverable Magnesium	7068.156	6395.789	4078.571	6069.189	4691.7647	9355.6757	3881.7204	7352.2727
Total Recoverable Manganese	237.9888	208.4632	184.1429	201.4919	177.50588	238.48649	132.77419	272.95455
Total Recoverable Molybdenum	<DL	<DL	<DL	<DL	<DL	<DL	<DL	<DL
Total Recoverable Sodium	219.5754	121.8947	160.3095	106.4	125.81176	261.62162	113.54839	557.72727
Total Recoverable Nickel	16.80447	18.84211	14.90476	22.48649	23.6	41.210811	25.462366	21.477273
Total Recoverable Phosphorous	556.2011	456.6316	285.9524	432.6486	330.82353	655.13514	185.11828	559.54545
Total Recoverable Lead	7.441341	<DL	16.45238	<DL	<DL	22.854054	<DL	22.136364
Total Recoverable Sulphur	<DL	<DL	216.4524	144.4541	139.01176	2322.1622	<DL	1926.3636
Total Recoverable Silicon	141.6536	134.6105	241.9048	130.1189	157.34118	145.34054	137.09677	129.65909
Total Recoverable Strontium	16.53631	15.70526	12.61905	13.03784	12.094118	10.681081	16.215054	24.068182
Total Recoverable Titanium	1010.503	848.4211	1150.952	756.973	1041.8824	685.18919	1220	1154.7727
Total Recoverable Vanadium	36.22346	30.63158	42	33.40541	34.305882	32.021622	31.591398	38.886364
Total Recoverable Zinc	261.4525	229.2632	1342.143	187.2	199.95294	1417.0811	635.69892	3900

Appendix D

Table D.1. Average root length (in millimetres) of *T. pratense* seedlings germinated on Hoagland's Nutrient Agar at various levels of As(III) contamination.

	Without LU-71		With LU-71	
As(III) Concentration (mM)	Root length (mm)	Std Dev	Root length (mm)	Std Dev
0	57.555	5.43836	37.3781746	2.44383
0.3	2.366666667	1.59304	11.92111111	5.141704
0.6	0	0	7.402380952	3.138583
0.9	0	0	5.38	1.678571
1.2	0	0	5.333333333	3.43673
1.5	0	0	3.3	2.088061
2	0	0	0.8	1.16619

Table D.2. Average shoot length (in millimetres) of *T. pratense* seedlings germinated on Hoagland's Nutrient Agar at various As(III) contamination.

	Without LU-71		With LU-71	
As(III) Concentration (mM)	Shoot length (mm)	Std Dev	Shoot length (mm)	Std Dev
0	12.6665873	1.23066	9.361507937	1.463647
0.3	0.7	0.4	4.519444444	2.354101
0.6	0	0	2.914285714	0.811147
0.9	0	0	2.253333333	0.460724
1.2	0	0	0.9	0.663325
1.5	0	0	1.6	1.2
2	0	0	0.6	1.2

Appendix E

Table E.1. Average root biomass of *T. pratense* seedlings after 45 days of growth, with and without inoculation by LU-71R at five different As(III) concentrations.

	Without LU-71		With LU-71	
As(III) Concentration (mM)	Root biomass (mg)	Std Dev	Root biomass (mg)	Std Dev
0	3.23	0.088	4.64	0.034
0.05	1.36	0.020	2.44	0.005
0.08	1.34	0.012	3.02	0.013
0.15	1.28	0.063	2.59	0.019
0.25	1.82	0.017	3.03	0.022
0.45	1.36	0.017	3.00	0.031

Table E.2. Average shoot biomass of *T. pratense* seedlings after 45 days of growth, with and without inoculation by LU-71R at five different As(III) concentrations.

	Without LU-71		With LU-71	
As(III) Concentration (mM)	Shoot biomass (mg)	Std Dev	Shoot biomass (mg)	Std Dev
0	6.32	1.09	5.38	0.005
0.05	3.08	0.044	5.00	0.048
0.08	3.68	0.039	4.98	0.014
0.15	3.02	0.050	4.43	0.024
0.25	2.98	0.051	4.81	0.030
0.45	2.48	0.070	5.20	0.081